Quaternary Science Reviews

Timing and amplitude of hydroclimate changes during the last glacial cycle in southwestern North America

--Manuscript Draft--

Manuscript Number:	JQSR-D-25-00358R2
Article Type:	Research Paper
Keywords:	Quaternary; paleoclimatology; North America; speleothems; U-Th series; Devils Hole; hydroclimate
Corresponding Author:	Simon Steidle University of Innsbruck Innsbruck, AUSTRIA
First Author:	Simon Steidle
Order of Authors:	Simon Steidle
	Yuri Dublyansky
	Marco Roman
	Gina E. Moseley
	Kathleen A. Wendt
	R. Lawrence Edwards
	Christoph Spötl
Abstract:	The presently (semi)arid southwestern North America experienced major shifts in hydroclimate during the Quaternary characterized by oscillations between pluvial and arid phases. On orbital timescales, regional moisture availability is attributed to latitudinal shifts of moisture-bearing storm tracks due to the expansion and retreat of North American ice sheets. Millennial-scale variability is superimposed on top of the broader glacial pluvial phases. Groundwater fluctuations recorded by calcite deposits in Devils Hole, Nevada, offer unique insights into the past hydroclimate of the southwestern USA covering both time scales. Here, we increase the resolution of the Devils Hole water table record with an additional 43 water-table markers covering the last interglacial-glacial cycle. The updated record of water-table changes enables a comparison with sea-level records between 120,000 to 70,000 years ago, revealing concurrent changes in both during this period. This strengthens the hypothesis that orbital-scale water-table changes are closely linked to ice-sheet expansion during Marine Isotope Stage 5. New water table markers of the last 60,000 years further support increased pluvial conditions during Heinrich events.
Response to Reviewers:	

Dear Editor,

Please find enclosed our manuscript, "Timing and amplitude of hydroclimate changes during the last glacial cycle in southwestern North America," which we submit for publication in *Quaternary Science Reviews*.

This manuscript presents a high-resolution speleothem-based hydroclimate record from Devils Hole 2 in the southern Great Basin. With this study, we conclude a long-term research effort that builds upon and complements a series of earlier high-impact publications (e.g., Moseley et al., 2016, Wendt et al., 2018 & 2020, Jackson et al., 2023, Steidle et al., 2024). The dataset was generated at the technical limits of U-Th dating on the exceptionally slow-growing subaqueous calcite, enabling precise chronologies in a particularly challenging time window. Our results reveal that during MIS 5, hydroclimate variability in the southern Great Basin was closely synchronized with global sea level and ice volume changes—an observation not previously documented at this timescale. This dataset provides a robust foundation for understanding hydroclimate controls across multiple temporal scales.

All authors have made substantial contributions and approved the final version of the manuscript. Individual contributions are detailed in the "Author contributions" section of the manuscript file. This is original work that has not been published elsewhere and is not under consideration for publication elsewhere.

We suggest the following reviewers:

1. David McGee, MIT, USA (davidmcg@mit.edu)
2. Daniel Ibarra, Brown University, USA (daniel_ibarra@brown.edu)
3. Jessica Oster, Vanderbilt University, USA (jessica.l.oster@vanderbilt.edu)
4. Kathleen Johnson, University of California, Irvine, USA (kathleen.johnson@uci.edu)
5. Russell Drysdale, University of Melbourne, Australia (rnd@unimelb.edu.au)
6. Isabel Montañez, University of California, Davis, USA (ipmontanez@ucdavis.edu)

Sincerely,
Simon Steidle
On behalf of all co-authors

Rebuttal Letter for Steidle et al. "Timing and amplitude of hydroclimate changes during the glacial cycle in southwestern North America" (QSR)

Reviewer #1:

Review of Steidle et al. "Timing and amplitude of hydro climate changes during the glacial cyclin southwestern North America" for QSR, June 2025

Summary
Steidle and coauthors present a detailed study with new ages and laser ablation data from the southwestern US Devils Hole site in Nevada. This dataset is largely additive to a suite of papers since 2016 from this group of authors. The paper was clearly originally written and formatted for a short format journal and my primary comment is that this work needs to be properly added to the long format for Quaternary Science Reviews in a way that makes this a distinctive contribution. Numerous parts of the supplemental including the figures could easily be incorporated into he main text and would make this work much more substantive. The geochronology is excellent but is largely not described in detail, all images of the samples and the laser ablation results are confined to the supplement, and the description of the millennial scale events (Heinrich events) in the last part of the discussion could really use much greater integration of the lake level datasets from the Great Basin as well as zoom-ins on the comparison to the Asian speleothem records. All of the pieces towards a really nice contribution are here but a more thorough job formatting and describing the results for a long format journal like QSR will make this work more impact and distinct from previous work on these samples from Devils Hole.

We extended the discussion including the usage of regional lake-level data (as also suggested by reviewer #2) and moved the trace element analysis description to the main text.

Major Comments
1) Section 4.1 - I would suggest you move the supplementary material showing these details to the main text, the paper is not overly long and it would substantially help with describing the dataset. This includes Figure S4 and S5 which should be moved to the main text.

We moved most of the petrographic description to the main text, forming the new section 4.1.

2) Description of the sampling and cores, Figures on page 19 and 22 (mislabelled as both being S2) - these should be moved to the main text to show the methods and the samples being analyzed. This would greatly improve the readability of the paper and describe what was done more thorough in one narrative.

The trace element analysis, including the pictures, was moved to the main text (see major comment #1 above)

We agree that showing the samples that were analysed (Figure S2) is an important part of the documentation. However, we would like to restrain from moving this complex picture into the main text as it isn't discussed in the main text in greater detail. We prefer to keep it in the supplementary material.

The figures were renumbered as they were moved to the main text.

3) Section 5.2 - I would suggest he authors also look at the records from Owens Lake, while the dating constraints are not great the oxygen isotope record from the Li et al. and Menking et al. papers on Owens lake during MIS 5 appear to line up with their datasets (see recent summary by Lowenstein et al. (2024, QSR). Additionally, at the end, 305-307: can the authors be more explicit here in what they are calling on for the different forcing mechanisms?

Li et al. (1999, Quaternary Research) only dealt with the last 1000 years - a time period that is not available for Devils Hole. The resolution of the study by Menking et al. (1997, Quaternary Research) is too low to compare it to Devils Hole. Lowenstein et al. is indeed a nice addition, and we updated the discussion for MIS 5 (new section 5.2).

Regarding the different forcing mechanisms, we changed the sentence to:

"This suggests MIS 4 and MIS 3 were influenced by a different forcing mechanism operating on shorter timescales, in contrast to MIS 5, where the dominant forcing mechanism appears to be linked to orbital variability"

We cannot determine how these mechanisms operate, but we can identify two distinct patterns, which we interpret as arising from two distinct forcing mechanisms.

A detailed description of the two most likely mechanisms according to literature for each time-scale is given in the first and second paragraph of the introduction.

4) 341-361: I generally agree with this but there is clearly a different response at H1, and the authors are confusing H5 to H2 vs. H1 as far as I understand the text.

Following our discussion on the second half of the first comment of reviewer #2, we have changed the wording of our discussion of the H1 interval. With only a single data point at 17.26 ka, our study cannot substantially inform this H event, so we keep the discussion and interpretation brief.

Further, the idea that the H events cause aridity in the north Great Basin is incorrect and in fact the papers cited on lines 342-346 like Munroe and Laabs (2012) show northern Great Basin wetting (see also Ibarra et al., 2014; Santi et al., 2020).

The papers cited in this paragraph and elsewhere in our study (Oster et al., 2020; Hudson et al., 2019; Heaton et al., 2019) discuss phases of varying aridity in the northern Great Basin associated with Heinrich events. We added wording to make it more explicit that this interpretation remains a subject of debate:

"Within the Great Basin, there is, although debated, evidence of increased aridity in the north (Oster et al., 2020; Benson et al., 2003; Zic et al., 2002; Heaton et al., 2019) and pluvial

conditions in the south (Munroe and Laabs, 20123; McGee et al., 2018; Oster et al., 2023) associated with H events."

"Some studies from the northern Great Basin suggest drying during H5 to H2 (Oster et al., 2020; Benson et al., 2003; Zic et al., 2002; Heaton et al., 2019)."

In general I think that the second half of section 5.3 should be more clearly written and ideally shown graphically more comprehensively than on Figure 2C.

The inherent limitations of our dataset —slow growing mammillary calcite, a discontinuous record, and sparse data coverage at several key intervals —limit our ability to discuss individual H events in a clear and straightforward manner. It is however needed for our interpretation stated in the end of the discussion section:

"Overall, it can be concluded that H events […] generally coincided with a high water table at Devils Hole"

"In the Great Basin, such shifts during H events have been associated with an intensification of the subtropical jet and a southeastward displacement of the Aleutian Low, ultimately increasing winter precipitation in the SW USA (McGee et al., 2018). Our study's findings support this climate scenario."

By adding a Conclusion section, we aim to make the take-away message of this discussion more apparent. Although we experimented with different types of figures, the inherent limitations of our dataset described above prevent us from presenting a more comprehensive synthesis.

5) A conclusion is needed summarizing the findings and discussion of the paper.

We added Conclusions

Minor Line-by-Line Comments
54: Oster et al. 2023 just used previous datasets, I would suggest you also cite Ibarra et al. (2014, GSA Bulletin; **2018, Geology)** and Hudson et al. (2019, Scientific Reports), as well as Munroe and Laabs (2013) as well as their 2012 paper.

We added Ibarra et al., 2014; Hudson et al., 2019 as they were also cited by Oster et al., 2023. We corrected the Munroe and Laabs citation from 2012 to 2013.

61-63: And across the deglaciation (e.g., Lora and Ibarra, 2019, QSR).

Our study does not include Termination I (nor T II). Hence we did not add this citation.

104-113: This is not really "regional setting", I would suggest you re-title this section or move this text relating to the texture of the carbonates.

We renamed the section REGIONAL SETTING AND CALCITE DEPOSITION.

140-141: Can you show this in a zoom in of the sample?

The samples are shown in Figure S2, where the presence of numerous thin mammillary calcite layers is evident (as described in the text). For reasons of consistent sample treatment and processing limitations, we chose not to extrapolate to boundaries in the few cases where this might have been possible. We do not see how a zoomed-in view of a portion of Figure S2 would meaningfully strengthen this point, and therefore have not made changes in response to this comment.

174-177: This is excellent that you have used a carbonate standard, which is not always the case. How does your data compare to recently reported measurements by others on SPLT-NP? (If available)

We have not added additional information on the measurement of this standard but provide the following information for the reviewer:

In general, we also confirm that SPLT-NP is an excellent calibration standard with respect to material homogeneity at the micro-scale, consistent with recent findings (Lores-Padin et al., J Anal At Spectrom, 2025, in press; Sekhom et al., Rapid Commun Mass Spectrom 39-9, 2025), and superior to both nanopressed and non-nanopressed alternatives. Conducting a detailed, direct quantitative comparison remains challenging. This is primarily because SPLT-NP is a very recent standard that has been utilized in only a limited number of published studies. Furthermore, these few studies often employed different instrumental or operational configurations (e.g., Lores-Padin et al. utilized a Time-of-flight mass spectrometer detector), or they do not provide full numerical information on the absolute performance of the standards themselves. To the extent that a comparison can be established with Sekhom et al. (2025), we achieve comparable LODs (limit of detection) for the absolute concentration of Mg, Sr, and Ba (ours are ~ 6 mg/g, ~ 200 µg/g, ~ 3 µg/g, compared to their reported ~ 6 mg/g, ~ 700 µg/g, ~ 30 µg/g, respectively). However, it is important to note that the LOD is not a particularly impactful parameter for these elements, as they are present at relatively high concentrations in the samples. Regarding the same authors' findings, we observed the matrix effect between the NIST 612 and SPLT-NP standards to be similar for Mg (approximately 20%), but significantly more pronounced for Sr and Ba (approximately 50%, compared to their reported >20%). Still, when normalized to Ca, the matrix effect in our study also reduces to <25% for all three elements. Quantitatively, these evaluations lack the robustness of a dedicated comparative study, because ablation conditions are slightly different (spot analysis for Sekhom et al. versus scan line for us, resulting in substantially different total energy delivered per analytical area - our choice was to analyse the standards under the exact same conditions as the samples). Also, in both our study and theirs, the underlying statistics are derived from a very limited number of analytical sessions. Nevertheless, at a qualitative level, our results strongly confirm the findings reported by others regarding the higher reliability of employing calibrations with nanopressed matrix-matching standards like SPLT-NP, compared to the NIST 612.

186-197: See major comment 1.

We added a new section 4.1 including the trace element analysis.

217-219: Do you mean to call on Figures 1 here? It would be better to show this texture in the core photos/images as in the supplementary figure. This relates to Major Comment 2 above.

Figure S2 is indeed a better reference here. We **changed** this part as follows:

“The subsequent water-table decline reached a lowstand less than +3.2 m but greater than +1.8 m between 104.3±0.3 ka and 97.5±0.3 ka during MIS 5c. However, the alternation between folia and mammillary calcite in core F (~~Figure 1C~~**Figure S2, between samples SS10 and SS14**) indicates that the water table was unstable, oscillating above and below +3.2 m multiple times during this period.”

In addition to our reply to major comment 2, we note that this is a qualitative statement, and therefore we do not consider it necessary to move Fig. S2 into the main text. We regard a decent quality picture as provided with Fig. S2 as sufficient to support the statement made in lines 217-219.

255: Does this imply that there are unconstrained hiatuses?

The comment refers to the following part:

“Despite actively searching for mammillary calcite above +9.9 m, none was found from the last 120 ka. However, no conclusions can be draw from this absence, as condensation corrosion – known to have occurred in the higher parts of Devils Hole (Dublyansky and Spötl, 2015) – may have removed calcite from the cave walls. It is therefore entirely plausible that mammillary calcite once existed at higher elevations.”

The short answer is no.

Condensation corrosion may have removed calcite from the exposed surface meaning younger deposits than found by us may have existed. However, calcite deposits that still exist today and were analysed and discussed in our study are unaffected by this. Furthermore, hiatuses in mammillary calcite (which we assume was meant by the reviewer here) were first of all not observed (see also "Controls on the southwest USA hydroclimate over the last six glacial-interglacial cycles" by Wendt et al., 2025; Nature Communications) and secondly are not an issue because we are interested in the boundary between folia and mammillary calcite which we are dating as close as possible to. Mammillary calcite indicates submergence, and the timing of folia formation adjacent to these layers is irrelevant to the conclusion that the water table rose or fell before or after mammillary calcite deposition at the boundary.

296: Agreed re: Oster et al. (2015) for MIS 2, but note that was an LGM focused study. Suggest you diversify the citations here that also look at the deglaciation (some mentioned above) and the work by Lachniet.
We are talking about times of extensive glaciation.

Figure 2: How was the grey shading actually produced?

It is a qualitative, hand-drawn visual aid and we found orientation within this type of figure is difficult without it. We acknowledge its limitations—particularly that the heights of highstands are not constrained. We emphasize that all interpretations and discussions in the manuscript are based solely on the direct ^{230}Th–U ages and do not rely on, or refer to, this shading.

Reviewer #2:

This study presents new U-Th dating results from calcite deposits in Devils Hole, Nevada, that record periods of high water tables during the last 120,000 years. The authors then

interpret the results in the context of regional and global climate changes over this period, concluding that regional groundwater tables respond to the presence of North American ice sheets and Heinrich stadial events. The authors also thoughtfully describe the deposits and use trace element analyses to identify portions of the deposits more likely to have remained closed systems with respect to U-Th.

This study offers important new constraints on the response of water availability in the southwestern U.S. to regional and global climate change, and it will be worthy of publication after moderate revisions. The U-Th data are robust, and the paper is well written. I also appreciate that the interpretations take into account the fact that water table elevations may be underestimated and that rises and falls cannot be directly dated. I have three main suggestions for improving the work, as well as one minor point.

First, I think the authors are too quick to highlight the points of consistency with previous understanding, and that the paper would benefit from more exploration of the more puzzling parts of the record. I'm surprised, for example, that water tables appear to be as high in MIS 5d and 5b as they were in MIS 2, given the substantially higher CO2 and sea levels (and thus higher temperatures and smaller ice sheets) in MIS 5.

Unfortunately, the Devils Hole record does not support this line of argument because all water-table markers represent minimum elevations. The lower bound is constrained by continuous mammillary calcite, but there is no upper bound. MIS 2 highstands could have been many meters higher than those of MIS 5 –or vice versa; our data cannot resolve this. We believe this limitation is already clearly described in the second half of section 5.1, and therefore we have not added further clarification.

I'm also puzzled by the fact that water tables begin falling early in Heinrich Stadial 1 (and show only a brief rise from the LGM into HS1, if I interpret Figure 2 correctly), given that so many Great Basin lakes (both north and south of Devils Hole) sustained their highstands in HS1. The authors attribute the falling water table during HS1 to the fact that the Termination was beginning, but the North American ice sheets were still quite large at this time (and sea level was substantially lower than sea levels during water table highstands in MIS 5d and 5b). Between the Heinrich stadial and the presence of large North American sheets, I would expect that the water table would remain high until ~15 ka. I don't expect the authors to have all the answers to these puzzling parts of the record, but the paper would benefit from more thoughtful discussion of them.

We acknowledge that our earlier statement suggesting that H1 is overprinted by the onset of Termination I was probably overstated, if not incorrect. Our record contains no data for the several thousand years following the brief rise at 17.3 ka. Aside from a single data point reported by Szabo et al., additional data only become available at 10 ka. We cannot evaluate the amplitude of the event: although all markers lie near +8.3 m, this does not provide a valid basis for interpretation, as discussed above. We changed the discussion about H1 as follows:

~~H1 is not clearly recorded at Devils Hole and instead appears to be overprinted by the onset of Termination I and associated drying of the southern Great Basin.~~

A single brief rise at 17.28±0.08 ka is recorded at Devils Hole, falling into the early part of H1, However, the absence of data for the subsequent few millennia, combined with the clustering of water-table markers near +8.3 m —which prevents estimating the event's amplitude— limits our ability to draw conclusions regarding H1 and the onset of Termination I.

Second, integration with regional lake records is important. At a minimum, the authors should

include Lowenstein et al.'s (QSR, 2024) recent revision of the Death Valley lake record, dating of highstands in the Death Valley drainage during Heinrich stadials by Reheis et al. (Quaternary Research 2015), and Adam Hudson's work on lakes both north and south of Devils Hole (Hudson et al., Scientific Reports 2019; Hudson et al., QSR 2023). How do the Devils Hole water table elevations (particularly those in MIS 5/4/3) compare to regional lake levels? If there are discrepancies, what might cause them?

Thank you for suggesting these studies. Since Reheis et al. (2015) investigated the time from 45 ka to 25 ka, their record barely overlaps with ours. Between 44 ka and 23 ka, we have only a single data point which, given its uncertainties, could coincide equally well with either a highstand or a lowstand of their record. For Hudson et al. (2023), no clear comparison can be made, as the Devils Hole record shows only oscillations around +8.3 m, and the amplitude cannot be determined. In contrast, we can provide a meaningful update to the MIS 5 interpretation of Lowenstein et al. (2024), and we find clear agreement with the hypothesized dipole proposed by Hudson et al. (2019) during the older half of their record (Devils Hole lacks data for the younger half). These elements now form the new section 5.2 of the main text.

Third, Moseley et al. (2016) demonstrated that deposits showed age offsets that increased linearly with depth below the water table, and I think it's important to consider these effects in the authors' discussion of the dating results. Figure 4 in that paper suggests that deposits ~30 m below the water table showed age offsets of ~10 kyr. Based on this relationship, deposits 3 m below the water table may have been biased old by ~1 kyr, causing substantial challenges with dating millennial-scale water table changes and relating them to Heinrich stadials. This uncertainty needs to be discussed, particularly since we don't know how far below the water table the dated deposits might have formed.

It is a well-recognized and important issue, which we now address in the manuscript in a new paragraph in section 5.1. However, it does not change any of the dating results or our interpretation of them.

“In Devils Hole, mammillary calcite sampled from depth and dated using the U-Th method has yielded inaccurate ages for glacial terminations that are systematically too old (Moseley et al., 2016). This age offset is hypothesized to be caused by an increase in excess ^{230}Th with depth in the water column, which specifically affects glacial terminations due to a change in sedimentation (Moseley et al., 2016). Moseley et al. (2016) observed that mamillary calcite deposited in shallow waters appeared to be unaffected by the age offset, and therefore represented the most accurate chronology at glacial terminations. The age offsets caused by increasing excess ^{230}Th at depth during glacial termination are thus not of relevance to this study given that: (1) the investigated time period is the last glacial period (and not a glacial termination), for which Moseley et al. (2016) produced reproducible chronologies from cores of different depths, and; (2) the samples dated in this study are largely from mamillary-folia boundaries indicating shallow water depths. Based on these two lines of argument, we consider the chronology presented here to be accurate within the stated precision. Still, since these are relatively young samples and it cannot be ruled out that the water table stood several meters higher during their formation, it must be noted that this represents a difficult-to-quantify uncertainty that could shift the true age of the samples to somewhat younger than reported here in particular during the intermediately glaciated phase of MIS 5 which was not analyzed by Moseley et al. (2016).”

Minor point: The word "Folia" is technically plural, and I encourage the authors to consider switching to treating the word as such (e.g. going from "Folia…forms" to "Folia…form" in lines 105-106; using "they" instead of "it" in lines 106-107) or using a different term that is clearly singular, like "Foliar calcite".

We checked the text and adjusted occurrences accordingly.

Nice work on this important set of deposits--
-David McGee

Rebuttal Letter #2 for Steidle et al. "Timing and amplitude of hydroclimate changes during the glacial cycle in southwestern North America" (QSR)

Reviewer #1:

The authors have done a thorough job revising the work based on my previous review and that of the other reviewer. My only replies/comments remaining are:

1) Figure 6, I think it's a bit odd to just say that the shading is "a visual aid". It would be much nicer to do this somewhat quantitatively as current this feels aribtrary. I note for example between 60 and 80 ka, I'm not sure why the light grey shading is so spread out on either side of the peak at ~70 ka.

We agree that there is room for discussion on this visual aid. We have carefully explored the possibility of developing a method, that 1) is quantitative, 2) meets scientific standards and 3) improves the readability of the figure. However, devising a method that fulfils all three criteria was found to be beyond the scope of this study.

The time interval between 80ka and 60ka is characterised by particularly low density of datapoints (especially between 70ka and 60ka), which results in substantial uncertainty and leaves room for unaccounted variability in the water table history. This higher level of uncertainty is reflected in the relatively broad extent of the light grey shading around the peak at ca 70 ka.

2) I apologize for vague reference to a Li et al. reference to Owens lake, I meant to refer the authors to Li et al. 2004 https://doi.org/10.1016/S0277-3791(03)00215-4

I see that both my comments and the other reviewer referred the authors to the Lowenstein et al. 2024 paper. I think this is sufficient. Lowenstein plots the Owens data from the various papers and USGS reports in their figures 2 and 5, and it's pretty coherent with Death Valley.

We thank the reviewer for the clarification of the reference, and we understand there are no changes suggested with this comment.

I look forward to seeing this work appear in QSR, congratulations.

We are very thankful for the time spend by the reviewer #1 to improve our work!

Reviewer #2:

Reviewer #2: The authors have adequately responded to my comments. I have a couple of small suggestions/corrections, and one strong request related to data availability.

-when discussing anti-phased responses in the northern vs. southern Great Basin (e.g. lines 351, 433-435), it might help to replace "northern" with "northwestern". The lakes and cave records that show the anti-phased response are in the NW, while Bonneville in the northeast Great Basin appears to be in phase with the southern lakes. When stated this way, I don't think this finding is controversial.

We have changed “northern” to “northwestern” in four places:

Line 60 & 449: “Studies from the northwestern Great Basin suggest dry conditions during H5 to H2 (Oster et al., 2020; Benson et al., 2003; Zic et al., 2002; Heaton et al., 2019).”

Line 350: “This anti-phased relationship is consistent with the proposed dipole pattern between northwestern and southern Great Basin during the interval leading into the early phase of H1 (Hudson et al., 2019).”

Line 433: “Within the Great Basin, there is, although debated, evidence of increased aridity in the northwest (Oster et al., 2020; Benson et al., 2003; Zic et al., 2002; Heaton et al., 2019) and pluvial conditions in the south (Munroe and Laabs, 2013; McGee et al., 2018; Oster et al., 2023) associated with…”

-line 334: change to "MIS 5d and MIS 5c" to start with the older interval

Changed it as suggested.

-line 349: replace comma with a decimal point in "21,76"

Changed it as suggested.

Data availability: dating results and elevations should be archived at a permanent online repository (e.g. NOAA Paleoclimate database), not just provided in the supplementary material.

Just after the submission of the last revision, our data has been made available online at Pangaea:

https://doi.org/10.1594/PANGAEA.988350

We have added this to the manuscript now.

We are very grateful for the efforts of reviewer #2 (David McGee) to help us improving our manuscript!

HIGHLIGHTS

- *Hydroclimate of SW USA linked to ice volume changes during MIS 5.*
- *A dry climate prevailed in the SW USA between 104.3±0.3 ka and 97.5±0.3 ka (MIS 5c).*
- *Heinrich events of the last 60 ka were associated with regional wet conditions.*

Declaration of Interest Statement

☒ The authors declare that they have no known competing financial interests or personal relationships that could have appeared to influence the work reported in this paper.

☐ The author is an Editorial Board Member/Editor-in-Chief/Associate Editor/Guest Editor for this journal and was not involved in the editorial review or the decision to publish this article.

☐ The authors declare the following financial interests/personal relationships which may be considered as potential competing interests:

AUTHOR CONTRIBUTIONS

Conceptualization: CS, KAW, SDS; Data curation: SDS; Formal analysis: SDS; Funding acquisition: CS, KAW, RLE; Investigation: CS, YD, SDS; Methodology: MR, KAW, SDS; Project administration: CS, YD; Resources: CS, RLE, MR; Supervision: CS, YD, RLE Visualization: SDS; Roles/Writing - original draft: SDS; Writing - review & editing: SDS, YD, KAW, MR, GEM, RLE, CS.

Timing and amplitude of hydroclimate changes during the last glacial cycle in southwestern North America

Simon D. Steidle[1], Yuri Dublyansky[1], Marco Roman[2], Gina E. Moseley[1], Kathleen A. Wendt[3], R. Lawrence Edwards[4], Christoph Spötl[1]

[1] *Institute of Geology, University of Innsbruck, Innrain 52, 6020 Innsbruck, Austria*

[2]*Department of Environmental Sciences, Informatics and Statistics, University Ca' Foscari of Venice, Via Torino 155, Venice Mestre, Italy*

[3]*College of Earth, Ocean, and Atmospheric Sciences, Oregon State University, 101 SW 26th Street, Corvallis, Oregon 97330*

[4]*School of Earth and Environmental Sciences, University of Minnesota, 116 Church Street SE, Minneapolis, MN 55455-0149, USA*

ABSTRACT

The presently (semi)arid southwestern North America experienced major shifts in hydroclimate during the Quaternary characterized by oscillations between pluvial and arid phases. On orbital timescales, regional moisture availability is attributed to latitudinal shifts of moisture-bearing storm tracks due to the expansion and retreat of North American ice sheets. Millennial-scale variability is superimposed on top of the broader glacial pluvial phases. Groundwater fluctuations recorded by calcite deposits in Devils Hole, Nevada, offer unique insights into the past hydroclimate of the southwestern USA covering both time scales. Here, we increase the resolution of the Devils Hole water table record with an additional 43 water-table markers covering the last interglacial-glacial cycle. The updated record of water-table changes enables a comparison with sea-level records between 120,000 to 70,000 years ago, revealing concurrent changes in both during this period. This strengthens the hypothesis that orbital-scale water-table changes are closely linked to ice-sheet expansion during Marine Isotope Stage 5. New water table markers of the last 60,000 years further support increased pluvial conditions during Heinrich events.

HIGHLIGHTS

Hydroclimate of SW USA linked to ice volume changes during MIS 5.
A dry climate prevailed in the SW USA between 104.3±0.3 ka and 97.5±0.3 ka (MIS 5c).
Heinrich events of the last 60 ka were associated with regional wet conditions.

KEYWORDS

Quaternary, paleoclimatology, North America, speleothems, U-Th series, Devils Hole, hydroclimate

1. INTRODUCTION

The endorheic Great Basin, which spans large portions of the arid southwestern USA, has experienced repeated periods of wetter and cooler climates during the Quaternary (e.g., Reheis et al., 2019; Wendt et al., 2018; Santi et al., 2020; Seltzer et al., 2019). Past pluvial periods have been attributed to an interplay of different forcing mechanisms operating on orbital to millennial timescales. For orbital timescales (i.e., a periodicity of ≥20 ka), the hydroclimate responded to the growth and decay of the North American ice sheets (Cheng et al., 2019; Lachniet et al., 2017) due to high-pressure systems positioned over these ice sheets that had a major role in steering Pacific moisture into the SW region of the USA during winter (Oster et al., 2015). This resulted in a lag of the SW USA hydroclimate response relative to Northern Hemisphere summer insolation of 3,000 to 5,000 years (Lachniet et al., 2017).

Heinrich (H) events (Hemming, 2004) were periodic millennial-scale events during the last glacial period, characterized by massive iceberg discharges into the North Atlantic, leading to widespread oceanographic and climatic impacts on a global scale. They occurred on shorter timescales than ice sheet growth and decay and are therefore linked to a different mechanism. In the southern Great Basin, the response to H events is well documented through evidence of enhanced pluvial conditions (Hudson et al., 2019; Ibarra et al., 2014; Munroe and Laabs, 2013; McGee et al., 2018; Oster et al., 2023). This phenomenon is hypothesized to result from cooling in the Northern Hemisphere that led to a southward shift of the Intertropical Convergence Zone and Hadley cell, a southeastward displacement of the Aleutian Low, and an intensification of the subtropical jet (McGee et al., 2018). These atmospheric changes collectively enhanced atmospheric river transport, bringing increased subtropical moisture into the western United States (McGee et al., 2018). Studies from the northwestern Great Basin suggest dry conditions during H5 to H2 (Oster et al., 2020; Benson et al., 2003; Zic et al., 2002; Heaton et al., 2019). The boundary between drier and wetter conditions in the North and South Great Basin, respectively, was temporally and spatially transgressive throughout the duration of a H Event (Oster et al., 2020).

This study focuses on the southern Great Basin, where calcite precipitated from groundwater in Devils Hole 2 (cave) provides a record of past still-stands and fluctuations in water table elevation. By analyzing these deposits, this research enhances the understanding of long-term hydroclimate variability and its driving mechanisms over time. Within the cave, two distinct types of calcite can be observed that formed simultaneously on the walls, each recording different aspects of the groundwater conditions. The first type, folia, forms at the water-air interface, while the second type, mammillary calcite, precipitates subaqueously. Transitions from mammillary calcite to folia at a given elevation therefore occurred during periods of water table decline, whereas rising water tables led to folia being overgrown by mammillary calcite. Water-table research at the study site was pioneered by Szabo et al. (1994), who established a record of the last 100 ka. This record was extended by Wendt et al. (2018) for the last 350 ka and more recently extended further back to 750 ka (Steidle et al. 2024). It has been shown that this long and continuous archive formed under constant temperature conditions (Kluge et al., 2014; Bajnai et al., 2021), minimal variation in growth rate (Li et al., 2021), and no significant influence from tectonic activity (Wendt et al., 2018) over the last three glacial-interglacial cycles. This record therefore provides a unique opportunity to investigate the water table's response to different climate events across different timescales throughout the last glacial period. Mammillary calcite has been dated in previous studies using a variety of U-series techniques (Winograd et al., 1988,

1992; Moseley et al., 2016; Wendt et al. 2018; Li et al., 2021). These studies have primarily focused on events lasting more than 5 ka, leaving shorter-term changes less well resolved. The aim of this study is therefore to enhance the resolution of the water-table record for the last glacial cycle and improve our understanding of the forcing mechanisms driving the regional hydroclimate on orbital and millennial timescales. Since the water-table history at Devils Hole is linked to the recharge of the regional aquifer (Jackson et al., 2023), understanding the impact of millennial-scale climate events on water availability is critical for balancing socio-economic needs and conservation efforts – both in the wider Great Basin region and at Devils Hole itself – amid future climate change (Deacon et al., 1991; Deacon et al., 2007; MacDonald, 2010).

2. REGIONAL SETTING AND CALCITE DEPOSITION

The Ash Meadows groundwater basin is a sub-basin of the Great Basin. At present, about 80% of the Ash Meadows recharge originates from snowmelt in the Spring Mountains and Sheep Range (Winograd et al., 1998; Halford and Jackson, 2020). The modern recharge of the Ash Meadows groundwater basin is 2.59×10^7 m^3/yr, with approximately 90% reaching the surface at the Ash Meadows discharge area – located downstream and near Devils Hole – where it subsequently evaporates (Halford and Jackson, 2020).

The calcite samples of this study originate from Devils Hole #2, a sub-vertical tectonic fracture intersecting the groundwater table of the Ash Meadows groundwater basin at 36.416°N, 116.283°W. Mammillary calcite, which forms under subaqueous conditions, is dense, translucent, and slow-growing. It has few impurities and can be reliably dated (Moseley et al., 2016). Dating a calcite layer at a specific elevation in the cave provides unambiguous evidence that the groundwater table was above that level at a given time. Folia, on the other hand, are porous, white, and form at higher rates at the water-air interface. Folia cannot be reliably dated using U-series techniques due to its open-system behavior. The presence of folia within a sequence, where they overlie mammillary calcite (indicating the folia are younger), signifies an episode of water table decline. Conversely, when mammillary calcite forms on top of folia (indicating the mammillary calcite is younger), it reflects a rise in the water table. Thin layers of mammillary calcite represent brief rises in the water table above a given elevation. In the absence of folia, mammillary calcite samples indicate submergence but do not offer further insights into water-table fluctuations. Together, mammillary calcite and folia represent two endmembers of a spectrum of calcite deposits (see Supplemental Material; Steidle et al. 2024).

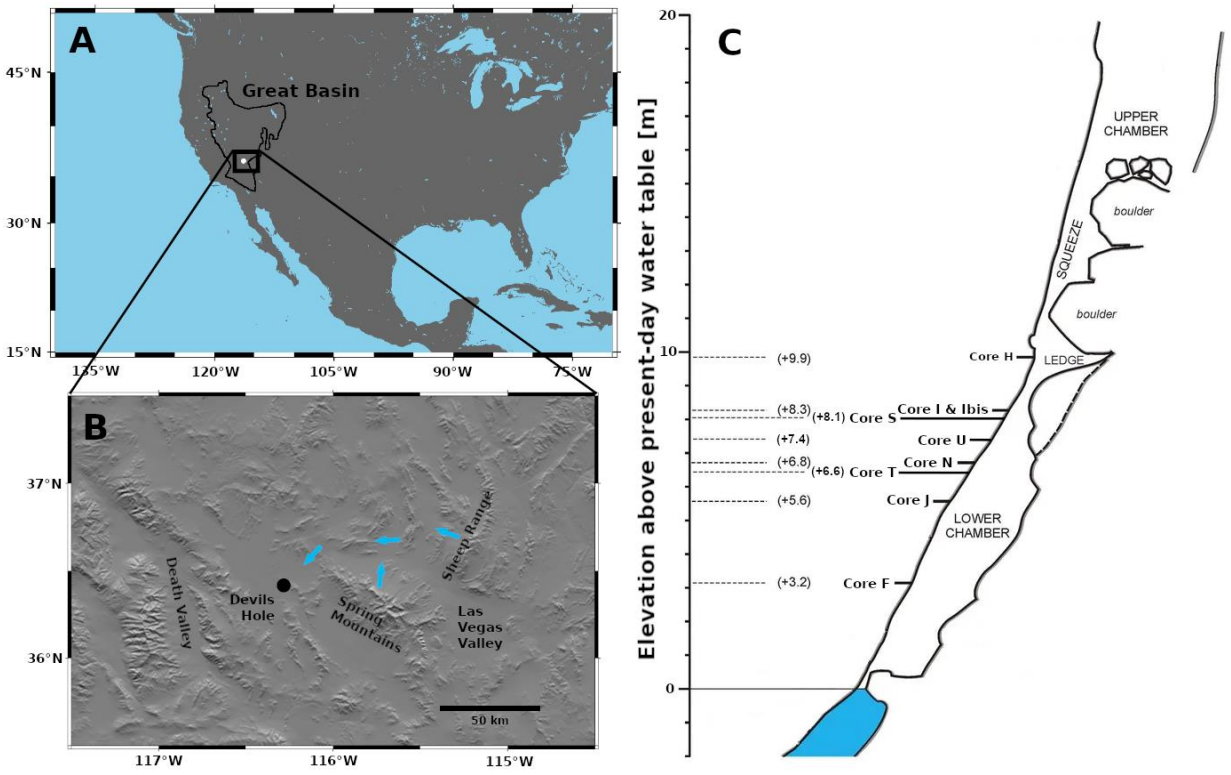

Fig. 1. *Study region and sampling positions. A: Overview map of North America and the Great Basin B: Shaded relief map of the area around Devils Hole showing major recharge areas of the regional aquifer, including the Spring Mountains and Sheep Range. Blue arrows indicate the main directions of groundwater flow. C: Simplified transect of Devils Hole #2 with the elevations of horizontally drilled cores examined in this study.*

3. METHODS

In this study, nine cores (2.5 cm diameter and 0.5-1.3 m in length) were horizontally drilled into the calcite deposits of the hanging wall in Devils Hole #2, at elevations ranging from +3.2 m to +9.9 m relative to the modern water table (Fig. S2). The cores were halved, polished, and 53 subsamples (5 to 30 mg) were prepared using a diamond burr-tipped dental drill under a clean laminar flow hood for U-Th dating. Furthermore, to further validate the chronology derived from thin calcite layers, the trace element composition of well-developed mammillary calcite and folia was analyzed. The trace element composition of all thin calcite layers dated to <60 ka was compared to that of well-developed mammillary calcite and folia to confirm their subaqueous formation as mammillary calcite.

Mammillary calcite has been shown to grow very slowly at an average rate of 0.9±0.3 mm/ka (Li et al., 2021). Due to the complex three-dimensional structure of the mammillary calcite and folia sequences, the drill bit size, and the sample quantity required for dating, the sampling resolution was limited to 1–2 mm. As a result, the dated calcite samples represent intervals of submergence exceeding 1 ka. The boundary between mammillary calcite and folia marks a rise or fall in the water table; however, only the mammillary calcite immediately above or below this boundary can be dated, not the boundary itself. Consequently, the recorded ages of water-table rises are systematically too young, while those of water-table falls are systematically too old by up to 1-2 ka. Unlike Wendt et al. (2018), extrapolation to the actual boundary was not possible in this study due to the sampled layers being too thin for multiple measurements.

The dating was performed at the Trace Metal Isotope Geochemistry Laboratory of the University of Minnesota, USA, following the chemical procedure of Edwards et al. (1987) and Shen et al. (2002, 2012) and the analytical procedures of Shen et al. (2012) and Cheng et al. (2013). In summary, samples were digested in HNO_3 and spiked with a mixed ^{236}U-^{233}U-^{229}Th spike. Spiked samples were co-precipitated with Fe, centrifuged, loaded onto anion exchange columns and separated and purified for uranium and thorium. Separate aliquots of uranium and thorium were measured on a multi-collector inductively coupled plasma mass spectrometer (Thermo Neptune Plus) via a secondary electron multiplier using a peak-jumping mode. Ages were calculated using the ^{230}Th and ^{234}U half-lives of Cheng et al. (2013). Chemical blanks were measured with each set of 12 samples and were found to be negligible (<30 ag ^{230}Th, <120 ag ^{234}U, <150 fg ^{232}Th, <1 pg ^{238}U). All ages are relative to the year 1950 common era (CE) and all uncertainties are reported at 2σ level where typical age uncertainties are on the order of 2-6 ‰.

Trace elements were measured by laser ablation inductively coupled plasma mass spectrometry (LA-ICP-MS) at the University of Venice using an excimer laser at 193 nm (Analyte Excite, Teledyne CETAC Photon Machines) coupled to a single quadrupole MS (iCAP-RQ, Thermo Scientific). Line scans parallel to the calcite growth direction were performed covering all sampled layers with ages younger than 60 ka. Laser fluence was set to 2 J/cm^2; pre-ablation was performed with a 85 µm square spot size at 80 Hz repetition rate and a fixed dosage of 20, whereas the ablation was performed with a 40 µm square spot size, 80 Hz repetition rate, and a fixed dosage of 10, resulting in a scan speed of 320 µm/s. Aerosol transfer was achieved using peek tubing and glass adapter (Glass Expansion) leading to a washout time of about 125 ms. Elemental 2D maps were recorded on a section of core H (+9.9 m) that shows a clear transition from folia to mammillary calcite and back to folia (Fig. 2). Laser fluence was set to 3 J/cm^2; pre-ablation was performed with a 150 µm square spot size at 6 Hz and a fixed dosage of 1, whereas the ablation was performed with a 20 µm square spot size, 300 Hz repetition rate and a fixed dosage of 6 resulting in a scan speed of 1000 µm/s. Aerosol transfer was achieved using peek tubing and ARIS adapter (Teledyne CETAC), leading to a washout time of about 30 ms. For both line scans and 2D maps, the ICP-MS acquisition included the elements (m/z) Mg (25), Ca (43), Sr (88) and Ba (137). Dwell times were adjusted to match the washout duration while being inversely proportional to the estimated average signal intensity of each element. This setup is designed to ensure synchronization between the LA and ICP-MS, thereby preventing artifacts such as aliasing in spatial analysis, as reported by vanElteren et al. (2019). Both line scans and 2D maps were quantitatively calibrated using the speleothem certified material SPLT-NP (µStandards) and quality checked (i.e. sensitivity drift correction) with the glass standard reference material NIST612 (National Institute of Standards and Technology). Raw signals were processed using the software HDIP (Teledyne CETAC), specifically by applying background (gas blank) correction, drift correction, possible outlier removal (to the SPLT-NP and NIST612 standards only, based on a 5 SD criterion) and normalization to the Ca signal to obtain molar ratios.

4. RESULTS

4.1 Trace element analysis of Devils Hole calcite

2D trace element maps were measured across a folia-to-mammillary calcite-to-folia transect (Fig. 2). Three distinct types of calcite were identified based on the trace element signatures. One of them characterizes folia and has low Mg/Ca, Sr/Ca and Ba/Ca ratios, with a relatively high standard deviation (Table S1). Mammillary calcite shows two types. Both have high Mg/Ca ratios, but one of them (referred to as "low concentration mammillary calcite" or "Mamm-l" in the following) has Sr/Ca and Ba/Ca ratios similar to folia, while the other (referred to as "high concentration mammillary calcite" or "Mamm-h" in the following) has 4x higher Sr/Ca and about 9x higher Ba/Ca ratios (Table S1).
Areas marked with the suffix "(d)" in Fig. 2 were used to define thresholds to distinguish these three types (Fig. 3). For Mg/Ca, a threshold of 15 mmol/mol was defined to distinguish folia from both mammillary calcite types. Thresholds of 0.6 mmol/mol for Sr/Ca and 0.025 for Ba/Ca distinguish high-concentration from low-concentration mammillary calcite.
These high-concentration mammillary calcite sections are not distinguishable petrographically from the low-concentration mammillary calcite sections. The high-concentration mammillary calcite is interpreted to be reliably datable because it is a subaqueous deposition. It is hypothesized to have formed within a few tens of centimetres of the water-air interface. These thresholds were validated (Fig. 4) in a different folia-to-mammillary calcite transition (areas marked by the suffix "(v)" in Fig. 2) showing similar trace element signatures (Table S1).

The trace element composition of 27 layers formed after 60 ka BP was analyzed and compared to folia and mammillary calcite thresholds (Fig. 5). 25 layers were associated with mammillary calcite due to their high Mg/Ca ratios. 20 of those 25 layers show the same Sr/Ca and Ba/Ca signature as high-concentration mammillary calcite. One sample (SS173) has a higher Ba/Ca ratio but lower Sr/Ca ratio. Two samples (SS17 and SS18) were associated with folia due to their low Mg/Ca ratio (Table S2) and consequently removed from the dataset.

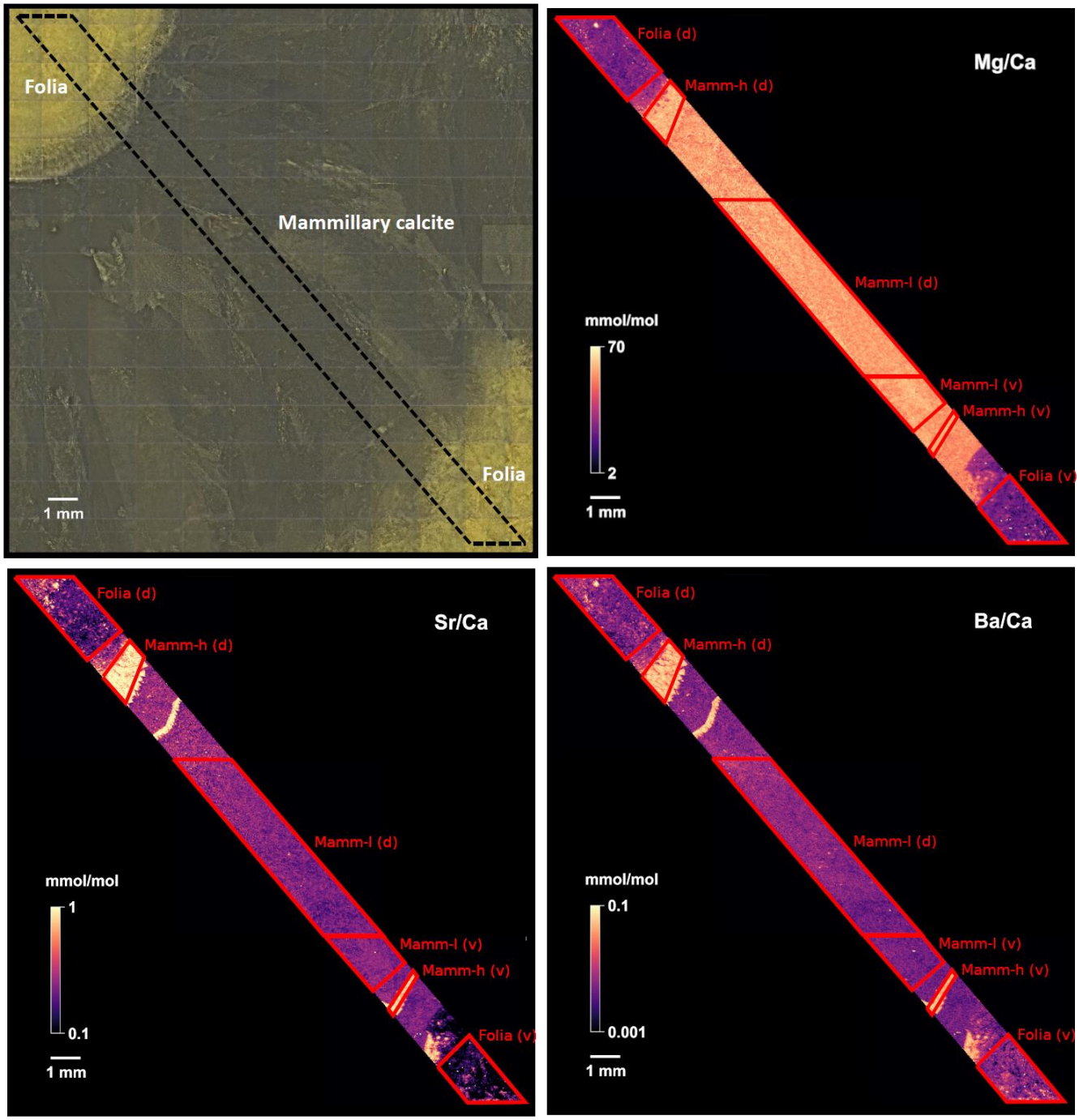

Fig. 2. *Reflected-light image of the analyzed folia – mammillary calcite – folia transition (upper left) and trace element ratios (Mg/Ca upper right, Sr/Ca lower left, Ba/Ca lower right). Regions associated with folia, mammillary calcite showing high trace element concentrations (Mamm-h) and mammillary calcite showing low trace element concentrations (Mamm-l) are highlighted respectively. Regions used to define the thresholds (Fig. 3) are labelled "(d)", regions used to validate the thresholds (Fig. 4) are labelled "(v)".*

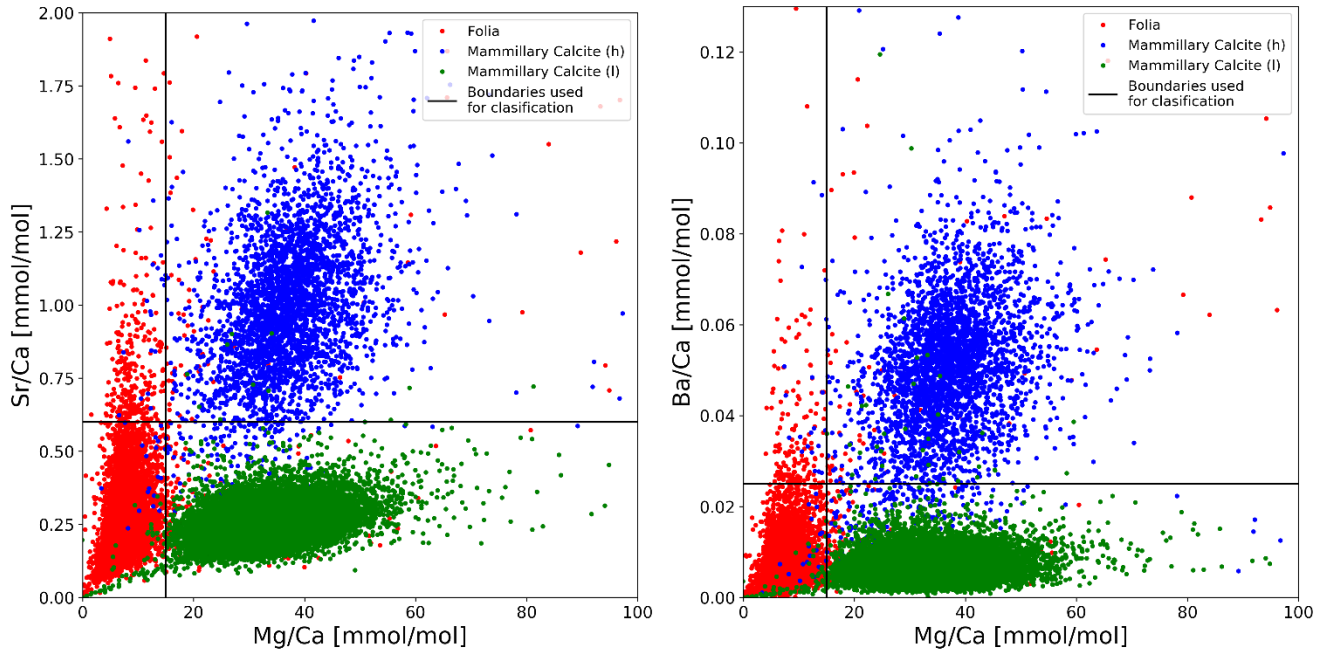

Fig. 3. *Trace element composition of folia and mammillary calcite used for defining typical ranges (labelled "(d)" in Fig. 2). Black lines are at 15 mmol/mol for Mg/Ca, 0.6 mmol/mol for Sr/Ca and 0.025 for Ba/Ca.*

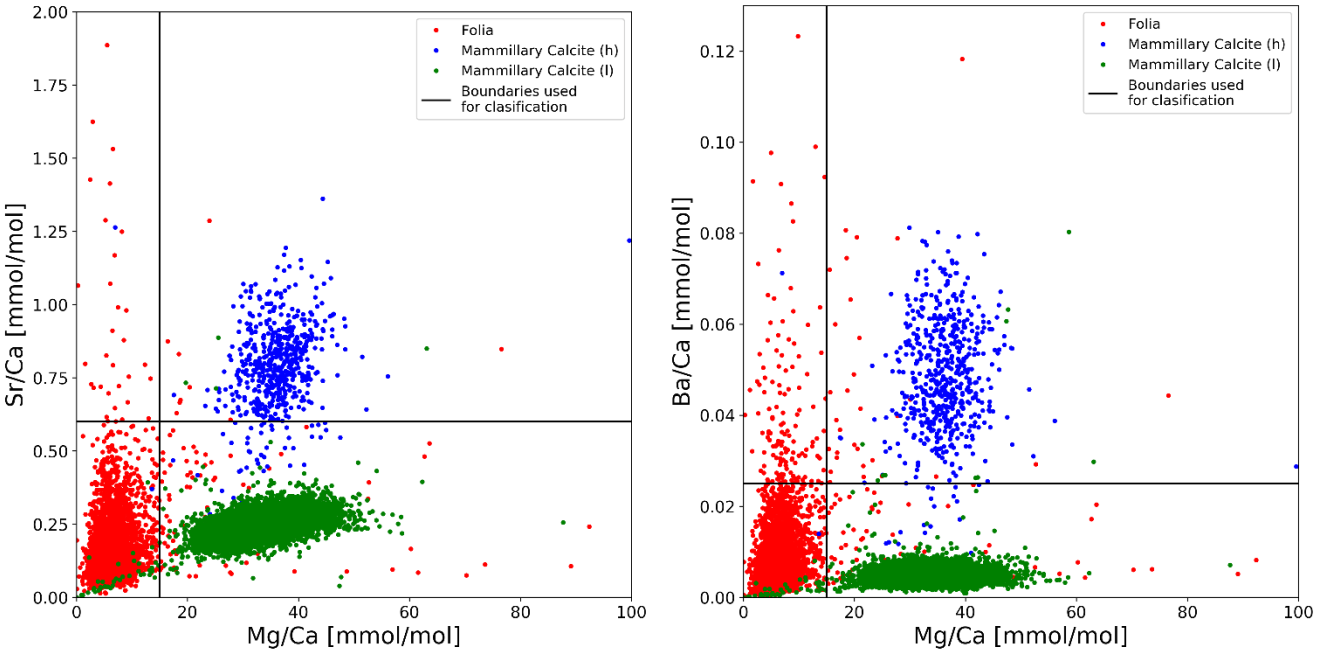

Fig. 4. *Trace element composition of folia and mammillary calcite in the areas used to verify the thresholds based on Fig. 3. Black lines as defined in Fig. 3.*

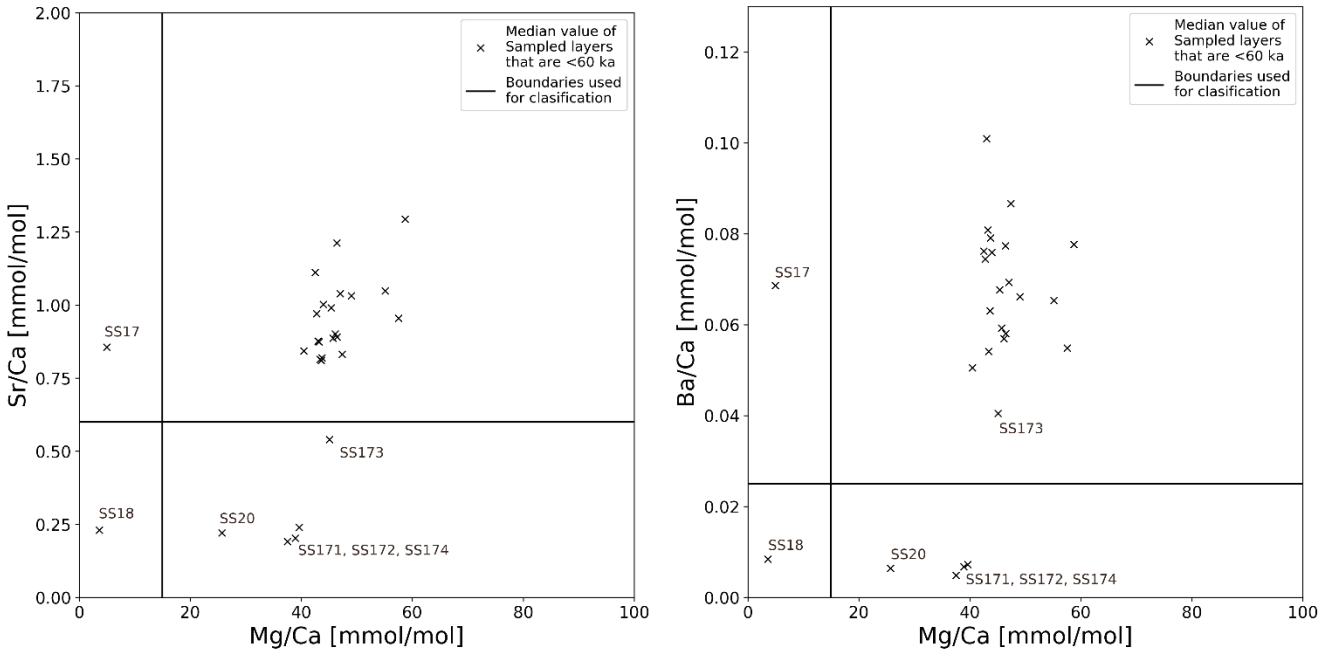

Fig. 5. *Trace element composition 27 layers younger than 60 ka. Black lines as defined in Fig. 3. Samples SS17 and SS18 were omitted due to their low Mg/Ca ratios as seen in folia which is not datable with U-series techniques. All other samples were classified as mammillary calcite.*

4.2 Construction of new water-table markers

Of the dated 53 samples, eight were omitted because their $\delta^{234}U_{initial}$ values deviate from the narrow range defined by Wendt et al. (2018), Li et al. (2021), and data from this study (see Supplementary Material for detailed information on outlier removal based on $\delta^{234}U_{initial}$). Folia were found to be associated with low trace element ratios (<15 mmol/mol of Mg/Ca, <0.6 mmol/mol of Sr/Ca, <0.025 mmol/mol of Ba/Ca). On the other hand, mammillary calcite exhibits two distinct trace element signatures, one of which – characterized by elevated trace element ratios – occurs near folia boundaries and is hypothesized to result from growth close to the water-air interface while still forming subaqueously (see section 4.1). Both signatures of mammillary calcite, however, have elevated Mg/Ca ratios (>15 mmol/mol), which was used as the main criterion to distinguish folia and mammillary calcite. Of the 27 investigated layers dated to be less than 60 ka, 25 were identified as mammillary calcite based on the trace element composition, while two were omitted because they partly consisted of folia (see Fig. 5).

4.3 Description of the refined water-table record

This study presents 43 new, reliable, high-precision U-Th ages from elevations between +3.2 m and +9.9 m relative to today's water table (Fig. 1C). These results are shown in Fig. 6 alongside water table markers from previous studies (Wendt et al., 2018; Szabo et al., 1994) and made available in a data repository (Steidle et al., 2026). Moseley et al. (2016) demonstrated that the water table remained continuously above +1.8 m between 116.1±0.4 ka and 4.89±0.05 ka. Two new data points from the highest-sampled elevation indicate that the water table exceeded +9.9 m

at least twice during the last glacial period, at 89.1±0.2 ka and 71.3±0.2 ka. The last glacial water table, however, was generally high and may have reached similar elevations at other times within this interval, as mammillary calcite deposits represent minimum water-table elevations. An additional 41 water table markers from this study dated to between 112.0±0.4 and 17.26±0.08 ka and from elevations of +3.2 m to +8.3 m improve the resolution of short-term water table variability during the last glacial period.

Following the last interglacial water-table lowstand, that dropped below 0 m after 120.4±0.5 ka (Wendt et al., 2018) and remained below +0.8 m between 117.5±0.5 ka and 116.2±0.3 ka and below +1.8 m between 121.4±0.4 ka and 116.1±0.4 ka (Moseley et al., 2016), the water table rose during the glacial inception, reaching a highstand of over +8.3 m around 105.6±0.4 ka. The subsequent water-table decline reached a lowstand less than +3.2 m but greater than +1.8 m between 104.3±0.3 ka and 97.5±0.3 ka during MIS 5c. However, the alternation between folia and mammillary calcite in core F (Fig. S2, between samples SS10 and SS14) indicates that the water table was unstable, oscillating above and below +3.2 m multiple times during this period. One such rise was dated to 98.4±0.3 ka. Dating the other oscillations was not feasible because the mammillary calcite layers were too thin to be sampled reliably without contamination from folia. The distinctive alternation of folia and mammillary calcite at +3.2 m during MIS 5c suggests that the water table did not drop significantly lower. This interpretation is supported by continuous mammillary calcite deposition at +1.8 m during this period (Moseley et al., 2016; Li et al., 2021; Fig. 6). The MIS 5b highstand, exceeding +9.9 m, was reached at 89.1±0.2 ka (MIS 5b). As previously mentioned, this represents one of the highest-known water tables of the entire last glacial period.

Interpreting the record between c.85 ka and 60 ka is challenging. Wendt et al. (2018) indicated submergence above +4.6 m after 79.5±0.3 ka, which is followed by a continuous, c. 2 cm-thick mammillary calcite layer without apparent hiatuses. This continuous mammillary calcite layer suggests that submergence at +4.6 m lasted for 18±6 ka (based on a growth rate of 0.9±0.3 ka; Li et al. 2021). In contrast, results from a lower core suggest that the water table dropped below +3.2 m between 78.9±0.4 ka and 74.4±0.4 ka (MIS 5a – Wendt et al., 2018). The lack of folia deposition at +4.6 during this time may be the result of a water table drop that was too rapid to form a layer of folia.

Following MIS 5a, the MIS 4 highstand peaked at 71.3±0.2 ka at +9.9 m before dropping below +7.4 m by 69.1±0.8 ka. A mammillary calcite layer at +8.1 m, dated to 57.1±0.3 ka to 56.0±0.2 ka, is present within an interval of short-lived rises documented in the core at +8.3 m between 57.3±0.2 ka and 53.9±0.1 ka. This suggests that the water table in Devils Hole oscillated around +8.3 m on centennial time scales during this period. Two markers at +6.6 m during MIS 3, dated to 53.3±0.3 ka and 52.9±0.3 ka, suggest a slight lowering of the water table before it rebounded to a series of highstands above +8.3 m between 48.9±0.2 ka and 44.2±0.1 ka. During the remainder of MIS 3, a mammillary calcite layer at +6.6 m, dated to 40.8±0.3 ka, aligns with a highstand exceeding +9 m, as documented by Szabo et al. (1994). As the last glacial maximum approached, the water table oscillated around +8.3 m between 23.84±0.05 ka and 17.26±0.08 ka, before gradually declining to its present elevation.

5. DISCUSSION

5.1 Limitations

In Devils Hole, mammillary calcite sampled from depth and dated using the U-Th method has yielded inaccurate ages for glacial terminations that are systematically too old (Moseley et al., 2016). This age offset is hypothesized to be caused by an increase in excess ^{230}Th with depth in the water column, which specifically affects glacial terminations due to a change in sedimentation (Moseley et al., 2016). Moseley et al. (2016) observed that mamillary calcite deposited in shallow waters appeared to be unaffected by the age offset, and therefore represented the most accurate chronology at glacial terminations. The age offsets caused by increasing excess ^{230}Th at depth during glacial termination are thus not of relevance to this study given that: (1) the investigated time period is the last glacial period (and not a glacial termination), for which Moseley et al. (2016) produced reproducible chronologies from cores of different depths, and; (2) the samples dated in this study are largely from mamillary-folia boundaries indicating shallow water depths. Based on these two lines of argument, we consider the chronology presented here to be accurate within the stated precision. Still, since these are relatively young samples and it cannot be ruled out that the water table stood several meters higher during their formation, it must be noted that this represents a difficult-to-quantify uncertainty that could shift the true age of the samples to somewhat younger than reported here in particular during the intermediately glaciated phase of MIS 5 which was not analyzed by Moseley et al. (2016).

While all lowstands of the water table remained above +1.8 m (Moseley et al., 2016), highstands are not constrained, and the elevations discussed represent minimum estimates. Despite actively searching for mammillary calcite above +9.9 m, none was found from the last 120 ka. However, no conclusions can be drawn from this absence, as condensation corrosion – known to have occurred in the higher parts of Devils Hole (Dublyansky and Spötl, 2015) – may have removed calcite from the cave walls. It is therefore entirely plausible that mammillary calcite once existed at higher elevations. Consequently, the peak water table highstands discussed may have been significantly higher than the stated elevations. Condensation corrosion is not expected to have affected any of the mammillary calcite analyzed in this study. However, it is possible that some calcite deposits were lost due to physical processes, such as detachment from the wall under their own weight or later depositions. A scarcity of mammillary calcite as seen around 45 ka to 25 ka is a possible result of this process.

5.2 Comparison with regional surface lakes

Regional surface lakes (Lowenstein et al., 2024) indicate a step-like transition from very arid conditions during MIS 5e, to arid conditions during MIS 5d and MIS 5c, followed by a shift to more humid conditions in MIS 5b and 5a. Brief rises above +6.8 m around 108.2±0.4 ka and above +8.3 m around 105.6±0.4 ka documented in this study provide evidence for significantly higher Devils Hole water table fluctuations during MIS 5 than previously recognized (Wendt et al., 2018; Lowenstein et al., 2024). The updated Devils Hole water table record indicates orbital-scale changes in MIS 5, which are not captured by deposits in surface lakes.

A comparison of sub-orbital variability is complicated by multi-millennial age uncertainties inherent in lake-level reconstructions and by the discontinuous nature of the Devils Hole water table record, which consists of individual snapshots rather than a continuous series. Even so, there are no apparent discrepancies between individual Devils Hole water-table events and

regional surface-lake records from the southern Great Basin and farther south on sub-orbital timescales during the last glacial cycle (Hudson et al., 2023; Lowenstein et al., 2024; Reheis et al., 2015).

A comparison with the lake Chewaucan record from the northern Great Basin shows that brief rises in the Devils Hole water table above +8.3 m around 17.26±0.08 ka, 19.4±0.3 ka and 21.76±0.07 ka occurred during Chewaucan lowstands that were separated by well-defined highstands. This anti-phased relationship is consistent with the proposed dipole pattern between northwestern and southern Great Basin during the interval leading into the early phase of H1 (Hudson et al., 2019).

5.3 Orbital-scale forcing

Given that the pluvial conditions in the Great Basin during glacial periods have been attributed to atmospheric reorganization driven by the extent of the North American ice sheets (Oster et al., 2015), changes in the Devils Hole water table are expected to correspond to the expansion and retreat of these ice sheets. Precisely dating the extent of North American ice sheets during MIS 5 remains challenging (Dalton et al., 2022). Although sea level reflects an integrated signal of the extent of global glaciation, it can be assumed that the timing of sea-level changes and North American ice sheet extent was strongly correlated (Lambeck and Chappell, 2001). Thus, precisely dated sea-level markers can be used to test the hypothesis that changes of the Devils Hole water table and ice sheet extent were near-synchronous. Simultaneous variations of Devils Hole water table and global sea level are apparent during MIS 5 (Fig. 6B). The water table lowstand associated with MIS 5c is the most well-constrained event in the refined record and was therefore compared to the timing of the MIS 5c sea-level highstand. A speleothem-based sea-level highstand in the Caribbean, documented from 103.9±0.6 ka to 96.8±0.4 ka (Steidle et al., 2021), aligns with other sea-level records that are less precisely dated (Wainer et al., 2017; Potter et al., 2004; Lundberg and Ford, 1994). There is very good agreement with the MIS 5c Devils Hole water-table lowstand between 104.3±0.3 ka and 97.5±0.3 ka, supporting a common link to ice-sheet extent.

The Devils Hole water table high- and lowstands followed the mid-July 65°N insolation with a delay of a few millennia during MIS 5 (i.e., from 120 ka to about 70 ka; Fig. 6A). Such a delayed response of the Great Basin hydroclimate agrees with other studies. Lachniet et al. (2017) found an average lag of 3240 years (-900 to 6600-year) in Great-Basin-stalagmite $\delta^{18}O$ data relative to Northern Hemisphere summer insolation, whereas Cheng et al. (2019) reported a ~5000-year lag in a similar study on the eastern side of North America. The delay is also apparent when comparing the MIS 5 Devils Hole water table to the Asian monsoon, which displays a strong response to precessional forcing on orbital timescales (Fig. 6C; Cheng et al., 2016). These delays result from the long response time of the North American ice sheets to insolation changes.

MIS 4 and MIS 2 were periods of low global sea level (Spratt and Lisiecki, 2016; Fig. 6B) and extensive North American glaciation (Dalton et al., 2022). In agreement with the mechanism described by Oster et al. (2015), Devils Hole water table was high during both of these stages (in excess of +8.3 m after 23.84±0.05 ka at MIS 2 and in excess of +9.9 m around 71.3±0.2 ka). While synchronous variations between the Devils Hole water table and sea level are evident during MIS 5 and across the MIS 1/2 transition, no such correspondence is observed during MIS 4. Between approximately 60 ka and 30 ka, sea level remained relatively low and stable.

Consequently, the North American ice sheets are likely present throughout this period, although a slight decrease in their extent around 40 ka has been documented (Dalton et al., 2022). The relationship between ice extent and additional moisture in the Great Basin is unlikely to be linear. Moreover, it remains unclear whether thresholds for moisture control exist and at what glacial extent they may occur. However, water table changes at Devils Hole recorded between 60 ka and 30 ka show no apparent correlation with sea level or North American ice sheet extent. This suggests MIS 4 and MIS 3 were influenced by a different forcing mechanism operating on shorter timescales, in contrast to MIS 5, where the dominant forcing mechanism appears to be linked to orbital variability.

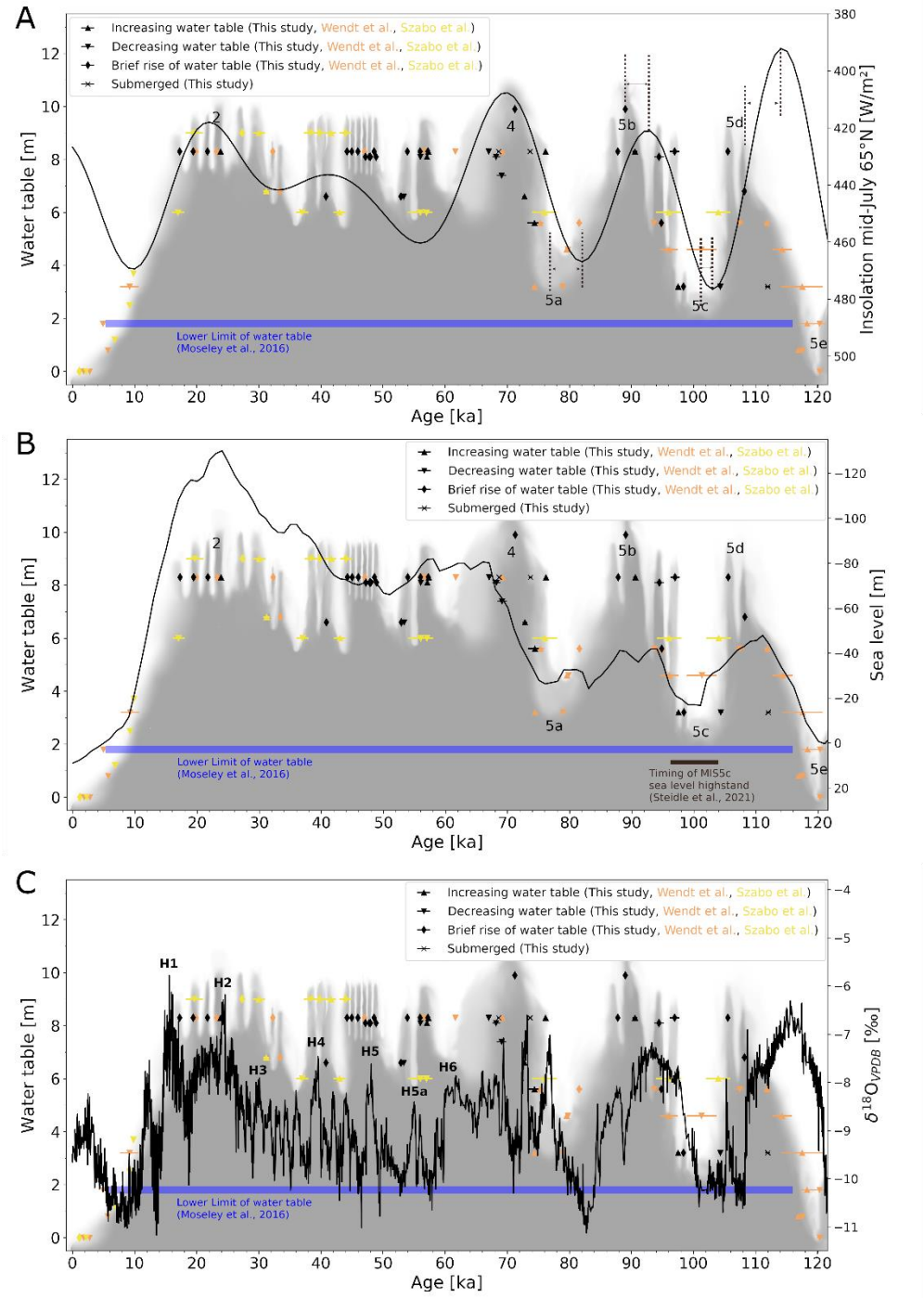

Fig. 6. *Devils Hole water table and insolation, sea level and Asian monsoon. Water table elevation relative to today's water table over the last glacial cycle. The grey shading is a visual aid to distinguish high probability of submergence (dark grey), high probability of no submergence (white), and intermediate probability (shades of gray). This is based on the data from three studies (Szabo et al., 1994; Moseley et al., 2016; Wendt et al., 2018; this study). The lower limit of water table during the last glacial cycle is defined by continuous mammillary calcite deposition (Moseley et al., 2016). The letters 2, 4 and 5a to 5e mark the timing of Marine Isotope Stages 2, 4 and 5a to 5e, which were associated with water table high- and lowstands in Devils Hole.* ***A:*** *Mid-July insolation at 65°N shown by the black curve (Berger, 1999). Dashed lines separated by arrows indicate the multi-millennial delay of water table low- and highstand with respect to insolation.* ***B:*** *Global sea level (Spratt and Lisiecki, 2016; note inverted Y axis). Black bar shows the timing of the MIS 5c Caribbean sea-level highstand (Steidle et al., 2021; y-coordinates are arbitrary).* ***C:*** *The Asian monsoon record as seen in speleothem $\delta^{18}O$ (Cheng et al., 2016). The letters H1 – H6 mark Heinrich events 1-6 as defined by positive $\delta^{18}O$ excursions by Cheng et al. (2016).*

5.4 Millennial-scale events

For the time interval between c. 60 and 20 ka (i.e., the start of Termination I), Devils Hole water table markers were consistently located at relatively high elevations between +6 m and +9 m (Szabo et al., 1994; Wendt et al., 2018; this study). Changes of the water table therefore occurred in excess of 3 m during MIS 4 to 2, which is significantly less than the amplitude of the changes during MIS 5 to 4, which were in excess of 6.7 m (Fig. 6).

As discussed in the previous section, water table variations are linked to North American ice sheet extent during MIS 5, as evidenced by the synchronicity with sea level changes (Fig. 6B) and a lag relative to mid-July 65°N insolation (Fig. 6A). However, no apparent link exists between these factors from about 60 ka to 30 ka. Instead, between 60 to 20 ka, multiple millennial-scale rises and falls of the water table overprint the high water table. Millennial-scale water table rises have been previously shown to coincide with H events (Wendt et al., 2018). H events mark the most important prolonged climatic disruptions during this period, serving as key reference points. These events triggered Northern Hemisphere cooling, resulting in global atmospheric reorganization, including southward shifts of the Intertropical Convergence Zone. This reorganization is documented by phases of weak Asian monsoon, precisely dated through positive excursions of rainfall $\delta^{18}O$ of East Asian speleothems (Cheng et al., 2016; Zhang et al., 2021).

The structure, forcing and global hydroclimate expressions of H events remain a topic of ongoing debate (Zhang et al., 2021; Oster et al., 2020). Within the Great Basin, there is, although debated, evidence of increased aridity in the northwest (Oster et al., 2020; Benson et al., 2003; Zic et al., 2002; Heaton et al., 2019) and pluvial conditions in the south (Munroe and Laabs, 2013; McGee et al., 2018; Oster et al., 2023) associated with H events and different mechanisms have been discussed (see introduction section; McGee et al., 2018; Oster et al., 2020; Heaton et al., 2019). Given its precise chronology aligned with H events, we use the Asian monsoon record as a reference for their timing.

H events were characterized by massive iceberg discharge into the North Atlantic with global impacts (Hemming, 2004). They occurred on shorter timescales than ice-sheet growth and decay and are therefore linked to a different mechanism. In the southern Great Basin, H events are widely associated with enhanced pluvial conditions (Munroe and Laabs, 2013; McGee et al., 2018; Oster et al., 2023). This response is hypothesized to result from Northern Hemisphere winter cooling, which triggered a southward shift of the Intertropical Convergence Zone and Hadley cell, a southeastward displacement of the Aleutian Low, and an intensification of the subtropical jet — ultimately increasing transport of subtropical moisture into the western United States (McGee et al., 2018). Some studies from the northwestern Great Basin suggest drying during H5 to H2 (Oster et al., 2020; Benson et al., 2003; Zic et al., 2002; Heaton et al., 2019). The boundary between wetter and drier regions was, however, likely temporally and spatially transgressive (Oster et al., 2020).

A single brief rise at 17.28±0.08 ka is recorded at Devils Hole, falling into the early part of H1, However, the absence of data for the subsequent few millennia, combined with the clustering of water-table markers near +8.3 m —which prevents estimating the event's amplitude— limits our ability to draw conclusions regarding H1 and the onset of Termination I.

The Asian monsoon record shows a weak phase from 24.4 ka to 23.6 ka associated with H2 (Qiu et al., 2024; Cui et al., 2024). This was simultaneous with a relatively high water table at Devils Hole marked by a rise at +8.3 m at 23.84±0.05 ka. The corresponding mammillary calcite layer is comparably thick (5 mm). This was the longest wet phase of the past 40 ka, as documented by the core at +8.3 m. It also coincided with peak MIS 2 and maximum extent of the North American ice sheets (Dalton et al., 2022), leaving it unclear to what extent the mechanism discussed in the previous section - or a different process related to this H event - gave rise to pluvial conditions in the aquifer's catchment that feeds Devils Hole.

H3 is weakly expressed in the Asian monsoon record around 30 ka (Cheng et al., 2016). We did not identify any corresponding highstand in Devils Hole around this time. Szabo et al. (1994) reported a rise in Devils Hole water table from +6.8 m at 31.2±0.5 ka to over +9 m at 30±1 ka that agree with the timing of H3 and could be attributed to the onset of a pluvial phase that lacks a well-defined end date.

H4 is strongly pronounced in the Asian monsoon record and lasted from 40.04±0.07 ka to 37.76±0.05 ka (Zhang et al., 2021). At Devils Hole, Szabo et al. (1994) dated a highstand at more than +9 m to around 40 ka, lasting for about 2 millennia. In the cores analyzed in this study, there is a remarkable absence of mammillary calcite above +6.6 m. While no additional evidence was found linking H4 to a wetter climate, this does not imply a more arid climate.

H5 is recorded from 48.1 ka to 46.9 ka in the Asian monsoon domain (Dong et al., 2018) and coincided with a relatively high (+8.3 m) water table between 48.9±0.2 ka and 44.2±0.1 ka at Devils Hole. Because this wet phase started before and ended after the weak monsoon interval, it remains unclear whether pluvial conditions at Devils Hole were specifically associated with H5. However, it can be concluded that no aridification occurred during this event.

Devils Hole shows a 1 ka-long highstand above +8.1 m between 57.1±0.3 ka and 56.0±0.2 ka, while multiple brief highstands at +8.3 m occurred between 57.3±0.2 ka and 53.9±0.1 ka. The highstand at +8.1 m falls mostly in between H5a (55.12 ka to 54.65 ka - Zhang et al., 2021b) and 6 (61.5±0.2 ka to 59.4±0.2 ka - Zhang et al., 2017) of the Asian monsoon record. This disagreement in the timing between this well-developed mammillary calcite layer at +8.1 m and known H events suggests that the latter were not associated with an increase in water table. With a water table decline at +6.6 m shortly after 53.3±0.3 ka, i.e. postdating H5a, there is also no indication of increased aridity, but rather of a constantly humid hydroclimate from before H6 to after H5a.

Overall, it can be concluded that H events, as defined by precisely dated speleothems recording weak Asian monsoon intervals, generally coincided with a high water table at Devils Hole with new data particularly around H5 and H5a. No clear conclusion can be drawn for H3 and H4 due to scarce or inconsistent data. In the case of H3, the climate change may have been too subtle to detect.

The synchronicity of high Devils Hole water tables and weak Asian monsoon intervals suggests a common underlying cause. For the Asian monsoon, this is attributed to southward shifts of the Intertropical Convergence Zone (Cheng et al., 2016; Zhang et al., 2021). In the Great Basin, such shifts during H events have been associated with an intensification of the subtropical jet and a southeastward displacement of the Aleutian Low, ultimately increasing winter precipitation in the SW USA (McGee et al., 2018). Our study's findings support this climate scenario.

6. CONCLUSIONS

This study refines the Devils Hole water-table record for the last glacial cycle and provides new constraints on the hydroclimatic evolution of the southern Great Basin. By integrating detailed characterization of mammillary calcite with high-resolution U-series dating, we identify previously unrecognized variability during MIS 5 and resolve multiple short-lived water-table events between 60 and 20 ka. Samples younger than 60 ka were examined petrographically and, after the removal of two outliers, show mammillary calcite fabrics. We also screened all samples for $\delta^{234}U_{initial}$ and excluded those with anomalous values. These steps ensure that the remaining data points are reliably dated.

During MIS 5, the Devils Hole water table displays a clear correspondence with global sea-level variability and Northern Hemisphere summer insolation on orbital timescales. The close alignment of the MIS 5c lowstand with the precisely dated Caribbean sea-level highstand indicates that water-table behavior in the southern Great Basin was strongly linked to the waxing and waning of North American ice sheets. The multi-millennial lag of Devils Hole water-table changes relative to insolation reflects the slow response time of continental ice sheets to orbital forcing and provides a clear indication that Devils Hole water table and ice sheet extent are directly linked.

In contrast, from ~60 to 30 ka, sea-level and ice-sheet changes remained relatively muted, and no systematic relationship with Devils Hole water-table variability can be identified, suggesting that different forcing mechanisms dominated this interval. During this time, our refined record reveals repeated, brief water-table rises on millennial timescales. Although Heinrich events generally coincide with high water tables at Devils Hole, the record does not provide sufficient resolution to reconstruct the history of individual events.

The overall synchronicity between high water tables at Devils Hole and weakened Asian monsoon phases supports a climate mechanism involving southward displacement of the Intertropical Convergence Zone, intensification of the subtropical jet, and enhanced winter moisture delivery to the southern Great Basin during Heinrich events.

Together, these findings show that the southern Great Basin hydroclimate responded to distinct forcing processes operating on different timescales. Orbital-scale water-table variations were governed by ice-sheet dynamics, whereas millennial-scale fluctuations were driven by rapid atmospheric reorganizations associated with Heinrich events. By extending the temporal resolution of the Devils Hole record, this study provides new insights into the mechanisms that controlled past groundwater recharge in the region. These insights underscore the sensitivity of the Great Basin hydroclimate to rapid climate perturbations and offer an improved framework for interpreting future hydroclimatic change in this water-limited region.

ACKNOWLEDGMENTS

This research was funded by grant P327510 of the Austrian Science Fund to CS. Fieldwork was possible under the scientific research and collecting permits of the United States National Park Services DEVA-2022-SCI-0014, DEVA-2017-SCI-0002 and DEVA-2015-SCI-0006. This contribution was partially supported by NSF grant 2202913 to RLE.

AUTHOR CONTRIBUTIONS

Conceptualization: CS, KAW, SDS; Data curation: SDS; Formal analysis: SDS; Funding acquisition: CS, KAW, RLE; Investigation: CS, YD, SDS; Methodology: MR, KAW, SDS; Project administration: CS, YD; Resources: CS, RLE, MR; Supervision: CS, YD, RLE Visualization: SDS; Roles/Writing - original draft: SDS; Writing - review & editing: SDS, YD, KAW, MR, GEM, RLE, CS.

DATA AVAILABILITY

The dating results are published on PANGAEA (https://doi.org/10.1594/PANGAEA.988350). Additionally they and all other data relevant to the discussion and conclusions are given as Supplementary Material to this study.

REFERENCES

Bajnai, D. et al., 2021 Devils Hole calcite was precipitated at ±1°C stable aquifer temperatures during the last half million years. Geophysical Research Letters 48 https://doi.org/10.1029/2021GL093257

Benson, L. et al., 2003 Response of North American Great Basin Lakes to Dansgaard–Oeschger oscillations. Quaternary Science Reviews 22:2239-2251 https://doi.org/10.1016/S0277-3791(03)00210-5

Berger, A., 1999 Parameters of the Earths orbit for the last 5 Million years in 1 kyr resolution. PANGAEA, https://doi.org/10.1594/PANGAEA.56040

Cheng, H. et al., 2013 Improvements in ^{230}Th dating, ^{230}Th and ^{234}U half-life values, and U–Th isotopic measurements by multi-collector inductively coupled plasma mass spectrometry. Earth and Planetary Science Letters. 371-372:82-91 https://doi.org/10.1016/j.epsl.2013.04.006

Cheng, H. et al., 2019 Eastern North American climate in phase with fall insolation throughout the last three glacial-interglacial cycles. Earth and Planetary Science Letters 522:125-134 https://doi.org/10.1016/j.epsl.2019.06.029

Cui, Y. et al., 2024 Chronological features of Heinrich Stadial 2 based on a high-resolution analysis of δ^{18}O stalagmite records from China, and possible links to changes in Atlantic Meridional Overturning Circulation. Paleogeography, Paleoclimatology, Paleoecology 633 https://doi.org/10.1016/j.palaeo.2023.111875

Dalton, A. S. et al., 2022 Evolution of the Laurentide and Innuitian ice sheets prior to the Last Glacial Maximum (115 ka to 25 ka). Earth-Science Reviews 224 https://doi.org/10.1016/j.earscirev.2021.103875

Deacon, J.E. and Williams, A.E., 1991 Ash Meadows and the legacy of the Devils Hole pupfish. In: Battle against extinction: native fish management in the American West: 69-87.

Deacon, J.E. et al., 2007 Fueling population growth in Las Vegas: How large-scale groundwater withdrawal could burn regional biodiversity. BioScience 57,8: 688-698 https://doi.org/10.1641/B570809

Dong, J. et al., 2018 Asian monsoon dynamics at Dansgaard/Oeschger events 14–8 and Heinrich events 5–4 in northern China. Quaternary Geochronology 47:72-80 https://doi.org/10.1016/j.quageo.2018.05.012

Dublyansky, Y. and Spötl, C., 2015 Condensation-corrosion speleogenesis above a carbonate-saturated aquifer: Devils Hole Ridge, Nevada. Geomorphology 229:17-29 http://dx.doi.org/10.1016/j.geomorph.2014.03.019

Edwards, R.L. et al., 1987 ^{238}U-^{234}U-^{230}Th-^{232}Th systematics and the precise measurement of time over the past 500,000 years. Earth and Planetary Science Letters. 81, 175–192 https://doi.org/10.1016/0012-821X(87)90154-3

Halford, K.J. and Jackson, T.R., 2020 Groundwater characterization and effects of pumping in the Death Valley regional groundwater flow system, Nevada and California, with special reference to Devils Hole. U.S. Geological Survey Professional Paper 1863. https://doi.org/10.3133/pp1863

Heaton, E.J. et al., 2019 A Great Basin lake-level response to 38–34 ka Dansgaard–Oeschger oscillations. Journal of Paleolimnology 61:263-278 https://doi.org/10.1007/s10933-018-0057-5

Hemming, S.R., 2004 Heinrich events: Massive late Pleistocene detritus layers of the North Atlantic and their global climate imprint. Reviews of Geophysics 42 https://doi.org/10.1029/2003RG000128

Hudson, A.M. et al., 2019 North-south dipole in winter hydroclimate in the western United States during the last deglaciation. Scientific Reports 9 https://doi.org/10.1038/s41598-019-41197-y

Hudson, A.M. et al., 2023 Paleohydrologic history of pluvial lake San Agustin, New Mexico: Tracking changing effective moisture in southwest North America through the last glacial transition. Quaternary Science Reviews 310 https://doi.org/10.1016/j.quascirev.2023.108110

Ibarra, D.E. et al., 2014 Rise and fall of late Pleistocene pluvial lakes in response to reduced evaporation and precipitation: Evidence from Lake Surprise, California. Geol. Soc. Am. Bull. 126 https://doi.org/10.1130/B31014.1

Jackson, T.R. and Steidle, S.D. et al., 2023 A 350,000-year history of groundwater recharge in the southern Great Basin, USA. Communications Earth and Environment 4: 98 https://doi.org/10.1038/s43247-023-00762-0

Kluge, T. et al., 2014 Devils Hole paleotemperatures and implications for oxygen isotope equilibrium fractionation. Earth and Planetary Science Letters 400: 251-260 https://doi.org/10.1016/j.epsl.2014.05.047

Lachniet, M.S., et al., 2017 Arctic cryosphere and Milankovitch forcing of Great Basin paleoclimate. Scientific Reports 7:12955 https://doi.org/10.1038/s41598-017-13279-2

Lambeck, K. and Chappell, J., 2001 Sea level change through the last glacial cycle. Science 292: 679-686 https://doi.org/10.1126/science.1059549

Li, X. et al., 2019 Novel method for determining ^{234}U–^{238}U ages of Devils Hole 2 cave calcite (Nevada). Geochronology 3: 49-58 https://doi.org/10.5194/gchron-3-49-2021

626 Lowenstein, T.K., et al., 2024 Unified 200 kyr paleohydrologic history of the Southern Great
627 Basin: Death Valley, Searles Valley, Owens Valley and Devils Hole cave. Quaternary
628 Science Reviews 336 https://doi.org/10.1016/j.quascirev.2024.108751
629 Lundberg, J. and Ford, D.C. 1994 Late Pleistocene sea level change in the Bahamas from mass
630 spectrometric U-series dating of submerged speleothem. Quaternary Science Reviews
631 13:1-14 https://doi.org/10.1016/0277-3791(94)90121-X
632 MacDonald, G.M., 2010 Water, climate change, and sustainability in the southwest. PNAS
633 107:21256-21262 https://doi.org/10.1073/pnas.0909651107
634 McGee, D. et al., 2018 Western U.S. lake expansions during Heinrich stadials linked to Pacific
635 Hadley circulation. Science Advances 4,11 https://doi.org/10.1126/sciadv.aav0118
636 Moseley, G.E. et al., 2016 Reconciliation of the Devils Hole climate record with orbital forcing.
637 Science 351: 165-168 https://doi.org/10.1126/science.aad4132
638 Munroe, J.S. and Laabs, B.J.C., 2013 Temporal correspondence between pluvial lake highstands
639 in the southwestern US and Heinrich Event 1. Journal of Quaternary Science 28:49-58
640 https://doi.org/10.1002/jqs.2586
641 Oster, J.L. et al., 2015 Steering of westerly storms over western North America at the Last
642 Glacial Maximum. Nat. Geosci. 8: 201-205 https://doi.org/10.1038/ngeo2365
643 Oster, J.L. et al., 2020 Multi-proxy stalagmite records from northern California reveal dynamic
644 patterns of regional hydroclimate over the last glacial cycle. Quaternary Science Reviews
645 241,106411 https://doi.org/10.1016/j.quascirev.2020.106411
646 Oster, J.L. et al., 2023 North Atlantic meltwater during Heinrich Stadial 1 drives wetter climate
647 with more atmospheric rivers in western North America. Science Advances 9(46)
648 https://doi.org/10.1126/sciadv.adj2225
649 Potter, E.K. et al., 2004 Suborbital-period sealevel oscillations during marine isotope substages
650 5a and 5c. Earth and Planetary Science Letters 225:191–204.
651 https://doi.org/10.1016/j.epsl.2004.05.034
652 Qiu, W. et al., 2024 Synchronous anti-phase variations between the East Asian summer monsoon
653 and South America Summer Monsoon during Heinrich stadial 2. Quaternary Science
654 Reviews 323 https://doi.org/10.1016/j.quascirev.2023.108434
655 Reheis, M.C. et al., 2015 Directly dated MIS 3 lake-level records from Lake Manix, Mojave
656 Desert, California, USA. Quaternary Research 83
657 http://dx.doi.org/10.1016/j.yqres.2014.11.003
658 Reheis, M.C. et al., 2019 Pleistocene lakes and paleohydrologic environments of the Tecopa
659 basin, California: Constraints on the drainage integration of the Amargosa River. GSA
660 Bulletin 132:1537-1565, https://doi.org/10.1130/B35282.1
661 Santi, L.M. et al., 2020 Clumped isotope constraints on changes in latest Pleistocene
662 hydroclimate in the northwestern Great Basin: Lake Surprise, California. GSA Bulletin
663 132:2669-2683 https://doi.org/10.1130/B35484.1
664 Seltzer, A.M. et al., 2019 Deglacial water-table decline in Southern California recorded by noble
665 gas isotopes. Nature Communications 10 https://doi.org/10.1038/s41467-019-13693-2
666 Shen, C.C. et al., 2002 Uranium and thorium isotopic and concentration measurements by
667 magnetic sector inductively coupled plasma mass spectrometry Chemical. Geology,
668 185:165–178 https://doi.org/10.1016/S0009-2541(01)00404-1
669 Shen, C.C. et al., 2012 High-precision and high-resolution carbonate ^{230}Th dating by MC-ICP-
670 MS with SEM protocols. Geochimica et Cosmochimica Acta. 99:71–86
671 https://doi.org/10.1016/j.gca.2012.09.018

Spratt, R.M. and Lisiecki, L.E., 2016 A Late Pleistocene sea level stack. Clim. Past 12:1079-1092 https://cp.copernicus.org/articles/12/1079/2016/

Steidle, S.D. et al., 2024 Moisture availability and groundwater recharge paced by orbital forcing over the past 750,000 years in the southwestern USA. Commun Earth Environ 5, 376 https://doi.org/10.1038/s43247-024-01550-0

Steidle, S.D. et al., 2021 Reconstruction of Middle to Late Quaternary sea level using submerged speleothems from the northeastern Yucatán Peninsula. Journal of Quaternary Science 36:1190-1200 https://doi.org/10.1002/jqs.3365

Steidle, S.D. et al., 2026 Th-U ages over the last 112,000 years from Devils Hole calcite (NV, USA) for palaeo water table reconstruction [dataset]. PANGAEA, https://doi.org/10.1594/PANGAEA.988350

Szabo, B.J. et al., 1994 Paleoclimatic inferences from a 120,000-Yr calcite record of water-table fluctuation in Browns Room of Devils Hole, Nevada. Quaternary Research 41: 59-69 https://doi.org/10.1006/qres.1994.1007

Van Elteren, J.T. et al., 2019 Insights into the selection of 2D LA-ICP-MS (multi)elemental mapping conditions. Journal of Analytical Atomic Spectrometry 34:1919-1931 https://doi.org/10.1039/C9JA00166B

Wainer, K.A.I. et al., 2017 Speleothem evidence for MIS 5c and 5a sea level above modern level at Bermuda. Earth and Planetary Science Letters 457:325–334. https://doi.org/10.1016/j.epsl.2016.10.005

Wendt, K.A. et al., 2018 Moisture availability in the southwest United States over the last three glacial-interglacial cycles. Science Advances 4,10 https://doi.org/10.1126/sciadv.aau1375

Wendt, K.A. et al., 2020 Paleohydrology of southwest Nevada (USA) based on groundwater $^{234}U/^{238}U$ over the past 475 k.y.. GSA Bulletin 132:793-802 https://doi.org/10.1130/B35168.1

Winograd, I.J. et al., 1992 Continuous 500,000-year climate record from vein calcite in Devils Hole, Nevada. Science 258: 255-260 https://doi.org/10.1126/science.258.5080.255

Winograd, I.J. et al., 1998 The relative contributions of summer and cool-season precipitation to groundwater recharge, Spring Mountains, Nevada, USA. Hydrogeology Journal 6: 77-93 https://doi.org/10.1007/s100400050135

Zhang, T.T. et al., 2017 Stalagmite-inferred centennial variability of the Asian summer monsoon in southwest China between 58 and 79 ka BP. Quaternary Science Reviews 160:1-12 https://doi.org/10.1016/j.quascirev.2017.02.003

Zhang, X. et al., 2021 Three-phase structure of the East Asia summer monsoon during Heinrich Stadial 4 recorded in Xianyun Cave, southeastern China. Quaternary Science Reviews 274 https://doi.org/10.1016/j.quascirev.2021.107267

Zhang, X. et al., 2021b A gradual transition into Greenland interstadial 14 in southeastern China based on a sub-decadally-resolved stalagmite record. Quaternary Science Reviews 253 https://doi.org/10.1016/j.quascirev.2020.106769

Zic, M. et al., 2002 Evidence of synchronous climate change across the Northern Hemisphere between the North Atlantic and the northwestern Great Basin, United States. Geology 30:635-638 https://doi.org/10.1130/0091-7613(2002)030%3C0635:EOSCCA%3E2.0.CO;2

Supplemental Material

Outlier detection based on $\delta^{234}U_{initial}$

The $\delta^{234}U_{initial}$ of Devils Hole calcite is narrowly defined (Wendt et al., 2019; Li et al., 2021) and reflects long-term water table changes and associated water-rock interactions in the aquifer upstream of Devils Hole (Wendt et al., 2019). It can therefore be used to check the integrity of samples of mammillary calcite because $\delta^{234}U_{initial}$ and age are interdependent. As an objective measure to identify outliers, data from Wendt et al. (2018), Li et al. (2021) and from this study that are both younger than 121.5 ka and have a $\delta^{234}U_{initial} < 1970$ were considered. A polynomial function of the form $y = a*x^5 + b*x^4 + c*x^3 + d*x^2 + e*x + f$ was fitted with a least squares algorithm to this dataset. With y as $\delta^{234}U_{initial}$ in ‰ and x as age in ka, the resulting parameters are: a = 1.12157714e-09, b = -3.13912768e-06, c = 5.57952974e-04, d = -6.10460779e-02, e = 3.66951373e+00 and f = 1.72895397e+03. Samples outside of a ±40 ‰ range were considered outliers and omitted (Fig. S1). Eight out of the 53 samples were removed: SS37, SS38, SS40, SS22, SS180, SS20, SS174 and SS13.

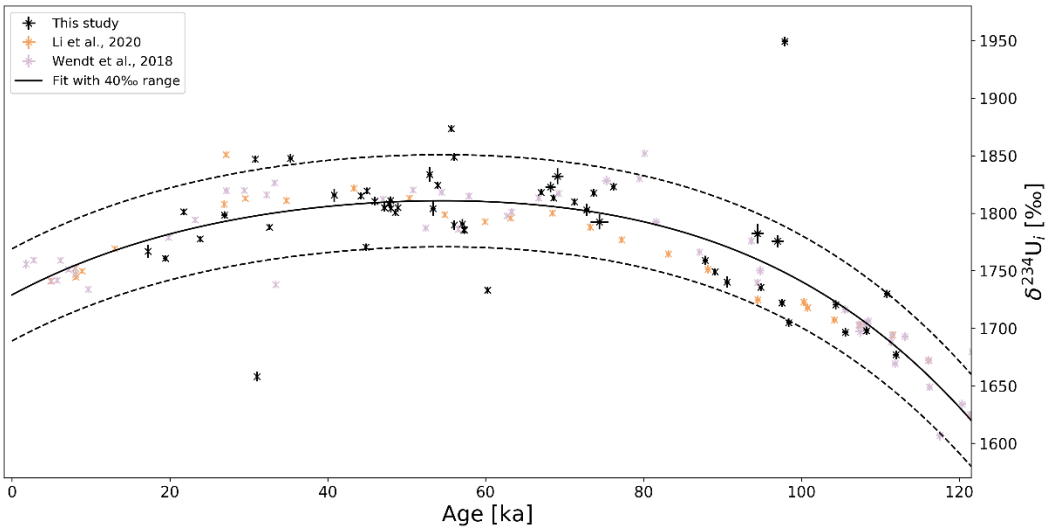

Fig. S1. *$\delta^{234}U_{initial}$ against time. A polynomial function was fitted to all data points. Samples from this study outside of the 40‰ range were not considered for the water table reconstruction.*

Changes in groundwater availability over the last 120 ka

Recharge is the measure that determines how much groundwater can be used for sustainable socio-economic needs. Its susceptibility to changes in climate forcing is therefore a crucial parameter for climate mitigation measures. A recent groundwater model (Jackson et al., 2023) makes it possible to infer the recharge to the Ash Meadows groundwater basin from the Devils Hole water table over the last glacial cycle. The new constraints on the Devils Hole water table allow for a more precise analysis of recharge changes during the last glacial period.

During MIS 5c, the water table lowstand at Devils Hole remained in a narrow range between +3.2 m and +1.8 m. Using the scaled-recharge scenario of Jackson et al. (2023), this translates into a recharge between 143% (for +3.2 m) and 120% (for +1.8 m) relative to today. MIS 5b experienced a water table rise to more than +9.9 m, which translates into a recharge of more than 363% relative to today. This suggests that recharge increased by at least +150% from peak MIS 5c to peak MIS 5b.

Between 60 ka and 20 ka, the water table oscillated between less than +6 m to more than +9 m. This corresponds to a change between less than 210% and more than 322% of today's recharge. The relative change was more than +50% (from +6 m to +9 m) or more than -35% (from +9 m to +6 m).

It is important to note that the link between external climate forcing and changes in recharge is non-linear. Given the generally higher recharge during the last glacial period compared to today, similar absolute changes in external climate forcing can lead to higher relative and smaller absolute changes during the presently hot and arid regional climate in the southern Great Basin.

Trace element analysis of Devils Hole calcite

Table S1. *Average trace element ratios and standard deviations of mammillary calcite and folia as shown in Fig. 2.*

[mmol/mol]	**Mamm-l (d)**	**Mamm-h (d)**	**Folia (d)**	**Mamm-l (v)**	**Mamm-h (v)**	**Folia (v)**
Mg/Ca	35.1±10	39.7±9.8	8.1±5.8	35.5±7.0	39.2±8.8	7.1±8.8
Sr/Ca	0.24±0.05	0.97±0.28	0.23±0.21	0.24±0.06	0.76±0.17	0.14±0.14
Ba/Ca	0.006±0.003	0.053±0.059	0.007±0.011	0.005±0.003	0.049±0.015	0.008±0.017

Table S2. *Averaged trace element ratios of calcite layers <60 ka BP. The classification (last column) is based on the scheme defined in Fig. 3.*

Sample ID	**Mg/Ca**	**Sr/Ca**	**Ba/Ca**	**Classification**
SS24	42.5±8.2	1.11±0.84	0.076±0.034	Mamm-h
SS25	46.4±13.0	1.21±0.75	0.077±0.025	Mamm-h
SS22	42.8±41.1	0.97±0.31	0.074±0.020	Mamm-h
SS4	45.3±8.6	0.99±0.24	0.068±0.023	Mamm-h
SS5	45.7±14.4	0.89±0.28	0.059±0.016	Mamm-h
SS35	43.7±12.1	0.82±0.42	0.079±0.097	Mamm-h
SS34	47.4±8.4	0.83±0.64	0.087±0.070	Mamm-h
SS33	43.0±11.0	0.88±1.48	0.101±0.037	Mamm-h
SS38	40.4±9.7	0.84±0.89	0.050±0.040	Mamm-h
SS37	43.6±33.0	0.81±0.88	0.063±0.026	Mamm-h
SS36	43.2±11.6	0.87±0.90	0.081±0.158	Mamm-h
SS30	44.0±31.6	1.00±0.37	0.076±0.022	Mamm-h
SS31	57.5±32.6	0.95±0.41	0.055±0.034	Mamm-h
SS17	5.0±13.7	0.86±0.53	0.069±0.034	Folia
SS18	3.6±10.8	0.23±1.25	0.008±0.086	Folia
SS20	25.7±5.4	0.22±0.23	0.006±0.030	Mamm-l
SS182	55.1±23.3	1.05±0.31	0.065±0.024	Mamm-h
SS183	58.7±13.1	1.29±0.40	0.078±0.023	Mamm-h
SS184	46.5±8.4	0.89±0.38	0.058±0.016	Mamm-h
SS185	43.4±7.8	0.81±0.26	0.054±0.020	Mamm-h
SS186	49.0±7.1	1.03±0.18	0.066±0.013	Mamm-h
SS187	47.0±8.5	1.04±0.29	0.069±0.021	Mamm-h
SS188	46.1±13.0	0.90±0.24	0.057±0.018	Mamm-h
SS171	39.6±13.3	0.24±0.34	0.007±0.030	Mamm-l
SS172	37.5±13.6	0.19±0.07	0.005±0.018	Mamm-l
SS173	45.1±24.2	0.54±0.45	0.041±0.033	Mamm-l/-h
SS174	38.9±26.7	0.20±0.49	0.007±0.016	Mamm-l

Scans of drill cores

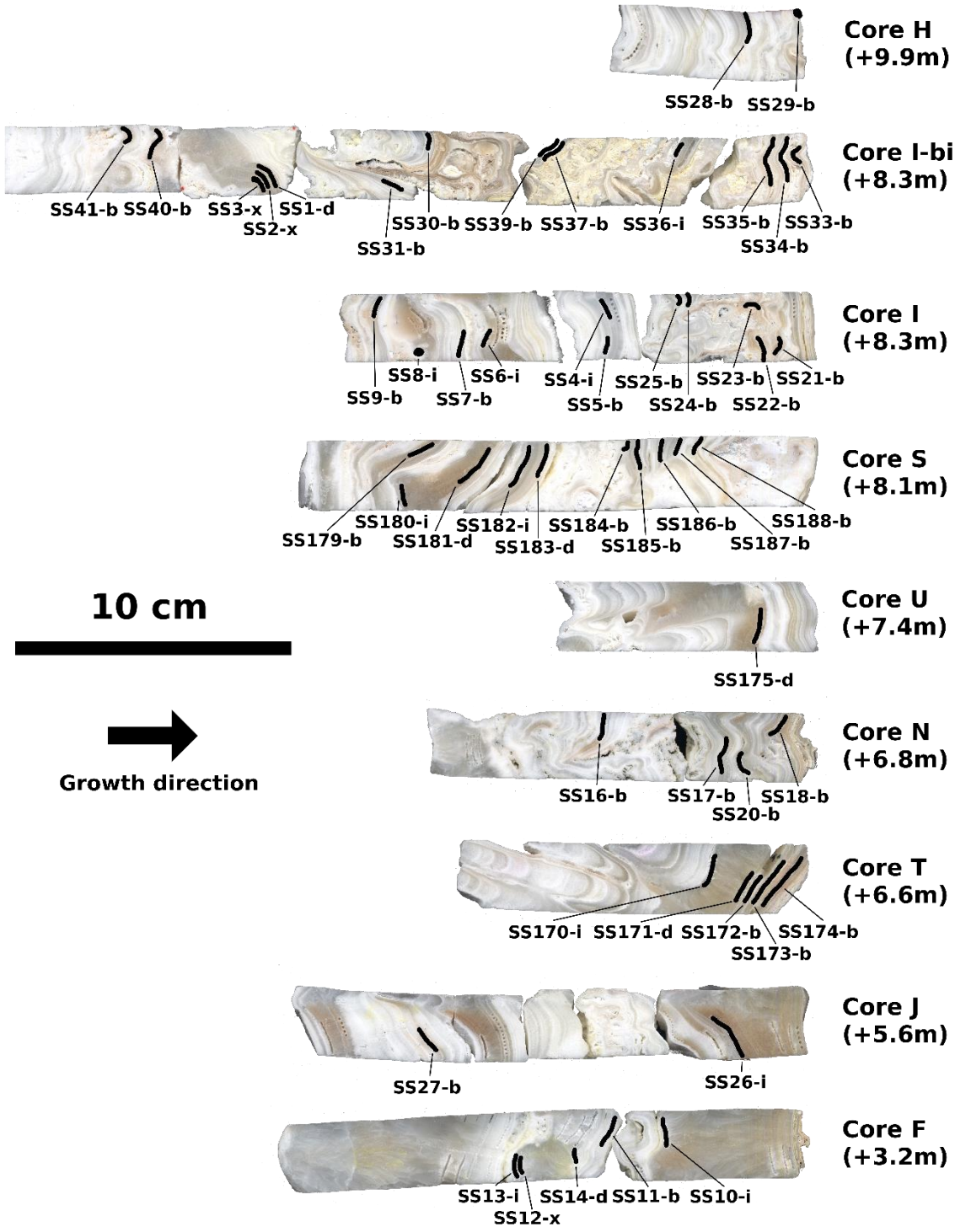

Fig. S2. *Positions of the 53 samples used for U-series dating sampled from nine horizontal drill cores (see Fig. 1).*

Table S3. *53 U-series dates.*

Sample Name	Core	Elev. [m]	type	note	^{238}U [ppb_{mass}]	^{232}Th [ppt_{mass}]	$^{230}Th/^{232}Th$ [at. ratio x10^{-6}]	$\delta^{234}U_{meas}$	$^{230}Th/^{238}U$ [act. Ratio]	^{230}Th-U age_{uncorr} [years]	^{230}Th-U age_{corr} [years]	$\delta^{234}U_{init}$	^{230}Th-U age_{corr} [years before 1950]
SS29	H	9,9	b		1641,4 ±2,1	1982 ±40	17186 ±346	1479,9 ±2,2	1,2587 ±0,0020	71337 ±173	**71325 ±173**	1810 ±3	**71255 ±173**
SS28	H	9,9	b		1593,3 ±2,1	867 ±18	42649 ±864	1360,2 ±2,2	1,4074 ±0,0024	89128 ±245	**89122 ±245**	1749 ±3	**89052 ±245**
SS33	I-bis	8,3	b		1955,3 ±17,7	3624 ±80	3956 ±94	1666,4 ±2,3	0,4446 ±0,0057	19529 ±271	**19509 ±271**	1761 ±3	**19439 ±271**
SS34	I-bis	8,3	b		1866,3 ±466,5	1294 ±324	9517 ±195	1682,6 ±5,6	0,4003 ±0,0015	17334 ±80	**17327 ±81**	1767 ±6	**17257 ±81**
SS35	I-bis	8,3	b		1357,2 ±1,6	6598 ±132	1692 ±34	1693,6 ±2,5	0,4990 ±0,0010	21876 ±54	**21826 ±65**	1801 ±3	**21756 ±65**
SS36	I-bis	8,3	i		1674,5 ±1,8	2237 ±45	6605 ±133	1661,7 ±2,4	0,5352 ±0,0008	23920 ±45	**23906 ±46**	1778 ±3	**23836 ±46**
SS37	I-bis	8,3	b	omitted	3967,1 ±12,9	29190 ±592	1441 ±29	1518,6 ±3,9	0,6430 ±0,0024	31197 ±144	**31117 ±154**	1658 ±4	**31047 ±154**
SS38	I-bis	8,3	b	omitted	1835,4 ±3,5	8225 ±165	3300 ±66	1559,7 ±2,8	0,8970 ±0,0021	44942 ±138	**44895 ±142**	1770 ±3	**44825 ±142**
SS31	I-bis	8,3	b		1435,8 ±2,1	1380 ±28	16508 ±332	1569,6 ±2,6	0,9622 ±0,0017	48637 ±121	**48627 ±122**	1800 ±3	**48557 ±122**
SS30	I-bis	8,3	b		1554,2 ±2,3	7300 ±146	3680 ±74	1566,5 ±2,5	1,0482 ±0,0020	54054 ±142	**54006 ±146**	1824 ±3	**53936 ±146**
SS1	I-bis	8,3	d		698,8 ±0,9	6755 ±135	2072 ±42	1504,3 ±2,4	1,2147 ±0,0023	67196 ±189	**67096 ±202**	1818 ±3	**67026 ±202**
SS2	I-bis	8,3	x		461,3 ±0,5	5761 ±115	1626 ±33	1493,7 ±2,3	1,2318 ±0,0020	68822 ±172	**68693 ±194**	1813 ±3	**68623 ±194**
SS3	I-bis	8,3	x		469,8 ±37,6	6604 ±529	1514 ±30	1476,0 ±2,6	1,2907 ±0,0027	73907 ±231	**73762 ±253**	1818 ±3	**73692 ±253**
SS40	I-bis	8,3	b	omitted	453,8 ±0,5	7133 ±143	1153 ±23	1461,9 ±2,4	1,0992 ±0,0017	60476 ±150	**60309 ±191**	1733 ±3	**60239 ±191**
SS41	I-bis	8,3	b		431,9 ±0,6	38961 ±781	273 ±5	1350,3 ±2,7	1,4964 ±0,0028	98002 ±326	**97053 ±745**	1776 ±5	**96983 ±745**
SS21	I	8,3	b		1438,4 ±2,0	2422 ±49	8952 ±181	1602,2 ±2,5	0,9142 ±0,0020	45057 ±127	**45040 ±127**	1819 ±3	**44970 ±127**
SS22	I	8,3	b	omitted	1447,9 ±2,0	4037 ±81	6443 ±130	1600,8 ±2,4	1,0895 ±0,0023	55746 ±161	**55718 ±163**	1873 ±3	**55648 ±163**
SS23	I	8,3	b		1407,4 ±1,8	990 ±20	21130 ±429	1601,9 ±2,5	0,9011 ±0,0020	44297 ±127	**44290 ±127**	1815 ±3	**44220 ±127**
SS24	I	8,3	b		1556,6 ±2,4	631 ±13	37671 ±764	1589,7 ±3,3	0,9263 ±0,0021	46035 ±145	**46031 ±145**	1810 ±4	**45961 ±145**
SS25	I	8,3	b		1601,5 ±2,1	541 ±11	52915 ±1073	1578,3 ±2,7	1,0848 ±0,0020	56070 ±148	**56066 ±148**	1849 ±3	**55996 ±148**
SS4	I	8,3	i		1475,7 ±2,0	1447 ±29	18150 ±365	1518,5 ±2,8	1,0791 ±0,0019	57395 ±150	**57385 ±151**	1785 ±3	**57315 ±151**
SS5	I	8,3	b		1526,5 ±1,7	358 ±7	75726 ±1529	1519,1 ±2,4	1,0778 ±0,0015	57293 ±119	**57290 ±119**	1786 ±3	**57220 ±119**
SS6	I	8,3	i		783,3 ±1,0	14051 ±282	1213 ±24	1470,0 ±2,4	1,3201 ±0,0023	76427 ±206	**76242 ±244**	1823 ±3	**76172 ±244**
SS7	I	8,3	b		1814,2 ±3,3	663 ±13	63194 ±1279	1372,6 ±2,9	1,4014 ±0,0034	87902 ±341	**87898 ±341**	1759 ±4	**87828 ±341**
SS8	I	8,3	i		569,6 ±1,1	568 ±11	23415 ±473	1347,4 ±3,6	1,4163 ±0,0031	90658 ±354	**90647 ±354**	1740 ±5	**90577 ±354**
SS9	I	8,3	b		1504,9 ±2,5	2227 ±45	16815 ±340	1259,2 ±2,5	1,5093 ±0,0032	105646 ±390	**105630 ±390**	1696 ±4	**105560 ±390**
SS188	S	8,1	b		1248,2 ±2,4	347 ±10	56799 ±1582	1581,3 ±3,1	0,9568 ±0,0031	48041 ±199	**48038 ±199**	1811 ±4	**47966 ±199**
SS187	S	8,1	b		1389,1 ±2,8	303 ±10	72048 ±2297	1579,6 ±3,2	0,9535 ±0,0029	47882 ±187	**47879 ±187**	1808 ±4	**47807 ±187**
SS186	S	8,1	b		1395,1 ±2,8	495 ±14	43778 ±1216	1579,7 ±3,2	0,9430 ±0,0031	47249 ±202	**47245 ±202**	1805 ±4	**47173 ±202**
SS185	S	8,1	b		1351,2 ±2,9	618 ±14	34439 ±795	1575,4 ±3,2	0,9549 ±0,0029	48062 ±193	**48057 ±193**	1804 ±4	**47985 ±193**
SS184	S	8,1	b		1641,1 ±3,5	1948 ±40	13454 ±278	1571,8 ±3,2	0,9687 ±0,0031	48985 ±201	**48973 ±201**	1805 ±4	**48901 ±201**
SS183	S	8,1	d		1411,3 ±3,1	708 ±15	34942 ±758	1527,6 ±3,2	1,0633 ±0,0034	56097 ±240	**56092 ±240**	1790 ±4	**56020 ±240**
SS182	S	8,1	i		1482,3 ±3,7	1066 ±22	24715 ±514	1524,0 ±3,4	1,0777 ±0,0036	57144 ±256	**57136 ±256**	1791 ±4	**57064 ±256**
SS181	S	8,1	d		503,3 ±0,6	42744 ±857	241 ±5	1503,2 ±2,7	1,2415 ±0,0026	69176 ±212	**68298 ±686**	1823 ±5	**68226 ±686**
SS180	S	8,1	i	omitted	520,4 ±0,6	2791 ±56	4865 ±99	1478,5 ±2,7	1,5825 ±0,0043	98026 ±420	**97973 ±421**	1949 ±4	**97901 ±421**
SS179	S	8,1	b		386,0 ±1,0	26285 ±531	358 ±7	1364,9 ±5,8	1,4769 ±0,0054	95230 ±617	**94516 ±793**	1782 ±9	**94444 ±793**
SS175	U	7,4	d		485,8 ±1,1	45283 ±911	222 ±5	1507,2 ±4,6	1,2567 ±0,0041	70137 ±348	**69175 ±762**	1832 ±7	**69103 ±762**
SS18	N	6,8	b	omitted	422,2 ±0,4	20143 ±404	210 ±4	1666,5 ±2,5	0,6081 ±0,0012	27480 ±68	**26983 ±358**	1798 ±3	**26913 ±358**
SS20	N	6,8	b	omitted	464,2 ±0,5	4476 ±90	1169 ±23	1692,9 ±2,8	0,6838 ±0,0013	30976 ±74	**30878 ±101**	1847 ±3	**30808 ±101**
SS17	N	6,8	b	omitted	1447,8 ±1,8	1278 ±26	13078 ±264	1630,3 ±2,4	0,7003 ±0,0014	32685 ±82	**32676 ±82**	1788 ±3	**32606 ±82**
SS16	N	6,8	b		746,2 ±1,0	7198 ±144	2613 ±53	1250,7 ±2,5	1,5288 ±0,0029	108396 ±368	**108292 ±375**	1698 ±4	**108222 ±375**
SS174	T	6,6	b	omitted	542,5 ±0,8	20933 ±420	329 ±7	1672,1 ±3,2	0,7703 ±0,0018	35768 ±108	**35373 ±299**	1848 ±4	**35301 ±299**
SS173	T	6,6	b		1097,8 ±3,7	14721 ±299	1045 ±21	1617,7 ±5,1	0,8496 ±0,0037	41036 ±230	**40897 ±250**	1816 ±6	**40825 ±250**
SS172	T	6,6	b		404,9 ±1,0	7845 ±158	884 ±18	1578,9 ±5,3	1,0393 ±0,0037	53170 ±269	**52971 ±303**	1834 ±6	**52899 ±303**
SS171	T	6,6	d		1112,6 ±3,3	7138 ±144	2654 ±54	1551,5 ±5,1	1,0329 ±0,0044	53480 ±311	**53413 ±314**	1804 ±6	**53341 ±314**
SS170	T	6,6	i		873,0 ±2,0	6285 ±127	2917 ±59	1467,9 ±4,0	1,2735 ±0,0039	72929 ±340	**72854 ±343**	1803 ±5	**72782 ±343**
SS26	J	5,6	i		431,0 ±0,5	64540 ####	144 ±3	1452,6 ±2,6	1,3058 ±0,0026	76057 ±233	**74487 ±1135**	1792 ±7	**74417 ±1135**
SS27	J	5,6	b		765,5 ±0,9	4416 ±89	4144 ±83	1327,9 ±2,3	1,4500 ±0,0022	94976 ±255	**94914 ±259**	1736 ±3	**94844 ±259**
SS10	F	3,2	i		1768,4 ±2,7	85 ±2	502249 ±10457	1307,5 ±2,4	1,4637 ±0,0029	97602 ±321	**97601 ±321**	1722 ±3	**97531 ±321**
SS11	F	3,2	b		1905,6 ±3,3	20 ±0	2269613 ±51951	1291,2 ±2,5	1,4616 ±0,0030	98467 ±342	**98467 ±342**	1705 ±4	**98397 ±342**
SS14	F	3,2	d		509,9 ±0,7	135 ±3	94432 ±1972	1281,4 ±2,7	1,5131 ±0,0027	104408 ±346	**104405 ±346**	1720 ±4	**104335 ±346**
SS12	F	3,2	x		439,9 ±0,5	1193 ±24	9372 ±189	1222,3 ±2,3	1,5411 ±0,0029	112075 ±384	**112045 ±385**	1677 ±4	**111975 ±385**
SS13	F	3,2	i	omitted	565,2 ±0,7	787 ±16	18487 ±375	1265,0 ±2,3	1,5621 ±0,0027	110930 ±353	**110915 ±354**	1730 ±4	**110845 ±354**

References

Wendt, K.A. et al. (2018) Moisture availability in the southwest United States over the last three glacial-interglacial cycles. Science Advances 4: eaau1375 https://doi.org/10.1126/sciadv.aau1375

Wendt, K.A. et al. (2019) Paleohydrology of southwest Nevada (USA) based on groundwater $^{234}U/^{238}U$ over the past 475 k.y.. GSA Bulletin 132(3-4): 793-802 https://doi.org/10.1130/B35168.1

Jackson, T.R. and Steidle, S.D. et al. (2023) A 350,000-year history of groundwater recharge in the southern Great Basin, USA. Communications Earth and Environment 4, 98 https://doi.org/10.1038/s43247-023-00762-0

Li, X. et al. (2020) Novel method for determining ^{234}U–^{238}U ages of Devils Hole 2 cave calcite (Nevada). Geochronology 3: 49-58 https://doi.org/10.5194/gchron-3-49-2021

Timing and amplitude of hydroclimate changes during the last glacial cycle in southwestern North America

Simon D. Steidle[1], Yuri Dublyansky[1], Marco Roman[2], Gina E. Moseley[1], Kathleen A. Wendt[3], R. Lawrence Edwards[4], Christoph Spötl[1]

[1] *Institute of Geology, University of Innsbruck, Innrain 52, 6020 Innsbruck, Austria*

[2]*Department of Environmental Sciences, Informatics and Statistics, University Ca' Foscari of Venice, Via Torino 155, Venice Mestre, Italy*

[3]*College of Earth, Ocean, and Atmospheric Sciences, Oregon State University, 101 SW 26th Street, Corvallis, Oregon 97330*

[4]*School of Earth and Environmental Sciences, University of Minnesota, 116 Church Street SE, Minneapolis, MN 55455-0149, USA*

ABSTRACT

The presently (semi)arid southwestern North America experienced major shifts in hydroclimate during the Quaternary characterized by oscillations between pluvial and arid phases. On orbital timescales, regional moisture availability is attributed to latitudinal shifts of moisture-bearing storm tracks due to the expansion and retreat of North American ice sheets. Millennial-scale variability is superimposed on top of the broader glacial pluvial phases. Groundwater fluctuations recorded by calcite deposits in Devils Hole, Nevada, offer unique insights into the past hydroclimate of the southwestern USA covering both time scales. Here, we increase the resolution of the Devils Hole water table record with an additional 43 water-table markers covering the last interglacial-glacial cycle. The updated record of water-table changes enables a comparison with sea-level records between 120,000 to 70,000 years ago, revealing concurrent changes in both during this period. This strengthens the hypothesis that orbital-scale water-table changes are closely linked to ice-sheet expansion during Marine Isotope Stage 5. New water table markers of the last 60,000 years further support increased pluvial conditions during Heinrich events.

HIGHLIGHTS

Hydroclimate of SW USA linked to ice volume changes during MIS 5.
A dry climate prevailed in the SW USA between 104.3±0.3 ka and 97.5±0.3 ka (MIS 5c).
Heinrich events of the last 60 ka were associated with regional wet conditions.

KEYWORDS

Quaternary, paleoclimatology, North America, speleothems, U-Th series, Devils Hole, hydroclimate

1. INTRODUCTION

The endorheic Great Basin, which spans large portions of the arid southwestern USA, has experienced repeated periods of wetter and cooler climates during the Quaternary (e.g., Reheis et al., 2019; Wendt et al., 2018; Santi et al., 2020; Seltzer et al., 2019). Past pluvial periods have been attributed to an interplay of different forcing mechanisms operating on orbital to millennial timescales. For orbital timescales (i.e., a periodicity of ≥20 ka), the hydroclimate responded to the growth and decay of the North American ice sheets (Cheng et al., 2019; Lachniet et al., 2017) due to high-pressure systems positioned over these ice sheets that had a major role in steering Pacific moisture into the SW region of the USA during winter (Oster et al., 2015). This resulted in a lag of the SW USA hydroclimate response relative to Northern Hemisphere summer insolation of 3,000 to 5,000 years (Lachniet et al., 2017).

Heinrich (H) events (Hemming, 2004) were periodic millennial-scale events during the last glacial period, characterized by massive iceberg discharges into the North Atlantic, leading to widespread oceanographic and climatic impacts on a global scale. They occurred on shorter timescales than ice sheet growth and decay and are therefore linked to a different mechanism. In the southern Great Basin, the response to H events is well documented through evidence of enhanced pluvial conditions (Hudson et al., 2019; Ibarra et al., 2014; Munroe and Laabs, 2013; McGee et al., 2018; Oster et al., 2023). This phenomenon is hypothesized to result from cooling in the Northern Hemisphere that led to a southward shift of the Intertropical Convergence Zone and Hadley cell, a southeastward displacement of the Aleutian Low, and an intensification of the subtropical jet (McGee et al., 2018). These atmospheric changes collectively enhanced atmospheric river transport, bringing increased subtropical moisture into the western United States (McGee et al., 2018). Studies from the northwestern Great Basin suggest dry conditions during H5 to H2 (Oster et al., 2020; Benson et al., 2003; Zic et al., 2002; Heaton et al., 2019). The boundary between drier and wetter conditions in the North and South Great Basin, respectively, was temporally and spatially transgressive throughout the duration of a H Event (Oster et al., 2020).

This study focuses on the southern Great Basin, where calcite precipitated from groundwater in Devils Hole 2 (cave) provides a record of past still-stands and fluctuations in water table elevation. By analyzing these deposits, this research enhances the understanding of long-term hydroclimate variability and its driving mechanisms over time. Within the cave, two distinct types of calcite can be observed that formed simultaneously on the walls, each recording different aspects of the groundwater conditions. The first type, folia, forms at the water-air interface, while the second type, mammillary calcite, precipitates subaqueously. Transitions from mammillary calcite to folia at a given elevation therefore occurred during periods of water table decline, whereas rising water tables led to folia being overgrown by mammillary calcite. Water-table research at the study site was pioneered by Szabo et al. (1994), who established a record of the last 100 ka. This record was extended by Wendt et al. (2018) for the last 350 ka and more recently extended further back to 750 ka (Steidle et al. 2024). It has been shown that this long and continuous archive formed under constant temperature conditions (Kluge et al., 2014; Bajnai et al., 2021), minimal variation in growth rate (Li et al., 2021), and no significant influence from tectonic activity (Wendt et al., 2018) over the last three glacial-interglacial cycles. This record therefore provides a unique opportunity to investigate the water table's response to different climate events across different timescales throughout the last glacial period. Mammillary calcite has been dated in previous studies using a variety of U-series techniques (Winograd et al., 1988,

1992; Moseley et al., 2016; Wendt et al. 2018; Li et al., 2021). These studies have primarily focused on events lasting more than 5 ka, leaving shorter-term changes less well resolved. The aim of this study is therefore to enhance the resolution of the water-table record for the last glacial cycle and improve our understanding of the forcing mechanisms driving the regional hydroclimate on orbital and millennial timescales. Since the water-table history at Devils Hole is linked to the recharge of the regional aquifer (Jackson et al., 2023), understanding the impact of millennial-scale climate events on water availability is critical for balancing socio-economic needs and conservation efforts – both in the wider Great Basin region and at Devils Hole itself – amid future climate change (Deacon et al., 1991; Deacon et al., 2007; MacDonald, 2010).

2. REGIONAL SETTING AND CALCITE DEPOSITION

The Ash Meadows groundwater basin is a sub-basin of the Great Basin. At present, about 80% of the Ash Meadows recharge originates from snowmelt in the Spring Mountains and Sheep Range (Winograd et al., 1998; Halford and Jackson, 2020). The modern recharge of the Ash Meadows groundwater basin is 2.59×10^7 m^3/yr, with approximately 90% reaching the surface at the Ash Meadows discharge area – located downstream and near Devils Hole – where it subsequently evaporates (Halford and Jackson, 2020).

The calcite samples of this study originate from Devils Hole #2, a sub-vertical tectonic fracture intersecting the groundwater table of the Ash Meadows groundwater basin at 36.416°N, 116.283°W. Mammillary calcite, which forms under subaqueous conditions, is dense, translucent, and slow-growing. It has few impurities and can be reliably dated (Moseley et al., 2016). Dating a calcite layer at a specific elevation in the cave provides unambiguous evidence that the groundwater table was above that level at a given time. Folia, on the other hand, are porous, white, and form at higher rates at the water-air interface. Folia cannot be reliably dated using U-series techniques due to its open-system behavior. The presence of folia within a sequence, where they overlie mammillary calcite (indicating the folia are younger), signifies an episode of water table decline. Conversely, when mammillary calcite forms on top of folia (indicating the mammillary calcite is younger), it reflects a rise in the water table. Thin layers of mammillary calcite represent brief rises in the water table above a given elevation. In the absence of folia, mammillary calcite samples indicate submergence but do not offer further insights into water-table fluctuations. Together, mammillary calcite and folia represent two endmembers of a spectrum of calcite deposits (see Supplemental Material; Steidle et al. 2024).

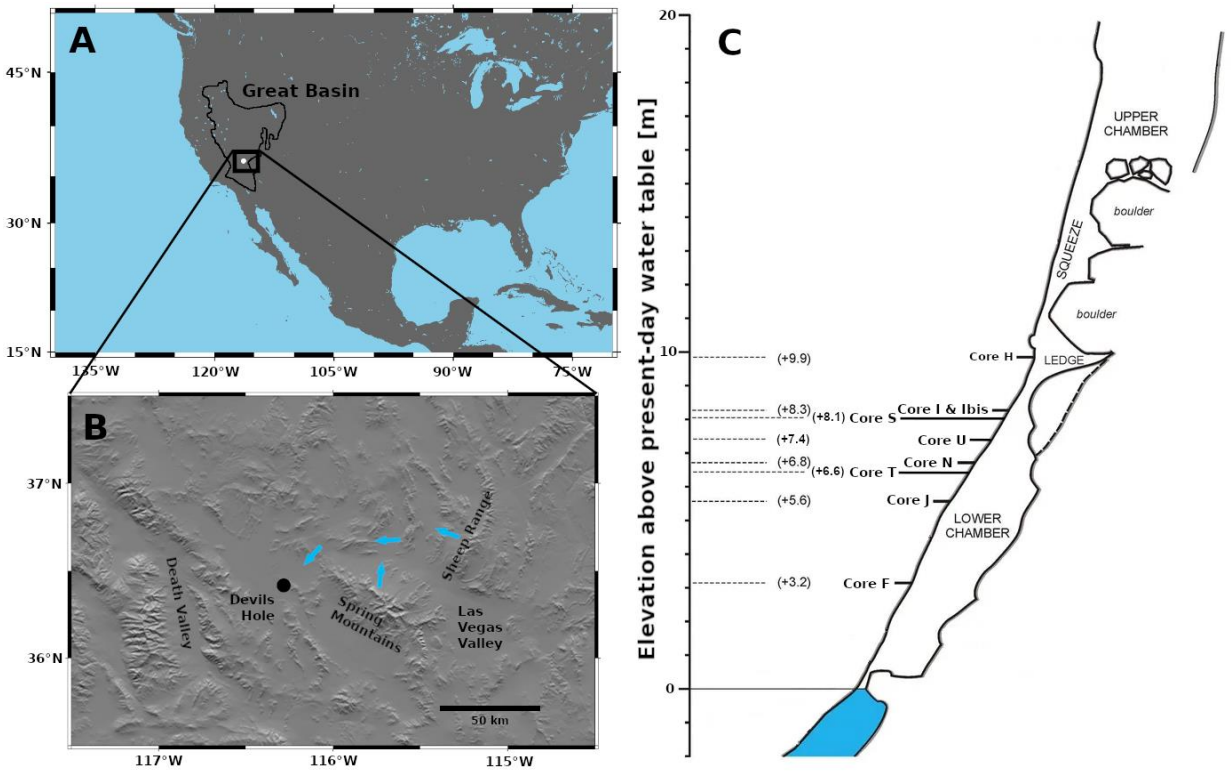

Fig. 1. *Study region and sampling positions. A: Overview map of North America and the Great Basin B: Shaded relief map of the area around Devils Hole showing major recharge areas of the regional aquifer, including the Spring Mountains and Sheep Range. Blue arrows indicate the main directions of groundwater flow. C: Simplified transect of Devils Hole #2 with the elevations of horizontally drilled cores examined in this study.*

3. METHODS

In this study, nine cores (2.5 cm diameter and 0.5-1.3 m in length) were horizontally drilled into the calcite deposits of the hanging wall in Devils Hole #2, at elevations ranging from +3.2 m to +9.9 m relative to the modern water table (Fig. S2). The cores were halved, polished, and 53 subsamples (5 to 30 mg) were prepared using a diamond burr-tipped dental drill under a clean laminar flow hood for U-Th dating. Furthermore, to further validate the chronology derived from thin calcite layers, the trace element composition of well-developed mammillary calcite and folia was analyzed. The trace element composition of all thin calcite layers dated to <60 ka was compared to that of well-developed mammillary calcite and folia to confirm their subaqueous formation as mammillary calcite.

Mammillary calcite has been shown to grow very slowly at an average rate of 0.9±0.3 mm/ka (Li et al., 2021). Due to the complex three-dimensional structure of the mammillary calcite and folia sequences, the drill bit size, and the sample quantity required for dating, the sampling resolution was limited to 1–2 mm. As a result, the dated calcite samples represent intervals of submergence exceeding 1 ka. The boundary between mammillary calcite and folia marks a rise or fall in the water table; however, only the mammillary calcite immediately above or below this boundary can be dated, not the boundary itself. Consequently, the recorded ages of water-table rises are systematically too young, while those of water-table falls are systematically too old by up to 1-2 ka. Unlike Wendt et al. (2018), extrapolation to the actual boundary was not possible in this study due to the sampled layers being too thin for multiple measurements.

The dating was performed at the Trace Metal Isotope Geochemistry Laboratory of the University of Minnesota, USA, following the chemical procedure of Edwards et al. (1987) and Shen et al. (2002, 2012) and the analytical procedures of Shen et al. (2012) and Cheng et al. (2013). In summary, samples were digested in HNO_3 and spiked with a mixed ^{236}U-^{233}U-^{229}Th spike. Spiked samples were co-precipitated with Fe, centrifuged, loaded onto anion exchange columns and separated and purified for uranium and thorium. Separate aliquots of uranium and thorium were measured on a multi-collector inductively coupled plasma mass spectrometer (Thermo Neptune Plus) via a secondary electron multiplier using a peak-jumping mode. Ages were calculated using the ^{230}Th and ^{234}U half-lives of Cheng et al. (2013). Chemical blanks were measured with each set of 12 samples and were found to be negligible (<30 ag ^{230}Th, <120 ag ^{234}U, <150 fg ^{232}Th, <1 pg ^{238}U). All ages are relative to the year 1950 common era (CE) and all uncertainties are reported at 2σ level where typical age uncertainties are on the order of 2-6 ‰.

Trace elements were measured by laser ablation inductively coupled plasma mass spectrometry (LA-ICP-MS) at the University of Venice using an excimer laser at 193 nm (Analyte Excite, Teledyne CETAC Photon Machines) coupled to a single quadrupole MS (iCAP-RQ, Thermo Scientific). Line scans parallel to the calcite growth direction were performed covering all sampled layers with ages younger than 60 ka. Laser fluence was set to 2 J/cm^2; pre-ablation was performed with a 85 µm square spot size at 80 Hz repetition rate and a fixed dosage of 20, whereas the ablation was performed with a 40 µm square spot size, 80 Hz repetition rate, and a fixed dosage of 10, resulting in a scan speed of 320 µm/s. Aerosol transfer was achieved using peek tubing and glass adapter (Glass Expansion) leading to a washout time of about 125 ms. Elemental 2D maps were recorded on a section of core H (+9.9 m) that shows a clear transition from folia to mammillary calcite and back to folia (Fig. 2). Laser fluence was set to 3 J/cm^2; pre-ablation was performed with a 150 µm square spot size at 6 Hz and a fixed dosage of 1, whereas the ablation was performed with a 20 µm square spot size, 300 Hz repetition rate and a fixed dosage of 6 resulting in a scan speed of 1000 µm/s. Aerosol transfer was achieved using peek tubing and ARIS adapter (Teledyne CETAC), leading to a washout time of about 30 ms. For both line scans and 2D maps, the ICP-MS acquisition included the elements (m/z) Mg (25), Ca (43), Sr (88) and Ba (137). Dwell times were adjusted to match the washout duration while being inversely proportional to the estimated average signal intensity of each element. This setup is designed to ensure synchronization between the LA and ICP-MS, thereby preventing artifacts such as aliasing in spatial analysis, as reported by vanElteren et al. (2019). Both line scans and 2D maps were quantitatively calibrated using the speleothem certified material SPLT-NP (µStandards) and quality checked (i.e. sensitivity drift correction) with the glass standard reference material NIST612 (National Institute of Standards and Technology). Raw signals were processed using the software HDIP (Teledyne CETAC), specifically by applying background (gas blank) correction, drift correction, possible outlier removal (to the SPLT-NP and NIST612 standards only, based on a 5 SD criterion) and normalization to the Ca signal to obtain molar ratios.

4. RESULTS

4.1 Trace element analysis of Devils Hole calcite

2D trace element maps were measured across a folia-to-mammillary calcite-to-folia transect (Fig. 2). Three distinct types of calcite were identified based on the trace element signatures. One of them characterizes folia and has low Mg/Ca, Sr/Ca and Ba/Ca ratios, with a relatively high standard deviation (Table S1). Mammillary calcite shows two types. Both have high Mg/Ca ratios, but one of them (referred to as "low concentration mammillary calcite" or "Mamm-l" in the following) has Sr/Ca and Ba/Ca ratios similar to folia, while the other (referred to as "high concentration mammillary calcite" or "Mamm-h" in the following) has 4x higher Sr/Ca and about 9x higher Ba/Ca ratios (Table S1).
Areas marked with the suffix "(d)" in Fig. 2 were used to define thresholds to distinguish these three types (Fig. 3). For Mg/Ca, a threshold of 15 mmol/mol was defined to distinguish folia from both mammillary calcite types. Thresholds of 0.6 mmol/mol for Sr/Ca and 0.025 for Ba/Ca distinguish high-concentration from low-concentration mammillary calcite.
These high-concentration mammillary calcite sections are not distinguishable petrographically from the low-concentration mammillary calcite sections. The high-concentration mammillary calcite is interpreted to be reliably datable because it is a subaqueous deposition. It is hypothesized to have formed within a few tens of centimetres of the water-air interface. These thresholds were validated (Fig. 4) in a different folia-to-mammillary calcite transition (areas marked by the suffix "(v)" in Fig. 2) showing similar trace element signatures (Table S1).

The trace element composition of 27 layers formed after 60 ka BP was analyzed and compared to folia and mammillary calcite thresholds (Fig. 5). 25 layers were associated with mammillary calcite due to their high Mg/Ca ratios. 20 of those 25 layers show the same Sr/Ca and Ba/Ca signature as high-concentration mammillary calcite. One sample (SS173) has a higher Ba/Ca ratio but lower Sr/Ca ratio. Two samples (SS17 and SS18) were associated with folia due to their low Mg/Ca ratio (Table S2) and consequently removed from the dataset.

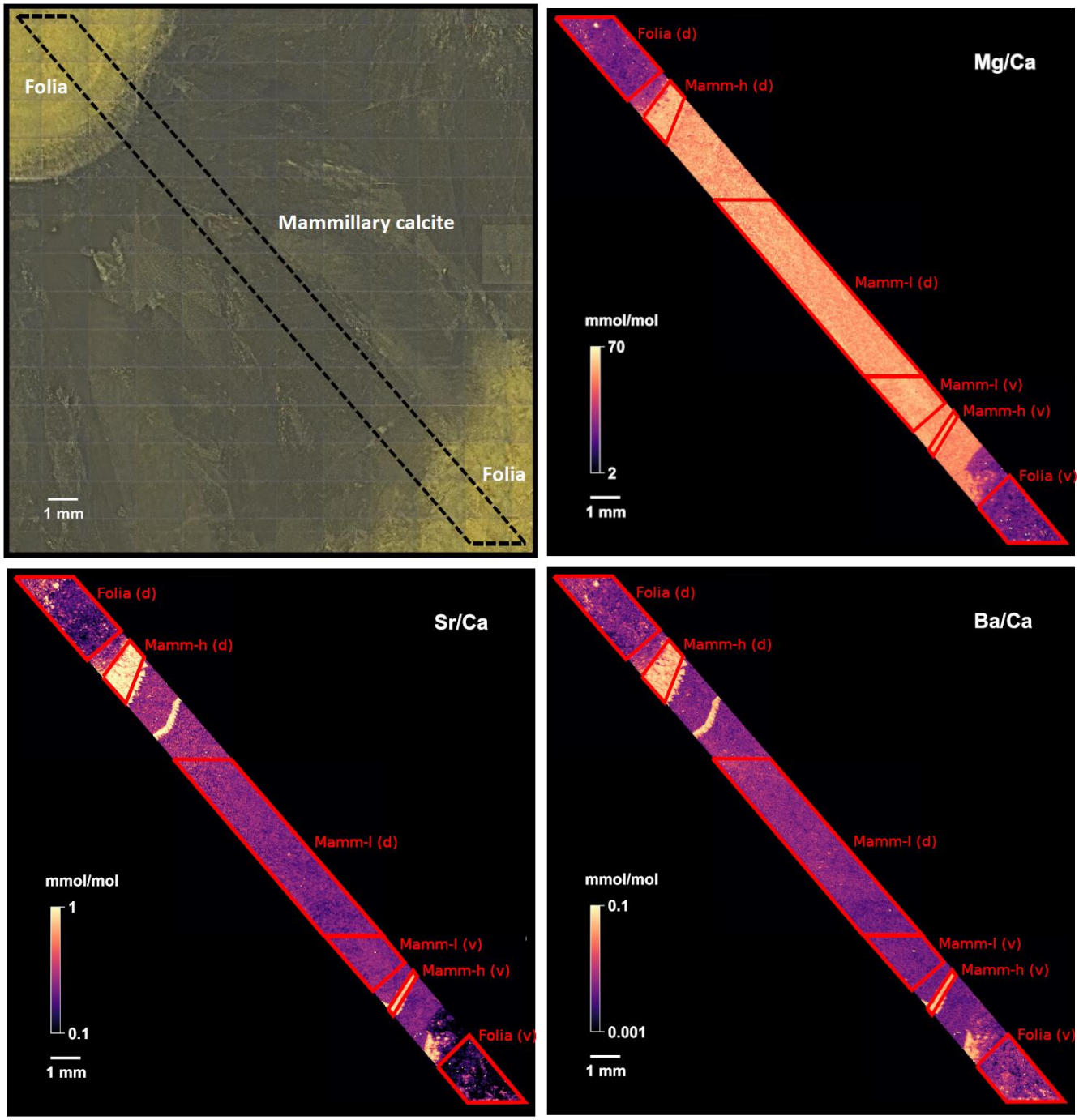

Fig. 2. *Reflected-light image of the analyzed folia – mammillary calcite – folia transition (upper left) and trace element ratios (Mg/Ca upper right, Sr/Ca lower left, Ba/Ca lower right). Regions associated with folia, mammillary calcite showing high trace element concentrations (Mamm-h) and mammillary calcite showing low trace element concentrations (Mamm-l) are highlighted respectively. Regions used to define the thresholds (Fig. 3) are labelled "(d)", regions used to validate the thresholds (Fig. 4) are labelled "(v)".*

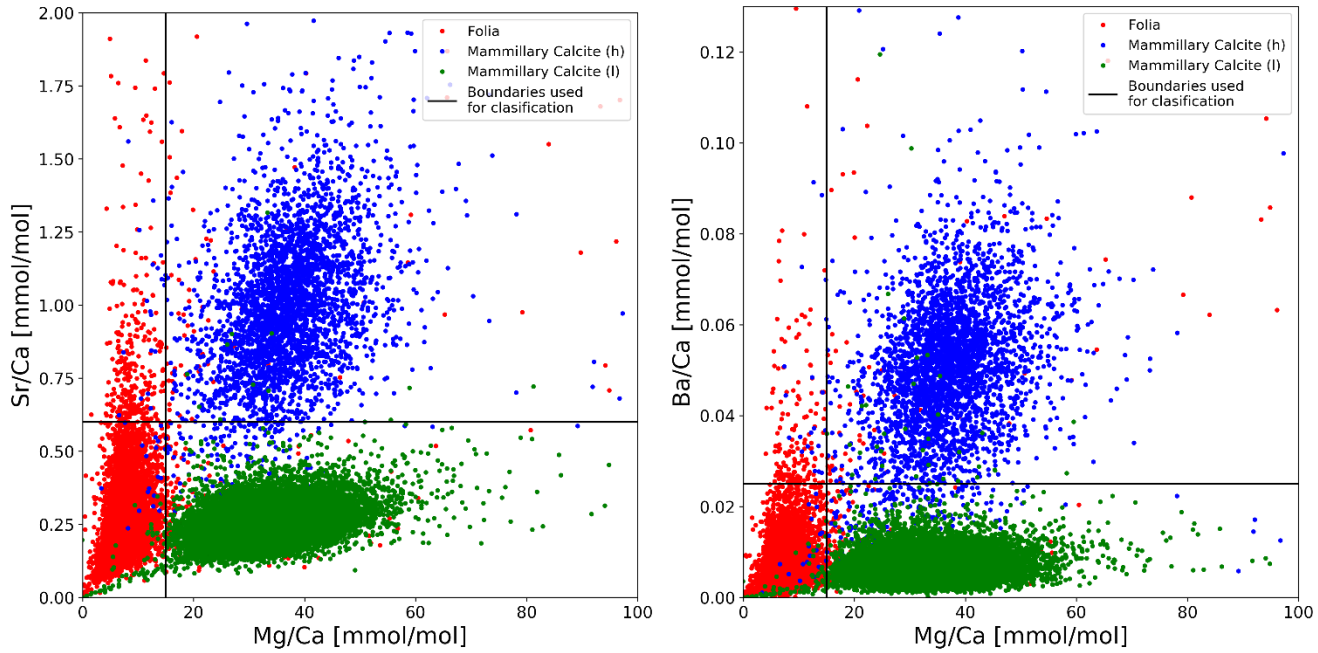

Fig. 3. *Trace element composition of folia and mammillary calcite used for defining typical ranges (labelled "(d)" in Fig. 2). Black lines are at 15 mmol/mol for Mg/Ca, 0.6 mmol/mol for Sr/Ca and 0.025 for Ba/Ca.*

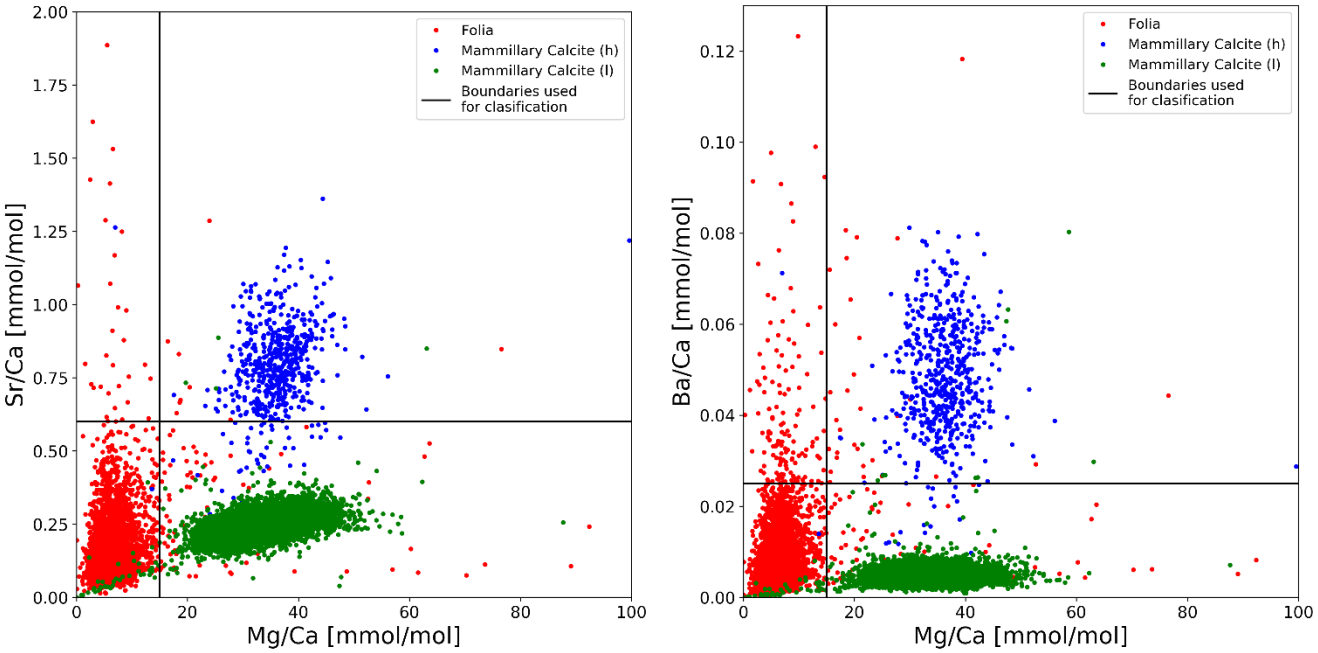

Fig. 4. *Trace element composition of folia and mammillary calcite in the areas used to verify the thresholds based on Fig. 3. Black lines as defined in Fig. 3.*

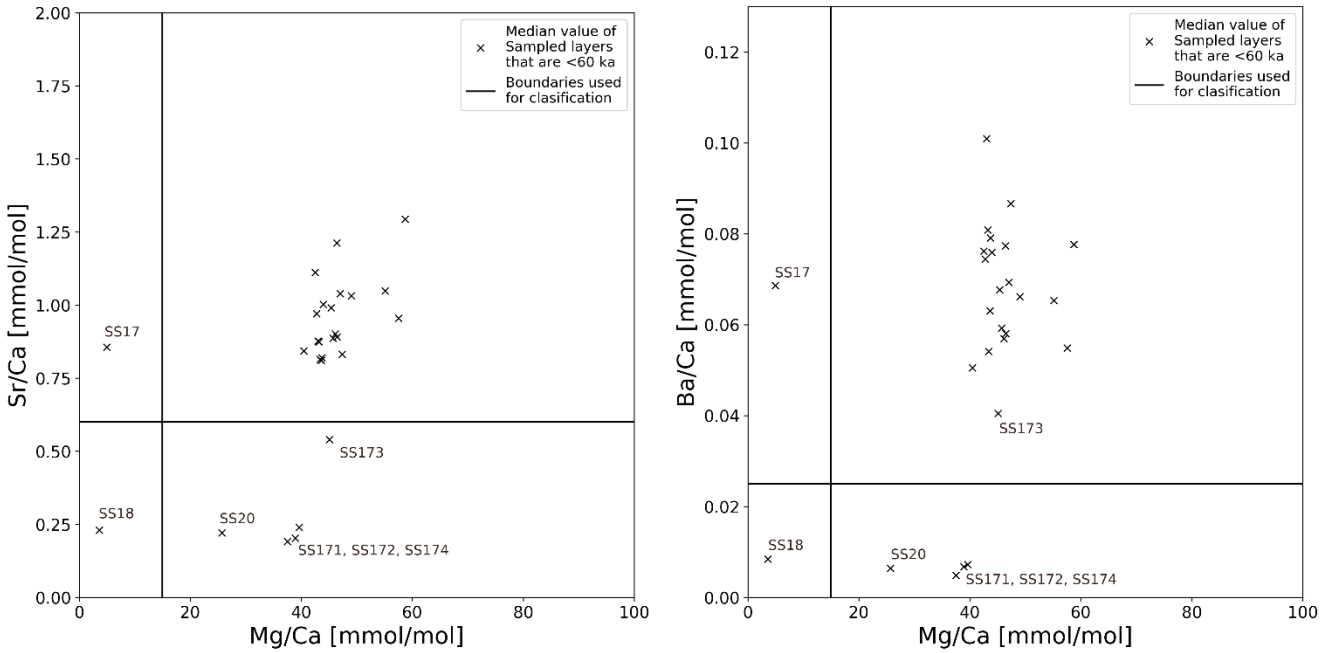

Fig. 5. *Trace element composition 27 layers younger than 60 ka. Black lines as defined in Fig. 3. Samples SS17 and SS18 were omitted due to their low Mg/Ca ratios as seen in folia which is not datable with U-series techniques. All other samples were classified as mammillary calcite.*

4.2 Construction of new water-table markers

Of the dated 53 samples, eight were omitted because their $\delta^{234}U_{initial}$ values deviate from the narrow range defined by Wendt et al. (2018), Li et al. (2021), and data from this study (see Supplementary Material for detailed information on outlier removal based on $\delta^{234}U_{initial}$). Folia were found to be associated with low trace element ratios (<15 mmol/mol of Mg/Ca, <0.6 mmol/mol of Sr/Ca, <0.025 mmol/mol of Ba/Ca). On the other hand, mammillary calcite exhibits two distinct trace element signatures, one of which – characterized by elevated trace element ratios – occurs near folia boundaries and is hypothesized to result from growth close to the water-air interface while still forming subaqueously (see section 4.1). Both signatures of mammillary calcite, however, have elevated Mg/Ca ratios (>15 mmol/mol), which was used as the main criterion to distinguish folia and mammillary calcite. Of the 27 investigated layers dated to be less than 60 ka, 25 were identified as mammillary calcite based on the trace element composition, while two were omitted because they partly consisted of folia (see Fig. 5).

4.3 Description of the refined water-table record

This study presents 43 new, reliable, high-precision U-Th ages from elevations between +3.2 m and +9.9 m relative to today's water table (Fig. 1C). These results are shown in Fig. ~~2~~6 alongside water table markers from previous studies (Wendt et al., 2018; Szabo et al., 1994) and made available in a data repository (Steidle et al., 2026). Moseley et al. (2016) demonstrated that the water table remained continuously above +1.8 m between 116.1±0.4 ka and 4.89±0.05 ka. Two new data points from the highest-sampled elevation indicate that the water table exceeded +9.9 m

at least twice during the last glacial period, at 89.1±0.2 ka and 71.3±0.2 ka. The last glacial water table, however, was generally high and may have reached similar elevations at other times within this interval, as mammillary calcite deposits represent minimum water-table elevations. An additional 41 water table markers from this study dated to between 112.0±0.4 and 17.26±0.08 ka and from elevations of +3.2 m to +8.3 m improve the resolution of short-term water table variability during the last glacial period.

Following the last interglacial water-table lowstand, that dropped below 0 m after 120.4±0.5 ka (Wendt et al., 2018) and remained below +0.8 m between 117.5±0.5 ka and 116.2±0.3 ka and below +1.8 m between 121.4±0.4 ka and 116.1±0.4 ka (Moseley et al., 2016), the water table rose during the glacial inception, reaching a highstand of over +8.3 m around 105.6±0.4 ka. The subsequent water-table decline reached a lowstand less than +3.2 m but greater than +1.8 m between 104.3±0.3 ka and 97.5±0.3 ka during MIS 5c. However, the alternation between folia and mammillary calcite in core F (Fig. S2, between samples SS10 and SS14) indicates that the water table was unstable, oscillating above and below +3.2 m multiple times during this period. One such rise was dated to 98.4±0.3 ka. Dating the other oscillations was not feasible because the mammillary calcite layers were too thin to be sampled reliably without contamination from folia. The distinctive alternation of folia and mammillary calcite at +3.2 m during MIS 5c suggests that the water table did not drop significantly lower. This interpretation is supported by continuous mammillary calcite deposition at +1.8 m during this period (Moseley et al., 2016; Li et al., 2021; Fig. 6). The MIS 5b highstand, exceeding +9.9 m, was reached at 89.1±0.2 ka (MIS 5b). As previously mentioned, this represents one of the highest-known water tables of the entire last glacial period.

Interpreting the record between c.85 ka and 60 ka is challenging. Wendt et al. (2018) indicated submergence above +4.6 m after 79.5±0.3 ka, which is followed by a continuous, c. 2 cm-thick mammillary calcite layer without apparent hiatuses. This continuous mammillary calcite layer suggests that submergence at +4.6 m lasted for 18±6 ka (based on a growth rate of 0.9±0.3 ka; Li et al. 2021). In contrast, results from a lower core suggest that the water table dropped below +3.2 m between 78.9±0.4 ka and 74.4±0.4 ka (MIS 5a – Wendt et al., 2018). The lack of folia deposition at +4.6 during this time may be the result of a water table drop that was too rapid to form a layer of folia.

Following MIS 5a, the MIS 4 highstand peaked at 71.3±0.2 ka at +9.9 m before dropping below +7.4 m by 69.1±0.8 ka. A mammillary calcite layer at +8.1 m, dated to 57.1±0.3 ka to 56.0±0.2 ka, is present within an interval of short-lived rises documented in the core at +8.3 m between 57.3±0.2 ka and 53.9±0.1 ka. This suggests that the water table in Devils Hole oscillated around +8.3 m on centennial time scales during this period. Two markers at +6.6 m during MIS 3, dated to 53.3±0.3 ka and 52.9±0.3 ka, suggest a slight lowering of the water table before it rebounded to a series of highstands above +8.3 m between 48.9±0.2 ka and 44.2±0.1 ka. During the remainder of MIS 3, a mammillary calcite layer at +6.6 m, dated to 40.8±0.3 ka, aligns with a highstand exceeding +9 m, as documented by Szabo et al. (1994). As the last glacial maximum approached, the water table oscillated around +8.3 m between 23.84±0.05 ka and 17.26±0.08 ka, before gradually declining to its present elevation.

5. DISCUSSION

5.1 Limitations

In Devils Hole, mammillary calcite sampled from depth and dated using the U-Th method has yielded inaccurate ages for glacial terminations that are systematically too old (Moseley et al., 2016). This age offset is hypothesized to be caused by an increase in excess ^{230}Th with depth in the water column, which specifically affects glacial terminations due to a change in sedimentation (Moseley et al., 2016). Moseley et al. (2016) observed that mamillary calcite deposited in shallow waters appeared to be unaffected by the age offset, and therefore represented the most accurate chronology at glacial terminations. The age offsets caused by increasing excess ^{230}Th at depth during glacial termination are thus not of relevance to this study given that: (1) the investigated time period is the last glacial period (and not a glacial termination), for which Moseley et al. (2016) produced reproducible chronologies from cores of different depths, and; (2) the samples dated in this study are largely from mamillary-folia boundaries indicating shallow water depths. Based on these two lines of argument, we consider the chronology presented here to be accurate within the stated precision. Still, since these are relatively young samples and it cannot be ruled out that the water table stood several meters higher during their formation, it must be noted that this represents a difficult-to-quantify uncertainty that could shift the true age of the samples to somewhat younger than reported here in particular during the intermediately glaciated phase of MIS 5 which was not analyzed by Moseley et al. (2016).

While all lowstands of the water table remained above +1.8 m (Moseley et al., 2016), highstands are not constrained, and the elevations discussed represent minimum estimates. Despite actively searching for mammillary calcite above +9.9 m, none was found from the last 120 ka. However, no conclusions can be drawn from this absence, as condensation corrosion – known to have occurred in the higher parts of Devils Hole (Dublyansky and Spötl, 2015) – may have removed calcite from the cave walls. It is therefore entirely plausible that mammillary calcite once existed at higher elevations. Consequently, the peak water table highstands discussed may have been significantly higher than the stated elevations. Condensation corrosion is not expected to have affected any of the mammillary calcite analyzed in this study. However, it is possible that some calcite deposits were lost due to physical processes, such as detachment from the wall under their own weight or later depositions. A scarcity of mammillary calcite as seen around 45 ka to 25 ka is a possible result of this process.

5.2 Comparison with regional surface lakes

Regional surface lakes (Lowenstein et al., 2024) indicate a step-like transition from very arid conditions during MIS 5e, to arid conditions during MIS 5~~c~~d and MIS ~~5d~~5c, followed by a shift to more humid conditions in MIS 5b and 5a. Brief rises above +6.8 m around 108.2±0.4 ka and above +8.3 m around 105.6±0.4 ka documented in this study provide evidence for significantly higher Devils Hole water table fluctuations during MIS 5 than previously recognized (Wendt et al., 2018; Lowenstein et al., 2024). The updated Devils Hole water table record indicates orbital-scale changes in MIS 5, which are not captured by deposits in surface lakes.

A comparison of sub-orbital variability is complicated by multi-millennial age uncertainties inherent in lake-level reconstructions and by the discontinuous nature of the Devils Hole water table record, which consists of individual snapshots rather than a continuous series. Even so, there are no apparent discrepancies between individual Devils Hole water-table events and

regional surface-lake records from the southern Great Basin and farther south on sub-orbital timescales during the last glacial cycle (Hudson et al., 2023; Lowenstein et al., 2024; Reheis et al., 2015).

A comparison with the lake Chewaucan record from the northern Great Basin shows that brief rises in the Devils Hole water table above +8.3 m around 17.26±0.08 ka, 19.4±0.3 ka and 21.76±0.07 ka occurred during Chewaucan lowstands that were separated by well-defined highstands. This anti-phased relationship is consistent with the proposed dipole pattern between northwestern and southern Great Basin during the interval leading into the early phase of H1 (Hudson et al., 2019).

5.3 Orbital-scale forcing

Given that the pluvial conditions in the Great Basin during glacial periods have been attributed to atmospheric reorganization driven by the extent of the North American ice sheets (Oster et al., 2015), changes in the Devils Hole water table are expected to correspond to the expansion and retreat of these ice sheets. Precisely dating the extent of North American ice sheets during MIS 5 remains challenging (Dalton et al., 2022). Although sea level reflects an integrated signal of the extent of global glaciation, it can be assumed that the timing of sea-level changes and North American ice sheet extent was strongly correlated (Lambeck and Chappell, 2001). Thus, precisely dated sea-level markers can be used to test the hypothesis that changes of the Devils Hole water table and ice sheet extent were near-synchronous. Simultaneous variations of Devils Hole water table and global sea level are apparent during MIS 5 (Fig. 6B). The water table lowstand associated with MIS 5c is the most well-constrained event in the refined record and was therefore compared to the timing of the MIS 5c sea-level highstand. A speleothem-based sea-level highstand in the Caribbean, documented from 103.9±0.6 ka to 96.8±0.4 ka (Steidle et al., 2021), aligns with other sea-level records that are less precisely dated (Wainer et al., 2017; Potter et al., 2004; Lundberg and Ford, 1994). There is very good agreement with the MIS 5c Devils Hole water-table lowstand between 104.3±0.3 ka and 97.5±0.3 ka, supporting a common link to ice-sheet extent.

The Devils Hole water table high- and lowstands followed the mid-July 65°N insolation with a delay of a few millennia during MIS 5 (i.e., from 120 ka to about 70 ka; Fig. 6A). Such a delayed response of the Great Basin hydroclimate agrees with other studies. Lachniet et al. (2017) found an average lag of 3240 years (-900 to 6600-year) in Great-Basin-stalagmite $\delta^{18}O$ data relative to Northern Hemisphere summer insolation, whereas Cheng et al. (2019) reported a ~5000-year lag in a similar study on the eastern side of North America. The delay is also apparent when comparing the MIS 5 Devils Hole water table to the Asian monsoon, which displays a strong response to precessional forcing on orbital timescales (Fig. 6C; Cheng et al., 2016). These delays result from the long response time of the North American ice sheets to insolation changes.

MIS 4 and MIS 2 were periods of low global sea level (Spratt and Lisiecki, 2016; Fig. 6B) and extensive North American glaciation (Dalton et al., 2022). In agreement with the mechanism described by Oster et al. (2015), Devils Hole water table was high during both of these stages (in excess of +8.3 m after 23.84±0.05 ka at MIS 2 and in excess of +9.9 m around 71.3±0.2 ka). While synchronous variations between the Devils Hole water table and sea level are evident during MIS 5 and across the MIS 1/2 transition, no such correspondence is observed during MIS 4. Between approximately 60 ka and 30 ka, sea level remained relatively low and stable.

Consequently, the North American ice sheets are likely present throughout this period, although a slight decrease in their extent around 40 ka has been documented (Dalton et al., 2022). The relationship between ice extent and additional moisture in the Great Basin is unlikely to be linear. Moreover, it remains unclear whether thresholds for moisture control exist and at what glacial extent they may occur. However, water table changes at Devils Hole recorded between 60 ka and 30 ka show no apparent correlation with sea level or North American ice sheet extent. This suggests MIS 4 and MIS 3 were influenced by a different forcing mechanism operating on shorter timescales, in contrast to MIS 5, where the dominant forcing mechanism appears to be linked to orbital variability.

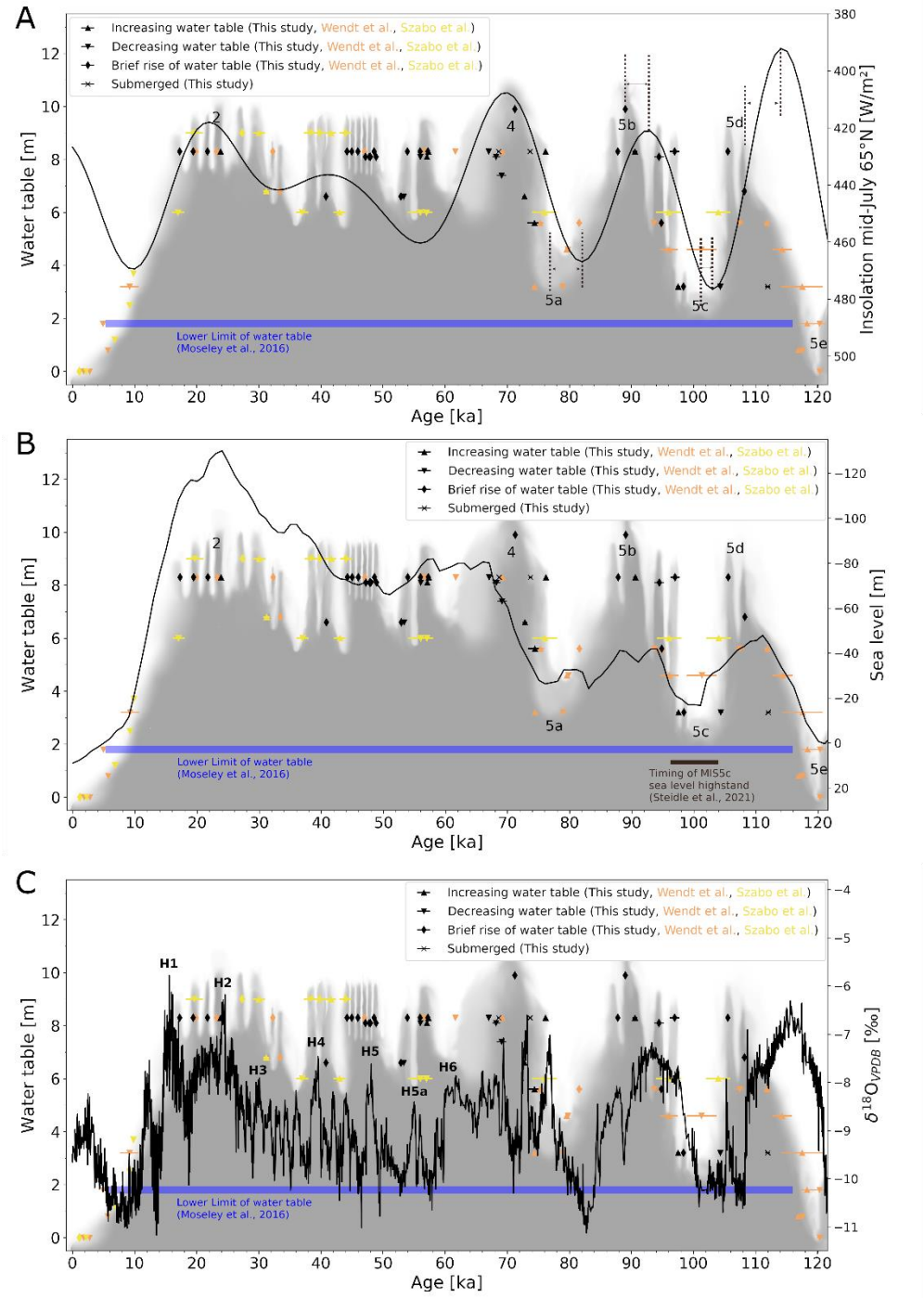

Fig. 6. *Devils Hole water table and insolation, sea level and Asian monsoon. Water table elevation relative to today's water table over the last glacial cycle. The grey shading is a visual aid to distinguish high probability of submergence (dark grey), high probability of no submergence (white), and intermediate probability (shades of gray). This is based on the data from three studies (Szabo et al., 1994; Moseley et al., 2016; Wendt et al., 2018; this study). The lower limit of water table during the last glacial cycle is defined by continuous mammillary calcite deposition (Moseley et al., 2016). The letters 2, 4 and 5a to 5e mark the timing of Marine Isotope Stages 2, 4 and 5a to 5e, which were associated with water table high- and lowstands in Devils Hole.* ***A:*** *Mid-July insolation at 65°N shown by the black curve (Berger, 1999). Dashed lines separated by arrows indicate the multi-millennial delay of water table low- and highstand with respect to insolation.* ***B:*** *Global sea level (Spratt and Lisiecki, 2016; note inverted Y axis). Black bar shows the timing of the MIS 5c Caribbean sea-level highstand (Steidle et al., 2021; y-coordinates are arbitrary).* ***C:*** *The Asian monsoon record as seen in speleothem $\delta^{18}O$ (Cheng et al., 2016). The letters H1 – H6 mark Heinrich events 1-6 as defined by positive $\delta^{18}O$ excursions by Cheng et al. (2016).*

5.4 Millennial-scale events

For the time interval between c. 60 and 20 ka (i.e., the start of Termination I), Devils Hole water table markers were consistently located at relatively high elevations between +6 m and +9 m (Szabo et al., 1994; Wendt et al., 2018; this study). Changes of the water table therefore occurred in excess of 3 m during MIS 4 to 2, which is significantly less than the amplitude of the changes during MIS 5 to 4, which were in excess of 6.7 m (Fig. 6).

As discussed in the previous section, water table variations are linked to North American ice sheet extent during MIS 5, as evidenced by the synchronicity with sea level changes (Fig. 6B) and a lag relative to mid-July 65°N insolation (Fig. 6A). However, no apparent link exists between these factors from about 60 ka to 30 ka. Instead, between 60 to 20 ka, multiple millennial-scale rises and falls of the water table overprint the high water table. Millennial-scale water table rises have been previously shown to coincide with H events (Wendt et al., 2018). H events mark the most important prolonged climatic disruptions during this period, serving as key reference points. These events triggered Northern Hemisphere cooling, resulting in global atmospheric reorganization, including southward shifts of the Intertropical Convergence Zone. This reorganization is documented by phases of weak Asian monsoon, precisely dated through positive excursions of rainfall $\delta^{18}O$ of East Asian speleothems (Cheng et al., 2016; Zhang et al., 2021).

The structure, forcing and global hydroclimate expressions of H events remain a topic of ongoing debate (Zhang et al., 2021; Oster et al., 2020). Within the Great Basin, there is, although debated, evidence of increased aridity in the northwest (Oster et al., 2020; Benson et al., 2003; Zic et al., 2002; Heaton et al., 2019) and pluvial conditions in the south (Munroe and Laabs, 2013; McGee et al., 2018; Oster et al., 2023) associated with H events and different mechanisms have been discussed (see introduction section; McGee et al., 2018; Oster et al., 2020; Heaton et al., 2019). Given its precise chronology aligned with H events, we use the Asian monsoon record as a reference for their timing.

H events were characterized by massive iceberg discharge into the North Atlantic with global impacts (Hemming, 2004). They occurred on shorter timescales than ice-sheet growth and decay and are therefore linked to a different mechanism. In the southern Great Basin, H events are widely associated with enhanced pluvial conditions (Munroe and Laabs, 2013; McGee et al., 2018; Oster et al., 2023). This response is hypothesized to result from Northern Hemisphere winter cooling, which triggered a southward shift of the Intertropical Convergence Zone and Hadley cell, a southeastward displacement of the Aleutian Low, and an intensification of the subtropical jet — ultimately increasing transport of subtropical moisture into the western United States (McGee et al., 2018). Some studies from the northwestern Great Basin suggest drying during H5 to H2 (Oster et al., 2020; Benson et al., 2003; Zic et al., 2002; Heaton et al., 2019). The boundary between wetter and drier regions was, however, likely temporally and spatially transgressive (Oster et al., 2020).

A single brief rise at 17.28±0.08 ka is recorded at Devils Hole, falling into the early part of H1, However, the absence of data for the subsequent few millennia, combined with the clustering of water-table markers near +8.3 m —which prevents estimating the event's amplitude— limits our ability to draw conclusions regarding H1 and the onset of Termination I.

The Asian monsoon record shows a weak phase from 24.4 ka to 23.6 ka associated with H2 (Qiu et al., 2024; Cui et al., 2024). This was simultaneous with a relatively high water table at Devils Hole marked by a rise at +8.3 m at 23.84±0.05 ka. The corresponding mammillary calcite layer is comparably thick (5 mm). This was the longest wet phase of the past 40 ka, as documented by the core at +8.3 m. It also coincided with peak MIS 2 and maximum extent of the North American ice sheets (Dalton et al., 2022), leaving it unclear to what extent the mechanism discussed in the previous section - or a different process related to this H event - gave rise to pluvial conditions in the aquifer's catchment that feeds Devils Hole.

H3 is weakly expressed in the Asian monsoon record around 30 ka (Cheng et al., 2016). We did not identify any corresponding highstand in Devils Hole around this time. Szabo et al. (1994) reported a rise in Devils Hole water table from +6.8 m at 31.2±0.5 ka to over +9 m at 30±1 ka that agree with the timing of H3 and could be attributed to the onset of a pluvial phase that lacks a well-defined end date.

H4 is strongly pronounced in the Asian monsoon record and lasted from 40.04±0.07 ka to 37.76±0.05 ka (Zhang et al., 2021). At Devils Hole, Szabo et al. (1994) dated a highstand at more than +9 m to around 40 ka, lasting for about 2 millennia. In the cores analyzed in this study, there is a remarkable absence of mammillary calcite above +6.6 m. While no additional evidence was found linking H4 to a wetter climate, this does not imply a more arid climate.

H5 is recorded from 48.1 ka to 46.9 ka in the Asian monsoon domain (Dong et al., 2018) and coincided with a relatively high (+8.3 m) water table between 48.9±0.2 ka and 44.2±0.1 ka at Devils Hole. Because this wet phase started before and ended after the weak monsoon interval, it remains unclear whether pluvial conditions at Devils Hole were specifically associated with H5. However, it can be concluded that no aridification occurred during this event.

Devils Hole shows a 1 ka-long highstand above +8.1 m between 57.1±0.3 ka and 56.0±0.2 ka, while multiple brief highstands at +8.3 m occurred between 57.3±0.2 ka and 53.9±0.1 ka. The highstand at +8.1 m falls mostly in between H5a (55.12 ka to 54.65 ka - Zhang et al., 2021b) and 6 (61.5±0.2 ka to 59.4±0.2 ka - Zhang et al., 2017) of the Asian monsoon record. This disagreement in the timing between this well-developed mammillary calcite layer at +8.1 m and known H events suggests that the latter were not associated with an increase in water table. With a water table decline at +6.6 m shortly after 53.3±0.3 ka, i.e. postdating H5a, there is also no indication of increased aridity, but rather of a constantly humid hydroclimate from before H6 to after H5a.

Overall, it can be concluded that H events, as defined by precisely dated speleothems recording weak Asian monsoon intervals, generally coincided with a high water table at Devils Hole with new data particularly around H5 and H5a. No clear conclusion can be drawn for H3 and H4 due to scarce or inconsistent data. In the case of H3, the climate change may have been too subtle to detect.

The synchronicity of high Devils Hole water tables and weak Asian monsoon intervals suggests a common underlying cause. For the Asian monsoon, this is attributed to southward shifts of the Intertropical Convergence Zone (Cheng et al., 2016; Zhang et al., 2021). In the Great Basin, such shifts during H events have been associated with an intensification of the subtropical jet and a southeastward displacement of the Aleutian Low, ultimately increasing winter precipitation in the SW USA (McGee et al., 2018). Our study's findings support this climate scenario.

6. CONCLUSIONS

This study refines the Devils Hole water-table record for the last glacial cycle and provides new constraints on the hydroclimatic evolution of the southern Great Basin. By integrating detailed characterization of mammillary calcite with high-resolution U-series dating, we identify previously unrecognized variability during MIS 5 and resolve multiple short-lived water-table events between 60 and 20 ka. Samples younger than 60 ka were examined petrographically and, after the removal of two outliers, show mammillary calcite fabrics. We also screened all samples for $\delta^{234}U_{initial}$ and excluded those with anomalous values. These steps ensure that the remaining data points are reliably dated.

During MIS 5, the Devils Hole water table displays a clear correspondence with global sea-level variability and Northern Hemisphere summer insolation on orbital timescales. The close alignment of the MIS 5c lowstand with the precisely dated Caribbean sea-level highstand indicates that water-table behavior in the southern Great Basin was strongly linked to the waxing and waning of North American ice sheets. The multi-millennial lag of Devils Hole water-table changes relative to insolation reflects the slow response time of continental ice sheets to orbital forcing and provides a clear indication that Devils Hole water table and ice sheet extent are directly linked.

In contrast, from ~60 to 30 ka, sea-level and ice-sheet changes remained relatively muted, and no systematic relationship with Devils Hole water-table variability can be identified, suggesting that different forcing mechanisms dominated this interval. During this time, our refined record reveals repeated, brief water-table rises on millennial timescales. Although Heinrich events generally coincide with high water tables at Devils Hole, the record does not provide sufficient resolution to reconstruct the history of individual events.

The overall synchronicity between high water tables at Devils Hole and weakened Asian monsoon phases supports a climate mechanism involving southward displacement of the Intertropical Convergence Zone, intensification of the subtropical jet, and enhanced winter moisture delivery to the southern Great Basin during Heinrich events.

Together, these findings show that the southern Great Basin hydroclimate responded to distinct forcing processes operating on different timescales. Orbital-scale water-table variations were governed by ice-sheet dynamics, whereas millennial-scale fluctuations were driven by rapid atmospheric reorganizations associated with Heinrich events. By extending the temporal resolution of the Devils Hole record, this study provides new insights into the mechanisms that controlled past groundwater recharge in the region. These insights underscore the sensitivity of the Great Basin hydroclimate to rapid climate perturbations and offer an improved framework for interpreting future hydroclimatic change in this water-limited region.

ACKNOWLEDGMENTS

This research was funded by grant P327510 of the Austrian Science Fund to CS. Fieldwork was possible under the scientific research and collecting permits of the United States National Park Services DEVA-2022-SCI-0014, DEVA-2017-SCI-0002 and DEVA-2015-SCI-0006. This contribution was partially supported by NSF grant 2202913 to RLE.

AUTHOR CONTRIBUTIONS

Conceptualization: CS, KAW, SDS; Data curation: SDS; Formal analysis: SDS; Funding acquisition: CS, KAW, RLE; Investigation: CS, YD, SDS; Methodology: MR, KAW, SDS; Project administration: CS, YD; Resources: CS, RLE, MR; Supervision: CS, YD, RLE Visualization: SDS; Roles/Writing - original draft: SDS; Writing - review & editing: SDS, YD, KAW, MR, GEM, RLE, CS.

DATA AVAILABILITY

The dating results are published on PANGAEA (https://doi.org/10.1594/PANGAEA.988350). Additionally they and all other~~All~~ data relevant to the discussion and conclusions ~~is~~ are given as ~~Supplemental~~ Supplementary Material to this study.

REFERENCES

Bajnai, D. et al., 2021 Devils Hole calcite was precipitated at ±1°C stable aquifer temperatures during the last half million years. Geophysical Research Letters 48 https://doi.org/10.1029/2021GL093257

Benson, L. et al., 2003 Response of North American Great Basin Lakes to Dansgaard–Oeschger oscillations. Quaternary Science Reviews 22:2239-2251 https://doi.org/10.1016/S0277-3791(03)00210-5

Berger, A., 1999 Parameters of the Earths orbit for the last 5 Million years in 1 kyr resolution. PANGAEA, https://doi.org/10.1594/PANGAEA.56040

Cheng, H. et al., 2013 Improvements in ^{230}Th dating, ^{230}Th and ^{234}U half-life values, and U–Th isotopic measurements by multi-collector inductively coupled plasma mass spectrometry. Earth and Planetary Science Letters. 371-372:82-91 https://doi.org/10.1016/j.epsl.2013.04.006

Cheng, H. et al., 2019 Eastern North American climate in phase with fall insolation throughout the last three glacial-interglacial cycles. Earth and Planetary Science Letters 522:125-134 https://doi.org/10.1016/j.epsl.2019.06.029

Cui, Y. et al., 2024 Chronological features of Heinrich Stadial 2 based on a high-resolution analysis of δ^{18}O stalagmite records from China, and possible links to changes in Atlantic Meridional Overturning Circulation. Paleogeography, Paleoclimatology, Paleoecology 633 https://doi.org/10.1016/j.palaeo.2023.111875

Dalton, A. S. et al., 2022 Evolution of the Laurentide and Innuitian ice sheets prior to the Last Glacial Maximum (115 ka to 25 ka). Earth-Science Reviews 224 https://doi.org/10.1016/j.earscirev.2021.103875

Deacon, J.E. and Williams, A.E., 1991 Ash Meadows and the legacy of the Devils Hole pupfish. In: Battle against extinction: native fish management in the American West: 69-87.

Deacon, J.E. et al., 2007 Fueling population growth in Las Vegas: How large-scale groundwater withdrawal could burn regional biodiversity. BioScience 57,8: 688-698 https://doi.org/10.1641/B570809

Dong, J. et al., 2018 Asian monsoon dynamics at Dansgaard/Oeschger events 14–8 and Heinrich events 5–4 in northern China. Quaternary Geochronology 47:72-80 https://doi.org/10.1016/j.quageo.2018.05.012

Dublyansky, Y. and Spötl, C., 2015 Condensation-corrosion speleogenesis above a carbonate-saturated aquifer: Devils Hole Ridge, Nevada. Geomorphology 229:17-29 http://dx.doi.org/10.1016/j.geomorph.2014.03.019

Edwards, R.L. et al., 1987 ^{238}U-^{234}U-^{230}Th-^{232}Th systematics and the precise measurement of time over the past 500,000 years. Earth and Planetary Science Letters. 81, 175–192 https://doi.org/10.1016/0012-821X(87)90154-3

Halford, K.J. and Jackson, T.R., 2020 Groundwater characterization and effects of pumping in the Death Valley regional groundwater flow system, Nevada and California, with special reference to Devils Hole. U.S. Geological Survey Professional Paper 1863. https://doi.org/10.3133/pp1863

Heaton, E.J. et al., 2019 A Great Basin lake-level response to 38–34 ka Dansgaard–Oeschger oscillations. Journal of Paleolimnology 61:263-278 https://doi.org/10.1007/s10933-018-0057-5

Hemming, S.R., 2004 Heinrich events: Massive late Pleistocene detritus layers of the North Atlantic and their global climate imprint. Reviews of Geophysics 42 https://doi.org/10.1029/2003RG000128

Hudson, A.M. et al., 2019 North-south dipole in winter hydroclimate in the western United States during the last deglaciation. Scientific Reports 9 https://doi.org/10.1038/s41598-019-41197-y

Hudson, A.M. et al., 2023 Paleohydrologic history of pluvial lake San Agustin, New Mexico: Tracking changing effective moisture in southwest North America through the last glacial transition. Quaternary Science Reviews 310 https://doi.org/10.1016/j.quascirev.2023.108110

Ibarra, D.E. et al., 2014 Rise and fall of late Pleistocene pluvial lakes in response to reduced evaporation and precipitation: Evidence from Lake Surprise, California. Geol. Soc. Am. Bull. 126 https://doi.org/10.1130/B31014.1

Jackson, T.R. and Steidle, S.D. et al., 2023 A 350,000-year history of groundwater recharge in the southern Great Basin, USA. Communications Earth and Environment 4: 98 https://doi.org/10.1038/s43247-023-00762-0

Kluge, T. et al., 2014 Devils Hole paleotemperatures and implications for oxygen isotope equilibrium fractionation. Earth and Planetary Science Letters 400: 251-260 https://doi.org/10.1016/j.epsl.2014.05.047

Lachniet, M.S., et al., 2017 Arctic cryosphere and Milankovitch forcing of Great Basin paleoclimate. Scientific Reports 7:12955 https://doi.org/10.1038/s41598-017-13279-2

Lambeck, K. and Chappell, J., 2001 Sea level change through the last glacial cycle. Science 292: 679-686 https://doi.org/10.1126/science.1059549

Li, X. et al., 2019 Novel method for determining ^{234}U–^{238}U ages of Devils Hole 2 cave calcite (Nevada). Geochronology 3: 49-58 https://doi.org/10.5194/gchron-3-49-2021

626 Lowenstein, T.K., et al., 2024 Unified 200 kyr paleohydrologic history of the Southern Great
627 Basin: Death Valley, Searles Valley, Owens Valley and Devils Hole cave. Quaternary
628 Science Reviews 336 https://doi.org/10.1016/j.quascirev.2024.108751
629 Lundberg, J. and Ford, D.C. 1994 Late Pleistocene sea level change in the Bahamas from mass
630 spectrometric U-series dating of submerged speleothem. Quaternary Science Reviews
631 13:1-14 https://doi.org/10.1016/0277-3791(94)90121-X
632 MacDonald, G.M., 2010 Water, climate change, and sustainability in the southwest. PNAS
633 107:21256-21262 https://doi.org/10.1073/pnas.0909651107
634 McGee, D. et al., 2018 Western U.S. lake expansions during Heinrich stadials linked to Pacific
635 Hadley circulation. Science Advances 4,11 https://doi.org/10.1126/sciadv.aav0118
636 Moseley, G.E. et al., 2016 Reconciliation of the Devils Hole climate record with orbital forcing.
637 Science 351: 165-168 https://doi.org/10.1126/science.aad4132
638 Munroe, J.S. and Laabs, B.J.C., 2013 Temporal correspondence between pluvial lake highstands
639 in the southwestern US and Heinrich Event 1. Journal of Quaternary Science 28:49-58
640 https://doi.org/10.1002/jqs.2586
641 Oster, J.L. et al., 2015 Steering of westerly storms over western North America at the Last
642 Glacial Maximum. Nat. Geosci. 8: 201-205 https://doi.org/10.1038/ngeo2365
643 Oster, J.L. et al., 2020 Multi-proxy stalagmite records from northern California reveal dynamic
644 patterns of regional hydroclimate over the last glacial cycle. Quaternary Science Reviews
645 241,106411 https://doi.org/10.1016/j.quascirev.2020.106411
646 Oster, J.L. et al., 2023 North Atlantic meltwater during Heinrich Stadial 1 drives wetter climate
647 with more atmospheric rivers in western North America. Science Advances 9(46)
648 https://doi.org/10.1126/sciadv.adj2225
649 Potter, E.K. et al., 2004 Suborbital-period sealevel oscillations during marine isotope substages
650 5a and 5c. Earth and Planetary Science Letters 225:191–204.
651 https://doi.org/10.1016/j.epsl.2004.05.034
652 Qiu, W. et al., 2024 Synchronous anti-phase variations between the East Asian summer monsoon
653 and South America Summer Monsoon during Heinrich stadial 2. Quaternary Science
654 Reviews 323 https://doi.org/10.1016/j.quascirev.2023.108434
655 Reheis, M.C. et al., 2015 Directly dated MIS 3 lake-level records from Lake Manix, Mojave
656 Desert, California, USA. Quaternary Research 83
657 http://dx.doi.org/10.1016/j.yqres.2014.11.003
658 Reheis, M.C. et al., 2019 Pleistocene lakes and paleohydrologic environments of the Tecopa
659 basin, California: Constraints on the drainage integration of the Amargosa River. GSA
660 Bulletin 132:1537-1565, https://doi.org/10.1130/B35282.1
661 Santi, L.M. et al., 2020 Clumped isotope constraints on changes in latest Pleistocene
662 hydroclimate in the northwestern Great Basin: Lake Surprise, California. GSA Bulletin
663 132:2669-2683 https://doi.org/10.1130/B35484.1
664 Seltzer, A.M. et al., 2019 Deglacial water-table decline in Southern California recorded by noble
665 gas isotopes. Nature Communications 10 https://doi.org/10.1038/s41467-019-13693-2
666 Shen, C.C. et al., 2002 Uranium and thorium isotopic and concentration measurements by
667 magnetic sector inductively coupled plasma mass spectrometry Chemical. Geology,
668 185:165–178 https://doi.org/10.1016/S0009-2541(01)00404-1
669 Shen, C.C. et al., 2012 High-precision and high-resolution carbonate ^{230}Th dating by MC-ICP-
670 MS with SEM protocols. Geochimica et Cosmochimica Acta. 99:71–86
671 https://doi.org/10.1016/j.gca.2012.09.018

Spratt, R.M. and Lisiecki, L.E., 2016 A Late Pleistocene sea level stack. Clim. Past 12:1079-1092 https://cp.copernicus.org/articles/12/1079/2016/

Steidle, S.D. et al., 2024 Moisture availability and groundwater recharge paced by orbital forcing over the past 750,000 years in the southwestern USA. Commun Earth Environ 5, 376 https://doi.org/10.1038/s43247-024-01550-0

Steidle, S.D. et al., 2021 Reconstruction of Middle to Late Quaternary sea level using submerged speleothems from the northeastern Yucatán Peninsula. Journal of Quaternary Science 36:1190-1200 https://doi.org/10.1002/jqs.3365

Steidle, S.D. et al., 2026 Th-U ages over the last 112,000 years from Devils Hole calcite (NV, USA) for palaeo water table reconstruction [dataset]. PANGAEA, https://doi.org/10.1594/PANGAEA.988350

Szabo, B.J. et al., 1994 Paleoclimatic inferences from a 120,000-Yr calcite record of water-table fluctuation in Browns Room of Devils Hole, Nevada. Quaternary Research 41: 59-69 https://doi.org/10.1006/qres.1994.1007

Van Elteren, J.T. et al., 2019 Insights into the selection of 2D LA-ICP-MS (multi)elemental mapping conditions. Journal of Analytical Atomic Spectrometry 34:1919-1931 https://doi.org/10.1039/C9JA00166B

Wainer, K.A.I. et al., 2017 Speleothem evidence for MIS 5c and 5a sea level above modern level at Bermuda. Earth and Planetary Science Letters 457:325–334. https://doi.org/10.1016/j.epsl.2016.10.005

Wendt, K.A. et al., 2018 Moisture availability in the southwest United States over the last three glacial-interglacial cycles. Science Advances 4,10 https://doi.org/10.1126/sciadv.aau1375

Wendt, K.A. et al., 2020 Paleohydrology of southwest Nevada (USA) based on groundwater $^{234}U/^{238}U$ over the past 475 k.y.. GSA Bulletin 132:793-802 https://doi.org/10.1130/B35168.1

Winograd, I.J. et al., 1992 Continuous 500,000-year climate record from vein calcite in Devils Hole, Nevada. Science 258: 255-260 https://doi.org/10.1126/science.258.5080.255

Winograd, I.J. et al., 1998 The relative contributions of summer and cool-season precipitation to groundwater recharge, Spring Mountains, Nevada, USA. Hydrogeology Journal 6: 77-93 https://doi.org/10.1007/s100400050135

Zhang, T.T. et al., 2017 Stalagmite-inferred centennial variability of the Asian summer monsoon in southwest China between 58 and 79 ka BP. Quaternary Science Reviews 160:1-12 https://doi.org/10.1016/j.quascirev.2017.02.003

Zhang, X. et al., 2021 Three-phase structure of the East Asia summer monsoon during Heinrich Stadial 4 recorded in Xianyun Cave, southeastern China. Quaternary Science Reviews 274 https://doi.org/10.1016/j.quascirev.2021.107267

Zhang, X. et al., 2021b A gradual transition into Greenland interstadial 14 in southeastern China based on a sub-decadally-resolved stalagmite record. Quaternary Science Reviews 253 https://doi.org/10.1016/j.quascirev.2020.106769

Zic, M. et al., 2002 Evidence of synchronous climate change across the Northern Hemisphere between the North Atlantic and the northwestern Great Basin, United States. Geology 30:635-638 https://doi.org/10.1130/0091-7613(2002)030%3C0635:EOSCCA%3E2.0.CO;2

Supplemental Material

Outlier detection based on $\delta^{234}U_{initial}$

The $\delta^{234}U_{initial}$ of Devils Hole calcite is narrowly defined (Wendt et al., 2019; Li et al., 2021) and reflects long-term water table changes and associated water-rock interactions in the aquifer upstream of Devils Hole (Wendt et al., 2019). It can therefore be used to check the integrity of samples of mammillary calcite because $\delta^{234}U_{initial}$ and age are interdependent. As an objective measure to identify outliers, data from Wendt et al. (2018), Li et al. (2021) and from this study that are both younger than 121.5 ka and have a $\delta^{234}U_{initial} < 1970$ were considered. A polynomial function of the form $y = a*x^5 + b*x^4 + c*x^3 + d*x^2 + e*x + f$ was fitted with a least squares algorithm to this dataset. With y as $\delta^{234}U_{initial}$ in ‰ and x as age in ka, the resulting parameters are: a = 1.12157714e-09, b = -3.13912768e-06, c = 5.57952974e-04, d = -6.10460779e-02, e = 3.66951373e+00 and f = 1.72895397e+03. Samples outside of a ±40 ‰ range were considered outliers and omitted (Fig. S1). Eight out of the 53 samples were removed: SS37, SS38, SS40, SS22, SS180, SS20, SS174 and SS13.

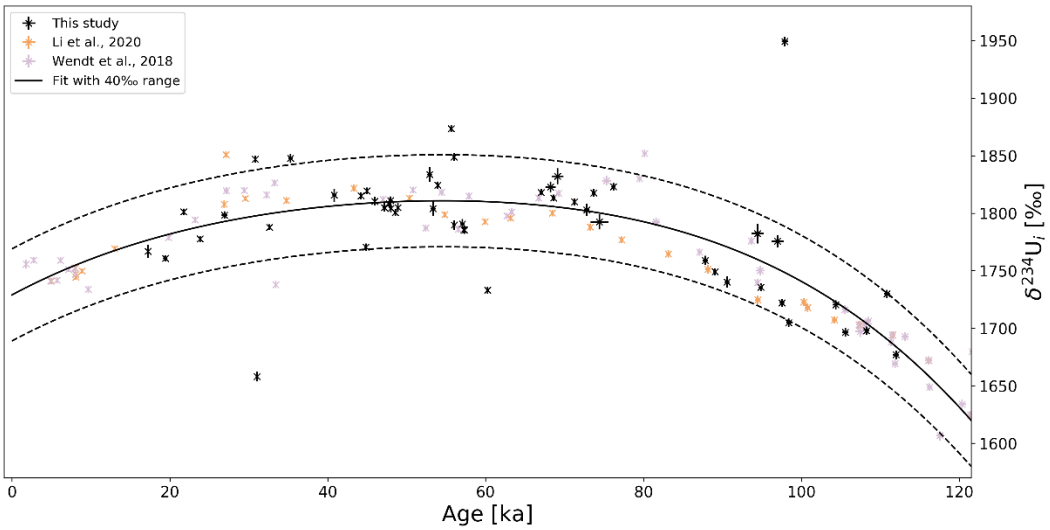

Fig. S1. *$\delta^{234}U_{initial}$ against time. A polynomial function was fitted to all data points. Samples from this study outside of the 40‰ range were not considered for the water table reconstruction.*

Changes in groundwater availability over the last 120 ka

Recharge is the measure that determines how much groundwater can be used for sustainable socio-economic needs. Its susceptibility to changes in climate forcing is therefore a crucial parameter for climate mitigation measures. A recent groundwater model (Jackson et al., 2023) makes it possible to infer the recharge to the Ash Meadows groundwater basin from the Devils Hole water table over the last glacial cycle. The new constraints on the Devils Hole water table allow for a more precise analysis of recharge changes during the last glacial period.

During MIS 5c, the water table lowstand at Devils Hole remained in a narrow range between +3.2 m and +1.8 m. Using the scaled-recharge scenario of Jackson et al. (2023), this translates into a recharge between 143% (for +3.2 m) and 120% (for +1.8 m) relative to today. MIS 5b experienced a water table rise to more than +9.9 m, which translates into a recharge of more than 363% relative to today. This suggests that recharge increased by at least +150% from peak MIS 5c to peak MIS 5b.

Between 60 ka and 20 ka, the water table oscillated between less than +6 m to more than +9 m. This corresponds to a change between less than 210% and more than 322% of today's recharge. The relative change was more than +50% (from +6 m to +9 m) or more than -35% (from +9 m to +6 m).

It is important to note that the link between external climate forcing and changes in recharge is non-linear. Given the generally higher recharge during the last glacial period compared to today, similar absolute changes in external climate forcing can lead to higher relative and smaller absolute changes during the presently hot and arid regional climate in the southern Great Basin.

Trace element analysis of Devils Hole calcite

Table S1. *Average trace element ratios and standard deviations of mammillary calcite and folia as shown in Fig. 2.*

[mmol/mol]	**Mamm-l (d)**	**Mamm-h (d)**	**Folia (d)**	**Mamm-l (v)**	**Mamm-h (v)**	**Folia (v)**
Mg/Ca	35.1±10	39.7±9.8	8.1±5.8	35.5±7.0	39.2±8.8	7.1±8.8
Sr/Ca	0.24±0.05	0.97±0.28	0.23±0.21	0.24±0.06	0.76±0.17	0.14±0.14
Ba/Ca	0.006±0.003	0.053±0.059	0.007±0.011	0.005±0.003	0.049±0.015	0.008±0.017

Table S2. *Averaged trace element ratios of calcite layers <60 ka BP. The classification (last column) is based on the scheme defined in Fig. 3.*

Sample ID	**Mg/Ca**	**Sr/Ca**	**Ba/Ca**	**Classification**
SS24	42.5±8.2	1.11±0.84	0.076±0.034	Mamm-h
SS25	46.4±13.0	1.21±0.75	0.077±0.025	Mamm-h
SS22	42.8±41.1	0.97±0.31	0.074±0.020	Mamm-h
SS4	45.3±8.6	0.99±0.24	0.068±0.023	Mamm-h
SS5	45.7±14.4	0.89±0.28	0.059±0.016	Mamm-h
SS35	43.7±12.1	0.82±0.42	0.079±0.097	Mamm-h
SS34	47.4±8.4	0.83±0.64	0.087±0.070	Mamm-h
SS33	43.0±11.0	0.88±1.48	0.101±0.037	Mamm-h
SS38	40.4±9.7	0.84±0.89	0.050±0.040	Mamm-h
SS37	43.6±33.0	0.81±0.88	0.063±0.026	Mamm-h
SS36	43.2±11.6	0.87±0.90	0.081±0.158	Mamm-h
SS30	44.0±31.6	1.00±0.37	0.076±0.022	Mamm-h
SS31	57.5±32.6	0.95±0.41	0.055±0.034	Mamm-h
SS17	5.0±13.7	0.86±0.53	0.069±0.034	Folia
SS18	3.6±10.8	0.23±1.25	0.008±0.086	Folia
SS20	25.7±5.4	0.22±0.23	0.006±0.030	Mamm-l
SS182	55.1±23.3	1.05±0.31	0.065±0.024	Mamm-h
SS183	58.7±13.1	1.29±0.40	0.078±0.023	Mamm-h
SS184	46.5±8.4	0.89±0.38	0.058±0.016	Mamm-h
SS185	43.4±7.8	0.81±0.26	0.054±0.020	Mamm-h
SS186	49.0±7.1	1.03±0.18	0.066±0.013	Mamm-h
SS187	47.0±8.5	1.04±0.29	0.069±0.021	Mamm-h
SS188	46.1±13.0	0.90±0.24	0.057±0.018	Mamm-h
SS171	39.6±13.3	0.24±0.34	0.007±0.030	Mamm-l
SS172	37.5±13.6	0.19±0.07	0.005±0.018	Mamm-l
SS173	45.1±24.2	0.54±0.45	0.041±0.033	Mamm-l/-h
SS174	38.9±26.7	0.20±0.49	0.007±0.016	Mamm-l

Scans of drill cores

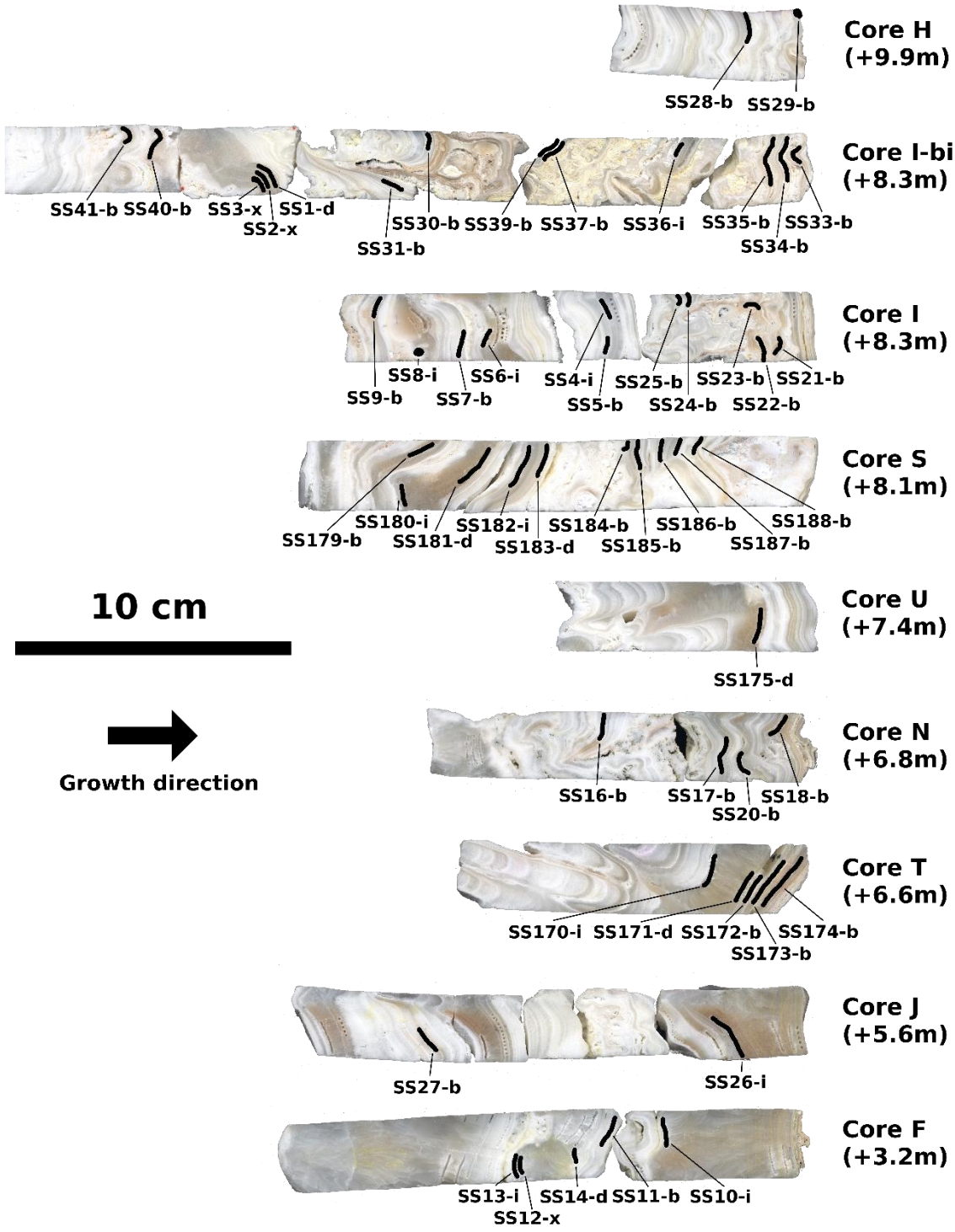

Fig. S2. *Positions of the 53 samples used for U-series dating sampled from nine horizontal drill cores (see Fig. 1).*

Table S3. *53 U-series dates.*

Sample Name	Core	Elev. [m]	type	note	^{238}U [ppb_{mass}]	^{232}Th [ppt_{mass}]	$^{230}Th/^{232}Th$ [at. ratio x10^{-6}]	$\delta^{234}U_{meas}$	$^{230}Th/^{238}U$ [act. Ratio]	^{230}Th-U age_{uncorr} [years]	^{230}Th-U age_{corr} [years]	$\delta^{234}U_{init}$	^{230}Th-U age_{corr} [years before 1950]
SS29	H	9,9	b		1641,4 ±2,1	1982 ±40	17186 ±346	1479,9 ±2,2	1,2587 ±0,0020	71337 ±173	**71325 ±173**	1810 ±3	**71255 ±173**
SS28	H	9,9	b		1593,3 ±2,1	867 ±18	42649 ±864	1360,2 ±2,2	1,4074 ±0,0024	89128 ±245	**89122 ±245**	1749 ±3	**89052 ±245**
SS33	I-bis	8,3	b		1955,3 ±17,7	3624 ±80	3956 ±94	1666,4 ±2,3	0,4446 ±0,0057	19529 ±271	**19509 ±271**	1761 ±3	**19439 ±271**
SS34	I-bis	8,3	b		1866,3 ±466,5	1294 ±324	9517 ±195	1682,6 ±5,6	0,4003 ±0,0015	17334 ±80	**17327 ±81**	1767 ±6	**17257 ±81**
SS35	I-bis	8,3	b		1357,2 ±1,6	6598 ±132	1692 ±34	1693,6 ±2,5	0,4990 ±0,0010	21876 ±54	**21826 ±65**	1801 ±3	**21756 ±65**
SS36	I-bis	8,3	i		1674,5 ±1,8	2237 ±45	6605 ±133	1661,7 ±2,4	0,5352 ±0,0008	23920 ±45	**23906 ±46**	1778 ±3	**23836 ±46**
SS37	I-bis	8,3	b	omitted	3967,1 ±12,9	29190 ±592	1441 ±29	1518,6 ±3,9	0,6430 ±0,0024	31197 ±144	**31117 ±154**	1658 ±4	**31047 ±154**
SS38	I-bis	8,3	b	omitted	1835,4 ±3,5	8225 ±165	3300 ±66	1559,7 ±2,8	0,8970 ±0,0021	44942 ±138	**44895 ±142**	1770 ±3	**44825 ±142**
SS31	I-bis	8,3	b		1435,8 ±2,1	1380 ±28	16508 ±332	1569,6 ±2,6	0,9622 ±0,0017	48637 ±121	**48627 ±122**	1800 ±3	**48557 ±122**
SS30	I-bis	8,3	b		1554,2 ±2,3	7300 ±146	3680 ±74	1566,5 ±2,5	1,0482 ±0,0020	54054 ±142	**54006 ±146**	1824 ±3	**53936 ±146**
SS1	I-bis	8,3	d		698,8 ±0,9	6755 ±135	2072 ±42	1504,3 ±2,4	1,2147 ±0,0023	67196 ±189	**67096 ±202**	1818 ±3	**67026 ±202**
SS2	I-bis	8,3	x		461,3 ±0,5	5761 ±115	1626 ±33	1493,7 ±2,3	1,2318 ±0,0020	68822 ±172	**68693 ±194**	1813 ±3	**68623 ±194**
SS3	I-bis	8,3	x		469,8 ±37,6	6604 ±529	1514 ±30	1476,0 ±2,6	1,2907 ±0,0027	73907 ±231	**73762 ±253**	1818 ±3	**73692 ±253**
SS40	I-bis	8,3	b	omitted	453,8 ±0,5	7133 ±143	1153 ±23	1461,9 ±2,4	1,0992 ±0,0017	60476 ±150	**60309 ±191**	1733 ±3	**60239 ±191**
SS41	I-bis	8,3	b		431,9 ±0,6	38961 ±781	273 ±5	1350,3 ±2,7	1,4964 ±0,0028	98002 ±326	**97053 ±745**	1776 ±5	**96983 ±745**
SS21	I	8,3	b		1438,4 ±2,0	2422 ±49	8952 ±181	1602,2 ±2,5	0,9142 ±0,0020	45057 ±127	**45040 ±127**	1819 ±3	**44970 ±127**
SS22	I	8,3	b	omitted	1447,9 ±2,0	4037 ±81	6443 ±130	1600,8 ±2,4	1,0895 ±0,0023	55746 ±161	**55718 ±163**	1873 ±3	**55648 ±163**
SS23	I	8,3	b		1407,4 ±1,8	990 ±20	21130 ±429	1601,9 ±2,5	0,9011 ±0,0020	44297 ±127	**44290 ±127**	1815 ±3	**44220 ±127**
SS24	I	8,3	b		1556,6 ±2,4	631 ±13	37671 ±764	1589,7 ±3,3	0,9263 ±0,0021	46035 ±145	**46031 ±145**	1810 ±4	**45961 ±145**
SS25	I	8,3	b		1601,5 ±2,1	541 ±11	52915 ±1073	1578,3 ±2,7	1,0848 ±0,0020	56070 ±148	**56066 ±148**	1849 ±3	**55996 ±148**
SS4	I	8,3	i		1475,7 ±2,0	1447 ±29	18150 ±365	1518,5 ±2,8	1,0791 ±0,0019	57395 ±150	**57385 ±151**	1785 ±3	**57315 ±151**
SS5	I	8,3	b		1526,5 ±1,7	358 ±7	75726 ±1529	1519,1 ±2,4	1,0778 ±0,0015	57293 ±119	**57290 ±119**	1786 ±3	**57220 ±119**
SS6	I	8,3	i		783,3 ±1,0	14051 ±282	1213 ±24	1470,0 ±2,4	1,3201 ±0,0023	76427 ±206	**76242 ±244**	1823 ±3	**76172 ±244**
SS7	I	8,3	b		1814,2 ±3,3	663 ±13	63194 ±1279	1372,6 ±2,9	1,4014 ±0,0034	87902 ±341	**87898 ±341**	1759 ±4	**87828 ±341**
SS8	I	8,3	i		569,6 ±1,1	568 ±11	23415 ±473	1347,4 ±3,6	1,4163 ±0,0031	90658 ±354	**90647 ±354**	1740 ±5	**90577 ±354**
SS9	I	8,3	b		1504,9 ±2,5	2227 ±45	16815 ±340	1259,2 ±2,5	1,5093 ±0,0032	105646 ±390	**105630 ±390**	1696 ±4	**105560 ±390**
SS188	S	8,1	b		1248,2 ±2,4	347 ±10	56799 ±1582	1581,3 ±3,1	0,9568 ±0,0031	48041 ±199	**48038 ±199**	1811 ±4	**47966 ±199**
SS187	S	8,1	b		1389,1 ±2,8	303 ±10	72048 ±2297	1579,6 ±3,2	0,9535 ±0,0029	47882 ±187	**47879 ±187**	1808 ±4	**47807 ±187**
SS186	S	8,1	b		1395,1 ±2,8	495 ±14	43778 ±1216	1579,7 ±3,2	0,9430 ±0,0031	47249 ±202	**47245 ±202**	1805 ±4	**47173 ±202**
SS185	S	8,1	b		1351,2 ±2,9	618 ±14	34439 ±795	1575,4 ±3,2	0,9549 ±0,0029	48062 ±193	**48057 ±193**	1804 ±4	**47985 ±193**
SS184	S	8,1	b		1641,1 ±3,5	1948 ±40	13454 ±278	1571,8 ±3,2	0,9687 ±0,0031	48985 ±201	**48973 ±201**	1805 ±4	**48901 ±201**
SS183	S	8,1	d		1411,3 ±3,1	708 ±15	34942 ±758	1527,6 ±3,2	1,0633 ±0,0034	56097 ±240	**56092 ±240**	1790 ±4	**56020 ±240**
SS182	S	8,1	i		1482,3 ±3,7	1066 ±22	24715 ±514	1524,0 ±3,4	1,0777 ±0,0036	57144 ±256	**57136 ±256**	1791 ±4	**57064 ±256**
SS181	S	8,1	d		503,3 ±0,6	42744 ±857	241 ±5	1503,2 ±2,7	1,2415 ±0,0026	69176 ±212	**68298 ±686**	1823 ±5	**68226 ±686**
SS180	S	8,1	i	omitted	520,4 ±0,6	2791 ±56	4865 ±99	1478,5 ±2,7	1,5825 ±0,0043	98026 ±420	**97973 ±421**	1949 ±4	**97901 ±421**
SS179	S	8,1	b		386,0 ±1,0	26285 ±531	358 ±7	1364,9 ±5,8	1,4769 ±0,0054	95230 ±617	**94516 ±793**	1782 ±9	**94444 ±793**
SS175	U	7,4	d		485,8 ±1,1	45283 ±911	222 ±5	1507,2 ±4,6	1,2567 ±0,0041	70137 ±348	**69175 ±762**	1832 ±7	**69103 ±762**
SS18	N	6,8	b	omitted	422,2 ±0,4	20143 ±404	210 ±4	1666,5 ±2,5	0,6081 ±0,0012	27480 ±68	**26983 ±358**	1798 ±3	**26913 ±358**
SS20	N	6,8	b	omitted	464,2 ±0,5	4476 ±90	1169 ±23	1692,9 ±2,8	0,6838 ±0,0013	30976 ±74	**30878 ±101**	1847 ±3	**30808 ±101**
SS17	N	6,8	b	omitted	1447,8 ±1,8	1278 ±26	13078 ±264	1630,3 ±2,4	0,7003 ±0,0014	32685 ±82	**32676 ±82**	1788 ±3	**32606 ±82**
SS16	N	6,8	b		746,2 ±1,0	7198 ±144	2613 ±53	1250,7 ±2,5	1,5288 ±0,0029	108396 ±368	**108292 ±375**	1698 ±4	**108222 ±375**
SS174	T	6,6	b	omitted	542,5 ±0,8	20933 ±420	329 ±7	1672,1 ±3,2	0,7703 ±0,0018	35768 ±108	**35373 ±299**	1848 ±4	**35301 ±299**
SS173	T	6,6	b		1097,8 ±3,7	14721 ±299	1045 ±21	1617,7 ±5,1	0,8496 ±0,0037	41036 ±230	**40897 ±250**	1816 ±6	**40825 ±250**
SS172	T	6,6	b		404,9 ±1,0	7845 ±158	884 ±18	1578,9 ±5,3	1,0393 ±0,0037	53170 ±269	**52971 ±303**	1834 ±6	**52899 ±303**
SS171	T	6,6	d		1112,6 ±3,3	7138 ±144	2654 ±54	1551,5 ±5,1	1,0329 ±0,0044	53480 ±311	**53413 ±314**	1804 ±6	**53341 ±314**
SS170	T	6,6	i		873,0 ±2,0	6285 ±127	2917 ±59	1467,9 ±4,0	1,2735 ±0,0039	72929 ±340	**72854 ±343**	1803 ±5	**72782 ±343**
SS26	J	5,6	i		431,0 ±0,5	64540 ####	144 ±3	1452,6 ±2,6	1,3058 ±0,0026	76057 ±233	**74487 ±1135**	1792 ±7	**74417 ±1135**
SS27	J	5,6	b		765,5 ±0,9	4416 ±89	4144 ±83	1327,9 ±2,3	1,4500 ±0,0022	94976 ±255	**94914 ±259**	1736 ±3	**94844 ±259**
SS10	F	3,2	i		1768,4 ±2,7	85 ±2	502249 ±10457	1307,5 ±2,4	1,4637 ±0,0029	97602 ±321	**97601 ±321**	1722 ±3	**97531 ±321**
SS11	F	3,2	b		1905,6 ±3,3	20 ±0	2269613 ±51951	1291,2 ±2,5	1,4616 ±0,0030	98467 ±342	**98467 ±342**	1705 ±4	**98397 ±342**
SS14	F	3,2	d		509,9 ±0,7	135 ±3	94432 ±1972	1281,4 ±2,7	1,5131 ±0,0027	104408 ±346	**104405 ±346**	1720 ±4	**104335 ±346**
SS12	F	3,2	x		439,9 ±0,5	1193 ±24	9372 ±189	1222,3 ±2,3	1,5411 ±0,0029	112075 ±384	**112045 ±385**	1677 ±4	**111975 ±385**
SS13	F	3,2	i	omitted	565,2 ±0,7	787 ±16	18487 ±375	1265,0 ±2,3	1,5621 ±0,0027	110930 ±353	**110915 ±354**	1730 ±4	**110845 ±354**

References

Wendt, K.A. et al. (2018) Moisture availability in the southwest United States over the last three glacial-interglacial cycles. Science Advances 4: eaau1375 https://doi.org/10.1126/sciadv.aau1375

Wendt, K.A. et al. (2019) Paleohydrology of southwest Nevada (USA) based on groundwater $^{234}U/^{238}U$ over the past 475 k.y.. GSA Bulletin 132(3-4): 793-802 https://doi.org/10.1130/B35168.1

Jackson, T.R. and Steidle, S.D. et al. (2023) A 350,000-year history of groundwater recharge in the southern Great Basin, USA. Communications Earth and Environment 4, 98 https://doi.org/10.1038/s43247-023-00762-0

Li, X. et al. (2020) Novel method for determining ^{234}U–^{238}U ages of Devils Hole 2 cave calcite (Nevada). Geochronology 3: 49-58 https://doi.org/10.5194/gchron-3-49-2021